

**ENGINEERING SURFACES TO DIRECT INTEGRIN BINDING AND
SIGNALING TO PROMOTE OSTEOBLAST DIFFERENTIATION**

A Doctoral Thesis
Presented to
The Academic Faculty

by

Benjamin G. Keselowsky

In Partial Fulfillment
of the Requirements for the Degree
Doctor of Philosophy in Bioengineering

Georgia Institute of Technology
May 2004

Copyright © Benjamin G. Keselowsky 2004

ENGINEERING SURFACES TO DIRECT INTEGRIN BINDING AND SIGNALING
TO PROMOTE OSTEOBLAST DIFFERENTIATION

Approved by:

Andrés J. García (Advisor)

David M. Collard

Elliot L. Chaikoff

Robert E. Guldberg

Harish Radhakrishna

Cheng Zhu

Date Approved: 2/24/2004

For my family

ACKNOWLEDGMENT

I would like to express my sincerest gratitude to a number of people, without whom, this undertaking would have been too overwhelming. Andrés García, my advisor, has provided both guidance and friendship that have been essential to my success. I've learned a lot from my labmates, la familia García, and they've made working at Tech enjoyable. Furthermore, I've had a lot of fun getting stupid with them. Ben Byers stuck it out with me from the first day in the lab until the end- thanks for the lab karaoke and being my pal. Nate Gallant has been the coolest hard-drinking calypso poet I've had the honor to be friends with- thanks. Thanks to Catherine Reyes for commiserating/being a sounding board during the trouble-shooting of numerous experiments, for letting me in on the literati secret to use the word: "acknowledgment" instead of "acknowledgements", and thank you for being a great friend. Back in the day, Kristin Michael had the nerve to tell me when I needed to wash the glassware... despite that- thank you for your friendship and the chili too. Thanks Jeff Capadona, for being a chemist, 'cause I like chemistry... additionally, thanks for sharing common interests like MMA and making me enjoy a Cubs game- I can forgive you for the country music. Thanks to Charlie Gersbach for "bringing etching to the lab", for making me freeze my feet off clamming and for having what I think is the "mullet-cut work ethic": all business during the day/at night-hardcore play. Yo, shout out to Jenn Philips for being the nicest workaholic and classiest b-balling chick ever, you off da hook! Thank you Lindsay Bryant, for managing the lab, taking over with the glassware, and being the sweetest South Carolinian I've had the pleasure to meet. Thanks to all of wing 2D. Thanks to Angela Lin for taking me out to

the *really* cool places in Atlanta, juggling, and being the only one who wouldn't get mad at me for trying out new ju-jitsu moves on them. Thanks to Srin Nagaraja for always finding a way to make us all laugh, even if it was at my expense. Thank you Blaise Porter, for your friendship. Thanks to my friends that started the program with me, especially Don Murphy, Tim Tolentino, Chad Johnson, Cherie Stabler and Matt Tate.

Most significantly, I must acknowledge the support and love my whole family has provided throughout these years. Thank you, Mom and Dad, for believing in me and never doubting that I'd get through this. Finally, I acknowledge that without my wife, Jennifer, and sons, Elijah and Ethan, none of this would be meaningful. Thank you for making my life this rich.

TABLE OF CONTENTS

DEDICATION	III
ACKNOWLEDGMENT	IV
TABLE OF CONTENTS	VII
LIST OF TABLES	VIII
LIST OF FIGURES	IX
SUMMARY	XI
CHAPTER 1: SPECIFIC AIMS	1
AIM 1	2
AIM 2	3
AIM 3	3
THESIS OUTLINE	4
CHAPTER 2: BACKGROUND AND SIGNIFICANCE	6
BONE TISSUE DEFICIENCIES	6
IMPLANT SURFACE TECHNOLOGIES.....	6
BONE GRAFT SUBSTRATES.....	8
TISSUE ENGINEERING STRATEGIES	9
BIOMIMETIC MATERIALS AND BONE REPAIR	10
CELL ADHESION TO ECM PROTEINS.....	11
INTEGRINS AND FOCAL ADHESIONS	12
FIBRONECTIN- AN ESSENTIAL ECM COMPONENT	14
CELL ADHESION TO BIOMATERIAL SURFACES.....	15
PROJECT SIGNIFICANCE.....	16
REFERENCES.....	20
CHAPTER 3: QUANTITATIVE METHODS FOR ANALYSIS OF INTEGRIN BINDING AND FOCAL ADHESION FORMATION ON BIOMATERIAL SURFACES	30
SUMMARY	30
INTRODUCTION.....	30
MATERIALS AND METHODS.....	31
<i>Cells and reagents</i>	31
<i>Integrin binding analysis</i>	32
<i>Focal adhesion assembly analysis</i>	34
RESULTS.....	35
<i>Integrin binding analysis</i>	35
<i>Focal adhesion assembly analysis</i>	37
DISCUSSION.....	38
ACKNOWLEDGMENT	40
REFERENCES.....	45
CHAPTER 4: SURFACE CHEMISTRY MODULATES FIBRONECTIN CONFORMATION AND DIRECTS INTEGRIN BINDING AND SPECIFICITY TO CONTROL CELL ADHESION	47
SUMMARY	47
INTRODUCTION.....	48
MATERIALS AND METHODS.....	50
<i>Reagents</i>	50
<i>Alkanethiols and Self-Assembled Monolayers</i>	51
<i>FN Adsorption to SAMs</i>	52
<i>FN Conformation on SAMs</i>	53

<i>Cell Model to Examine Adhesive Interactions</i>	54
<i>Integrin Binding Analyses</i>	54
<i>Cell Adhesion Assay</i>	55
<i>Curve-Fits and Statistics</i>	56
RESULTS	56
<i>Model Surfaces with Well-Defined Chemistry</i>	56
<i>FN Adsorption onto SAMs</i>	57
<i>SAM-dependent Changes in Adsorbed FN Conformation</i>	58
<i>Integrin Binding to FN-coated SAMs</i>	59
<i>Cell Adhesion to FN-coated SAMs</i>	62
DISCUSSION.....	63
ACKNOWLEDGMENT	68
REFERENCES	85
CHAPTER 5: SURFACE CHEMISTRY MODULATES FOCAL ADHESION COMPOSITION AND SIGNALING THROUGH CHANGES IN INTEGRIN BINDING	90
SUMMARY	90
INTRODUCTION	91
MATERIALS AND METHODS	92
<i>Cells and reagents</i>	92
<i>Model surfaces with well-defined chemistries</i>	93
<i>Cell adhesion assay</i>	94
<i>Integrin binding and focal adhesion assembly</i>	95
<i>FAK phosphorylation</i>	96
<i>Statistical analyses</i>	96
RESULTS	96
<i>Surface chemistry modulates integrin binding and cell adhesion</i>	96
<i>Surface chemistry alters focal adhesion assembly</i>	98
<i>Surface chemistry modulates site-specific FAK phosphorylation</i>	99
DISCUSSION.....	99
ACKNOWLEDGMENT	103
REFERENCES	110
CHAPTER 6: SURFACE CHEMISTRY DIRECTS OSTEOBLASTIC DIFFERENTIATION	115
SUMMARY	115
INTRODUCTION	116
MATERIALS AND METHODS	118
<i>Cells and Reagents</i>	118
<i>Model Surfaces with Well-Defined Chemistries</i>	118
<i>Proliferation</i>	119
<i>Osteoblast-Specific Gene Expression</i>	120
<i>Alkaline Phosphatase Activity</i>	121
<i>Matrix Mineralization</i>	121
<i>Statistical Analyses</i>	122
RESULTS	122
<i>Cell Proliferation</i>	123
<i>Osteoblastic Gene Expression is Surface Chemistry-Dependent</i>	123
<i>Alkaline Phosphatase Activity</i>	124
<i>Surface Chemistry-Dependent Differences in Matrix Mineralization</i>	124
DISCUSSION.....	125
ACKNOWLEDGMENT	128
REFERENCES	136
CHAPTER 7: CONCLUSIONS AND RECOMMENDATIONS FOR FUTURE WORK	141

LIST OF TABLES

Table 4.1. Variable-angle XPS measurements of SAMs.....	69
Table 4.2. Hyperbolic curve-fit parameters for FN adsorption.....	70
Table 4.3. HFN7.1 monoclonal antibody FN_{AB-50} values for FN-coated SAMs.....	71
Table 4.4. 3E3 monoclonal antibody FN_{AB-50} values for FN-coated SAMs.....	72
Table 4.5. $FN_{\alpha 5-50}$ values for MC3T3-E1 cells on FN-coated SAMs.....	73
Table 4.6. FN_{ADH-50} values for MC3T3-E1 adhesion to FN-coated SAMs.....	74
Table 4.7. Summary of FN conformation/integrin binding/cell adhesion results.....	75
Table 5.1. Recruitment of structural and signaling components to focal adhesions.....	104
Table 6.1. Real-time PCR oligonucleotides for murine genes.....	129

LIST OF FIGURES

Figure 2.1. Diagram of a focal adhesion.....	14
Figure 2.2. Schematic model of fibronectin.....	15
Figure 3.1. Analysis of integrin binding via cross-linking/extraction method.....	41
Figure 3.2. Quantitative analysis of integrin binding via cross-linking/extraction method.....	42
Figure 3.3. Analysis of focal adhesion formation by wet-cleaving method.....	43
Figure 3.4. Quantification of focal adhesion assembly by wet-cleaving method.....	44
Figure 4.1. SAM structure and characterization by contact angle.....	76
Figure 4.2. FN adsorption on SAMs as a function of coating concentration.....	77
Figure 4.3. Bound HFN7.1 monoclonal antibody as a function of FN surface density....	78
Figure 4.4. Bound 3E3 monoclonal as a function of FN surface density.....	79
Figure 4.5. $\alpha_5\beta_1$ integrin binding as a function of FN surface density.....	80
Figure 4.6. Immunofluorescence staining for α_5 and α_v integrin subunits on MC3T3-E1 cells.....	81
Figure 4.7. Adherent fraction of MC3T3-E1 cells seeded on FN-coated SAMs, as a function of FN surface density.....	82
Figure 4.8. Minimum “active” FN surface density to produce maximum cell adhesion.....	83
Figure 4.9. Relationship between FN_{α_5-50} and FN_{ADH-50} showing positive correlation between $\alpha_5\beta_1$ integrin binding and cell adhesion strength.....	84
Figure 5.1. Surface chemistry modulates integrin binding affinity.....	105
Figure 5.2. Surface chemistry modulates cell adhesion strength.....	106
Figure 5.3. Surface chemistry differentially alters recruitment and organization of structural component, vinculin, to focal adhesions.....	107

Figure 5.4. Surface chemistry differentially alters recruitment and organization of structural component, talin, to focal adhesions.....	108
Figure 5.5. Surface chemistry modulates site-specific phosphorylation of FAK.....	109
Figure 6.1 Osteoblast proliferation shows little dependence on surface chemistry.....	130
Figure 6.2. Surface chemistry modulates osteoblastic gene expression.....	131
Figure 6.3. Osteoblast alkaline phosphatase activity shows little dependence on surface chemistry.....	132
Figure 6.4. Surface chemistry modulates matrix mineralization.....	133
Figure 6.5. Surface chemistry modulates composition and structure of matrix mineralization as shown by FT-IR.....	134
Figure 6.6. Osteoblast differentiation requires integrin binding to fibronectin.....	135

SUMMARY

Cell adhesion to proteins adsorbed onto implanted surfaces is particularly important to host responses in biomedical and tissue engineering applications. Biomaterial surface properties influence the type, quantity and functional presentation (activity) of proteins adsorbed upon contact with physiological fluids, and modulate subsequent cell response. Cell adhesion to extracellular matrix proteins (e.g. fibronectin) is primarily mediated by the integrin family of cell-surface receptors. Integrins not only anchor cells, supporting cell spreading and migration, but also trigger signals that regulate survival, proliferation and differentiation. A fundamental understanding of the adhesive interactions at the biomaterial interface is critical to the rational design of biomaterial surfaces. Using model surfaces of self-assembled monolayers of alkanethiols on gold presenting well-defined surface chemistries (CH₃, OH, COOH, NH₂), we investigated the effects of surface chemistry on osteoblastic differentiation. We report that surface chemistry effectively modulates fibronectin adsorption, integrin binding, focal adhesion assembly and signaling to direct the osteoblast cellular functions of adhesion strength, gene expression and matrix mineralization. Specifically, surfaces presenting OH and NH₂ functionalities provide enhanced functional presentation of adsorbed fibronectin, promoting specificity of integrin binding as well as elevating focal adhesion assembly and signaling. Furthermore, the OH and NH₂ surfaces supported elevated levels of osteoblast differentiation as evidenced by osteoblast-specific gene expression and matrix mineralization. These results contribute to the development of design principles for the engineering of surfaces that direct cell adhesion for biomedical

and tissue engineering applications. In particular, the understanding provided by this analysis may be useful in the engineering of surface properties for bone tissue repair and regeneration.

CHAPTER 1

SPECIFIC AIMS

The focus of this project was the engineering of surfaces that modulate cell adhesion in order to direct cell function. Cell adhesion to extracellular matrix (ECM) proteins is critical to physiological and pathological processes such as tissue development and homeostasis, blood clotting, wound healing and cancer metastasis. In addition, cell adhesion to proteins adsorbed onto synthetic surfaces directs cell function in numerous biomedical applications. Cell adhesion is a highly regulated process involving receptor-ligand binding, cell spreading and formation of focal adhesions and actin stress fibers. Cell adhesion to ECM proteins is primarily mediated by the integrin family of transmembrane adhesion receptors. Integrins provide a connection between the cytoskeleton and the ECM, anchoring cells to provide tissue structure and integrity. Integrins also function as signal transducers, relaying information contained in the surrounding ECM to intracellular signaling pathways that control cell survival, proliferation and differentiation. Upon ligand binding, integrins cluster to form focal adhesions. Focal adhesions are the closest points of contact between the cell membrane and ECM, and are the sites of greatest cell adhesion. Focal adhesions are complexes that consist of not only adhesion receptors and cytoskeletal proteins (e.g., vinculin, talin, actin fibers), but also include abundant signaling molecules (e.g., focal adhesion kinase (FAK) and src-family kinases).

The ECM protein fibronectin (FN) plays a central role in the proliferation and differentiation of numerous cell types. For example, in osteoblasts, integrin-mediated adhesion to FN regulates cell survival, proliferation and expression of osteoblast-specific

genes and matrix mineralization, and integrin- and fibronectin-blocking antibodies inhibit osteoblastic gene expression and matrix mineralization. The critical importance of integrin-FN interactions in cell function has significant implications in the development of surfaces for biomaterial and tissue engineering applications. **The overall objective of this project was to identify surface chemistries that modulate adsorbed FN conformation to direct integrin-FN binding in order to direct cell function.** Our central hypothesis was that surface chemistry directs cell function by altering integrin-FN binding due to surface-dependent modulation of FN conformation. This hypothesis is supported by previous studies in our laboratory demonstrating that substrate-dependent differences in FN conformation modulate integrin binding and control switching between myoblast proliferation and differentiation. A significant advantage of our experimental system over previous studies is the use of model surfaces consisting of self-assembled monolayers (SAMs) of alkanethiols on gold presenting well-defined chemistries. This system, coupled with robust bioengineering and cell biology approaches, allows a systematic analysis of the effects of surface chemistry on cell function.

AIM 1: TO ANALYZE DIFFERENCES IN ADSORBED FN CONFORMATION AS A FUNCTION OF SURFACE CHEMISTRY (CH₃, OH, COOH, NH₂) USING MONOCLONAL ANTIBODIES. The structure of FN adsorbed onto SAMs was investigated using a panel of monoclonal antibodies directed against different FN domains. Differences in antibody binding affinity reflect differences in adsorbed FN conformation among SAMs.

Hypothesis: Surface chemistry significantly alters the structure of adsorbed FN, including regions within the central integrin-binding domain.

AIM 2: TO QUANTIFY INTEGRIN RECEPTOR BINDING TO FN ADSORBED ONTO SAMS AND ANALYZE SUBSTRATE-DEPENDENT DIFFERENCES IN FOCAL ADHESION FORMATION AND SIGNALING. Integrin binding to adsorbed FN was quantified via a cross-linking/extraction biochemical method. Cytoskeletal and signaling proteins (vinculin, talin, paxillin and α -actinin, FAK) localized to focal adhesions were quantified as a function of FN density by a wet-cleaving/ELISA technique as well as immunofluorescence staining. FAK phosphorylation, a measure of integrin-mediated signaling, was analyzed by Western blotting.

Hypothesis: Substrate-dependent changes in FN conformation modulate integrin receptor binding, focal adhesion formation (composition and distribution) and signaling.

AIM 3: TO ANALYZE OSTEObLAST-SPECIFIC GENE EXPRESSION AND MATRIX MINERALIZATION OF MC3T3-E1 CELLS CULTURED ON FN-COATED SAMS. Osteoblast-specific gene expression of a cell model representing immature osteoblasts, MC3T3-E1 cells, was analyzed through real-time RT-PCR. Alkaline phosphatase activity and matrix mineralization was quantified using a biochemical assay and von Kossa staining, respectively.

Hypothesis: Substrate-dependent changes in integrin binding and focal adhesion assembly direct osteoblast differentiation and matrix mineralization.

Control of cell receptor-ligand interactions through the underlying substrata represents a versatile approach for the rational design of materials to manipulate cellular responses for biotechnological and biomedical applications. Currently, a major obstacle in biomaterial and tissue engineering applications is the *in vitro* loss of differentiated phenotypes. By implementing a bioengineering analysis of integrin-mediated adhesion as a function of the underlying chemistry, we established a fundamental framework for the engineering of surfaces to direct cell function. By focusing on osteoblasts, the cells responsible for bone matrix production and mineralization, this research is directly relevant to the engineering of surfaces that promote osteoblast function, which may lead to improvements in bioactive implant coatings, and 3-D scaffolds for bone tissue engineering.

THESIS OUTLINE

This thesis addresses the Specific Aims outlined above, and is organized in the following manner. Chapter 2 provides background of the field and the significance of this project. Chapter 3 details the validation of new techniques developed to quantify integrin binding and focal adhesion assembly. These techniques were then used as described in Chapter 4 and Chapter 5 to address topics in Specific Aim 2. Chapter 4 presents results demonstrating that surface chemistry modulates fibronectin conformation and directs integrin binding (Specific Aim 1 and part of Specific Aim 2). Chapter 5 provides data showing that surface chemistry modulates focal adhesion composition and signaling through changes in integrin binding, addressing the remainder of Specific Aim 2. Chapter 6 details data demonstrating that surface chemistry directs osteoblastic differentiation

(Specific Aim 3). Finally, Chapter 7 gives overall conclusions and recommendations for future work.

CHAPTER 2

BACKGROUND AND SIGNIFICANCE

BONE TISSUE DEFICIENCIES

Complications associated with bone tissue reconstruction procedures including poor prosthesis-bone integration, non-union fractures, and bone loss associated with trauma, joint replacements and tumors, have an enormous socioeconomic impact in the U.S., in terms of both personal disability and resultant health care costs. For example, over 700,000 joint arthroplasties were performed in 2000, incurring a cost of approximately \$15 billion.¹ Although joint replacements are relatively successful, often able to function for over 10 years, the long-term success of these arthroplasties is limited by implant loosening and wear, causing patient discomfort and pain and requiring revision surgery.² Similarly, bone grafting to treat non-unions and bone loss is critical to numerous orthopedic and craniofacial applications.³ For example, approximately 600,000 spinal fusion and general orthopedic grafting procedures are performed yearly in the U.S.⁴ In addition, about 10% of the 6 million bone fractures treated annually require auxiliary grafting.⁵ Treatments using auto- and allo-grafts have had the most success, however, these treatments are limited by donor bone supply and morbidity, reduced bioactivity and risk of disease transmission.

IMPLANT SURFACE TECHNOLOGIES

Considerable efforts have focused on implant surface technologies, particularly porous coatings for bone ingrowth and bone-bonding ceramic coatings, to promote

integration with surrounding bone.⁶ Osseous implants often fail by a combination of factors, including inflammatory responses to wear debris, infection, implant motion, and inadequate mechanical loading.⁷ These factors result in a reduction of local bone production, an increase in bone resorption, or both.⁷ One critical parameter in the long-term success of osseous implants is initial mechanical fixation. Most orthopedic implants with poor initial fixation eventually fail clinically, a problem that is exacerbated by wear debris.⁸⁻¹⁰ Consequently, considerable effort has focused on the development of implant surface technologies, particularly micro- and macro-textured implants for bone ingrowth and bone-bonding ceramics, to promote osseointegration, defined as direct bone apposition and load transfer.^{11,12}

Implants with porous metal coatings have been used to provide cavities of several hundred micrometers available for bone ingrowth and fixation.¹³ While these designs generally perform well clinically, bone ingrowth and implant fixation are highly variable, especially in revision surgeries.¹⁴⁻¹⁷ Micro-textured surfaces, such as grit-blasted titanium, have exhibited excellent osseointegration and performance in dental applications.^{18,19} However, they have had limited success in orthopedic settings due to inadequate initial fixation.^{20,21} An alternative strategy to promote osseointegration focuses on bioactive coatings.²² Bioactive materials, namely calcium phosphate and bioactive ceramics such as hydroxyapatite, react with physiological fluids to enhance bone formation and bond directly to bone.²³ Bioactive ceramics have been generally successful in non-load bearing applications, but poor fracture properties and loss of bioactivity resulting from manufacturing-related alterations in composition/structure have limited their application as implant coatings and structural replacements.²⁴ Therefore

there is still a significant need for surface technologies that enhance implant osseointegration.

BONE GRAFT SUBSTRATES

Bone grafting is critical to numerous orthopedic and craniofacial applications.³ Autogenous bone, harvested from the patient's iliac crest, is presently the preferred material.³ Autografts, however, are limited by donor bone supply, donor site morbidity and pain, anatomical and structural complications and graft resorption.²⁵ Because of these complications, allogenic bone has been used as grafting material.²⁶ Although tissue processing minimizes immune complications, allografts suffer from poor mechanical properties, graft resorption, reduced osteogenic capacity, and risk of disease transmission.²⁵ Consequently, extensive research has focused on the development of synthetic materials as alternatives to biological grafts. However, synthetic materials generally incite foreign body/inflammatory responses and exhibit poor osteogenic cell interactions and bone formation.²⁷ Notable exceptions are bioactive ceramics and glasses, which exhibit osteoconductive properties.^{23,24} These materials, however, are limited by poor mechanical properties and inadequate dissolution/precipitation rates as well as difficulties in manufacturing and processing.^{28,29}

Delivery of osteoinductive factors, such as BMPs, has been successfully applied to augment local bone repair and several formulations are available for clinical applications.³⁰⁻³² However, the clinical efficacy of these treatments continues to be hampered by inadequate delivery carriers, release kinetics, dosage, and potency.^{31,33} Genetic engineering strategies to deliver osteoinductive genes to osseous defects have emerged as efficient approaches to enhance bone formation.^{34,35} Recent studies have

demonstrated significant healing rates in fractures and segmental defects treated with vectors encoding for BMP or BMP-expressing cells.³⁶⁻⁴¹ Although these initiatives are promising, further studies are required to establish the efficacy, immunogenicity, and long-term safety of these genetic engineering approaches.

TISSUE ENGINEERING STRATEGIES

Due to the limitations associated with current grafting methods, recent research efforts have concentrated on tissue engineering strategies, incorporating cells dispersed in 3D scaffolds, in order to create functional bone grafts.⁴² Tissue engineering strategies include the use of bioactive factors, osteogenic precursor or stem cells, and natural and artificial matrices to support cell attachment, proliferation and differentiation *in vivo* or, alternatively, for *in vitro* construct development as a preliminary step to implantation.⁴³ Several groups have demonstrated *in vitro* development of mineralized constructs by combining immature osteoblasts or bone marrow stromal cells with polymeric or ceramic scaffolds.⁴⁴⁻⁵² For example, the polymeric scaffolds of poly(lactic acid) (PLA), poly(glycolic acid) (PGA) and their copolymers of poly(lactic/glycolic acid) (PLGA) have been extensively investigated for tissue engineering applications and support osteoblast differentiation, matrix mineralization *in vitro* and *in vivo*.⁵³ However, for these scaffolds, a severe limitation is that 200-500 μm penetration depths of mineralized tissue are typical.⁵⁴ Correspondingly, in critical size defect models, PLA scaffolds, empty or containing osteoprogenitor cells, have failed to close the non-healing defect at 4 weeks.⁵⁵ Further illustrating this point, *in vitro* studies comparing various metals and alloys, as well as polymers of PLA, PGA, PLGA, hydroxyapatite, poly(methylmethacrylate), and

poly(hydroxyethyl methacrylate), demonstrated no improvement in cell attachment, proliferation collagen synthesis and alkaline phosphatase activity with respect to reference materials of tissue culture and glass.⁵⁶

Recent studies have demonstrated *in vivo* bone formation and repair of bone defects with scaffolds loaded with osteogenic cells, in particular, marrow-derived mesenchymal stem cells.⁵⁷⁻⁶³ While these studies establish the potential of tissue engineering strategies for bone repair, these cell-based approaches fall short of providing mechanically robust, osteoconductive grafting templates, especially for large, non-healing defects. A critical limitation of these strategies is the inability of current scaffold materials to direct osteogenic cells to proliferate, differentiate and produce robust bone tissue. Thus, there is an essential need for bioactive materials that promote osteoblastic differentiation and mineralization for the development of improved grafting templates.

BIOMIMETIC MATERIALS AND BONE REPAIR

Because cell adhesion to extracellular matrices provides signals critical to osteoblast survival, proliferation and differentiation,⁶⁴ researchers have engineered substrates presenting ligands to provide recognition sites in an effort to direct cellular adhesion. These biomimetic substrates have led to incorporation of the RGD adhesive peptide onto surfaces and into scaffolds. Work *in vitro* with RGD adhesive peptide grafted substrates showed enhancement in cell adhesion and modest improvement in mineralization at three weeks.^{65,66} Furthermore, RGD coating of PLGA scaffolds implanted into rat tibial defects enhanced early-stage osteocompatibility and ingrowth.⁶⁷ Similarly, matrix metalloproteinase-degradable hydrogels presenting tethered RGD, in

conjunction with delivery of bone morphogenetic protein-2, were able to bridge a rat cranial critical size defect.⁶⁸ Taken together, these results suggest that improved adhesive interactions at the biomaterial interface could enhance tissue engineered construct outcomes.

CELL ADHESION TO ECM PROTEINS

Cell adhesion to extracellular matrix (ECM) proteins including collagen, laminin, fibrinogen, and fibronectin (FN), is essential to such physiological processes as development, organogenesis, wound healing and tissue homeostasis.^{69,70} Cell adhesion not only anchors cells, providing tissue structure and integrity and supporting cell migration, but also triggers signals that regulate survival, proliferation and differentiation.⁷¹ Several pathological conditions, including blood clotting defects and tumor metastases, involve abnormal adhesion processes.⁷² Cell adhesion interactions are critical to many biomedical and biotechnological applications.⁷³ Cell adhesion to implant surfaces via engineered adhesive motifs, proteins pre-adsorbed or proteins adsorbed from physiological fluids, is particularly important to host response in biomaterial and tissue engineering applications.^{74,75} Many proteins including albumin, immunoglobulins, vitronectin, fibrinogen and FN adsorb onto implant surfaces immediately upon contact with physiological fluids and modulate subsequent inflammatory responses.⁷⁵ For example, FN plays an important role in clot formation through its interactions with fibrin and activated platelets.⁷⁶ Adsorbed FN also mediates the attachment and activation of neutrophils, macrophages and other inflammatory cells.⁷⁷ Cell-ECM interactions also play a central role in clot retraction, matrix contraction and wound healing.^{76a} Adhesion

to proteins endogenously secreted or adsorbed from serum-containing media provides mechanical coupling to the underlying substrate for in vitro applications such as tissue-engineered constructs, bioreactors and cell culture supports, and activates signaling pathways that control cell morphology, proliferation and differentiation.⁶⁹

INTEGRINS AND FOCAL ADHESIONS

Cell adhesion to the ECM is a highly regulated process involving cell attachment through integrin receptor-ligand binding, cell spreading, and the formation of focal adhesions in conjunction with actin stress fibers. The dominant family of cell adhesion receptors mediating attachment to ECM is the integrin receptor family.⁶⁹ The critical physiological importance of integrin receptors and focal adhesion components is highlighted by knockout studies in mice where deletions in the genes encoding for integrin receptors, focal adhesion components (FAK, vinculin) and ECM ligands (FN, laminin) are lethal in the early stages of embryonic development.⁷⁸

Integrins are heterodimeric transmembrane receptors consisting of non-covalently associated α and β subunits with short cytoplasmic tails and large extracellular regions that interact to bind specific amino acid sequences in the ligand. For example, several integrins bind the arginine-glycine-aspartic acid (RGD) recognition sequence present in several ECM proteins such as FN, vitronectin and thrombospondin.⁷⁹ As seen by rotary shadowing electron microscopy, the extracellular, N-terminal portions of both integrin subunits contribute to form a globular head domain approximately 8 nm long by 12 nm wide with two extended tails about 2 nm thick and 18-20 nm long constituting the transmembrane and cytoplasmic tail domains, with the whole complex being

approximately 28 nm long.⁸⁰ Nuclear magnetic resonance and electron microscopy have revealed that the cytoplasmic tail of the β subunit binds cytoskeletal and signaling proteins, whereas the cytoplasmic tail of the α subunit functions to mask β tail interactions until receptor-ligand binding occurs.⁸¹⁻⁸³ X-ray diffraction studies of unbound and bound $\alpha_v\beta_3$ integrin to cyclic RGD ligand has revealed that ligand binding induces small changes in the orientation of the α chain with respect to the β chain.⁸⁴ In contrast, molecular electron microscopy of $\alpha_5\beta_1$ binding to FN fragments reveal much larger conformational differences.⁸⁵

Integrins connect the ECM to the cytoskeleton to anchor cells, providing tissue structure and integrity. Integrins also function as signal transducers, transmitting information contained in the ECM to intracellular signaling pathways and cytoskeletal rearrangements that control survival, proliferation and differentiation.⁸⁶ This process is termed “outside-in signaling”.⁸⁷ Conversely, “inside-out signaling” consists of a conformational change in integrin subunits to an activated state in order to modulate ligand binding affinity and cellular adhesion.⁸⁷

Upon binding ligand, integrins cluster together to form focal adhesions, the sites of greatest cell adhesion and closest points of contact between the cell membrane and the ECM substrate (Figure 2.1).⁸⁸ Focal adhesions are complexes that consist of not only cell-surface receptors and cytoskeletal proteins, but also include abundant signaling molecules.⁸⁹ Upon integrin binding to FN, bound receptors rapidly associate with the actin cytoskeleton and cluster together giving rise to focal adhesions containing cytoplasmic structural proteins such as vinculin, talin and α -actinin, and signaling molecules including src, FAK and paxillin, as well as transmembrane proteoglycans.⁹⁰

Focal adhesions are crucial to the adhesion process, directing growth and differentiation.⁹¹⁻⁹³

FIBRONECTIN- AN ESSENTIAL ECM COMPONENT

The ECM consists of a dynamic network of heterogeneous macromolecules secreted by many cell types to serve tissue-specific functions.⁹⁴ By supporting cell adhesion and storing growth factors, the ECM provides structure and signals vital for cells, playing an active and complex role in regulation, influencing development, migration, proliferation, shape and function. The ECM glycoprotein FN, the first cell adhesion protein identified,⁹⁵ has been investigated extensively.⁹⁶ The physiological importance of FN is demonstrated by the embryonic lethality of the FN-gene deletion.⁹⁷ FN has been shown to be involved in numerous physiological and pathological processes including tissue and organ development, tissue homeostasis, hemostasis, wound healing and cancer metastasis.⁹⁶ Cellular interactions with FN are primarily mediated by integrins. Integrin binding to FN plays a critical role in the survival, proliferation and differentiation of numerous cell types, including fibroblasts, myoblasts, chondrocytes and keratinocytes.⁹⁸ For example, $\alpha_5\beta_1$ integrin-mediated adhesion to FN regulates osteoblast survival and expression of osteoblast-specific genes and matrix mineralization, as well as myoblast differentiation, *in vitro*.^{64,115}

Plasma FN is a dimer of two polypeptide chains of approximately 220 kDa each, covalently linked by two interchain disulfide bridges close to the C-terminus (Figure 2.2). Each polypeptide chain is composed of a series of flexible, repeating functional domains of type I, II or III. The central integrin-binding site in FN localizes to the RGD motif in

the 10th type III repeat.⁹⁹ Additional integrin-binding domains include the PHSRN site in the 9th type III repeat, which in conjunction with the RGD site, binds synergistically to several integrins.⁹⁹ FN is secreted by many cell types in different splice-variants and is expressed in most tissues and body fluids.⁹⁴ FN is synthesized as soluble dimers which can then undergo cell-mediated polymerization into insoluble fibrillar networks by numerous cell types including fibroblasts, chondrocytes, myoblasts, smooth muscle cells, endothelial cells and epithelial cells.⁹⁶ Some cell types synthesize and secrete FN, but do not assemble fibrils, including macrophages, activated neutrophils and activated T-lymphocytes.¹⁰⁰

CELL ADHESION TO BIOMATERIAL SURFACES

Numerous studies have shown that surface properties influence the type, amount and conformation of adsorbed proteins.¹⁰¹⁻¹⁰⁴ For example, hydrophilic ethylene glycol-terminated SAMs resist protein adsorption and consequently, cell adhesion, as opposed to the hydrophobic hexadecanethiolate-functionalized SAM that supports protein adsorption, cell adhesion and spreading.¹⁰⁵ The conformation, or three-dimensional structure, of many proteins including FN, is sensitive to surface chemistry.^{77,106} Upon adsorption onto natural and synthetic substrates, FN undergoes conformational changes as demonstrated by electron spin resonance,¹⁰⁷ infrared spectroscopy,¹⁰⁸ fluorescence polarization,¹⁰⁹ rotary shadowing,¹¹⁰ and antibody binding.¹¹¹ Changes in FN conformation alter its ability to support cell adhesion and spreading.¹¹¹⁻¹¹⁴ Substrate-dependent changes in FN conformation have been shown to alter integrin binding and modulate myogenic and osteoblastic differentiation.^{115,115a}

PROJECT SIGNIFICANCE

While the examples provided illustrate progress in engineering of orthopedic implants, there is clearly a need to further the development of improved implant surfaces and bone graft materials. Therefore, we propose that a mechanistic understanding of the factors governing biological responses to surfaces *in vitro* and *in vivo* is necessary for the continued development of materials to repair and regenerate lost tissue function. This project analyzes osteoblast adhesion and differentiation as a function of the underlying surface chemistry in an effort identify chemistries that modulate the activity of the ECM protein FN to control integrin receptor binding, which in turn directs cell function. Engineered surfaces that direct cell function could improve osteoconductive scaffolds by not just simply allowing mineralized tissue to penetrate the scaffold, but by inducing osteoblastic differentiation within the scaffold itself. Previous studies have examined osteoblast function grown on various materials, including metals, polymers and ceramics,⁵⁶ demonstrating that different substrates support different levels of expression of the osteoblastic phenotype. However, these studies do not provide an understanding of the underlying mechanisms of the cell-matrix-surface interactions due to poorly defined substrates and the complex nature of these interactions. In an effort to understand the fundamental role of the underlying substrate, recent work has investigated osteoblast function on surfaces with well-defined chemistries and biomimetic surfaces.^{62,116-118} Although these studies indicate that substrate chemistry and RGD peptides influence osteoblast function, and that cell adhesion is important, the cell-matrix-surface interactions were not analyzed in depth. Understanding these adhesive interactions is

critical to the rational design of surfaces, as recent studies have shown that modulation of specific adhesive interactions controls cell function.^{115,119-121}

The approach of controlling cell receptor-ligand interactions through underlying substrata represents a versatile method to manipulate cellular responses for biomaterial and tissue engineering applications. By focusing on a bioengineering analysis of integrin-FN binding as a function of the underlying substrate, a fundamental framework is established for the rational design of substrates to direct cell function. Although this project deals with model surfaces, the understanding provided by this analysis may be useful in the engineering of surface properties for bone tissue repair and regeneration. The results from this project identified surface chemistries that modulate FN conformation to promote specific integrin receptor binding and osteoblast differentiation. These chemistries can then be incorporated into implant surface coatings or polymer backbones of three-dimensional scaffolds, potentially addressing limitations in the current therapies available for bone tissue deficiencies.

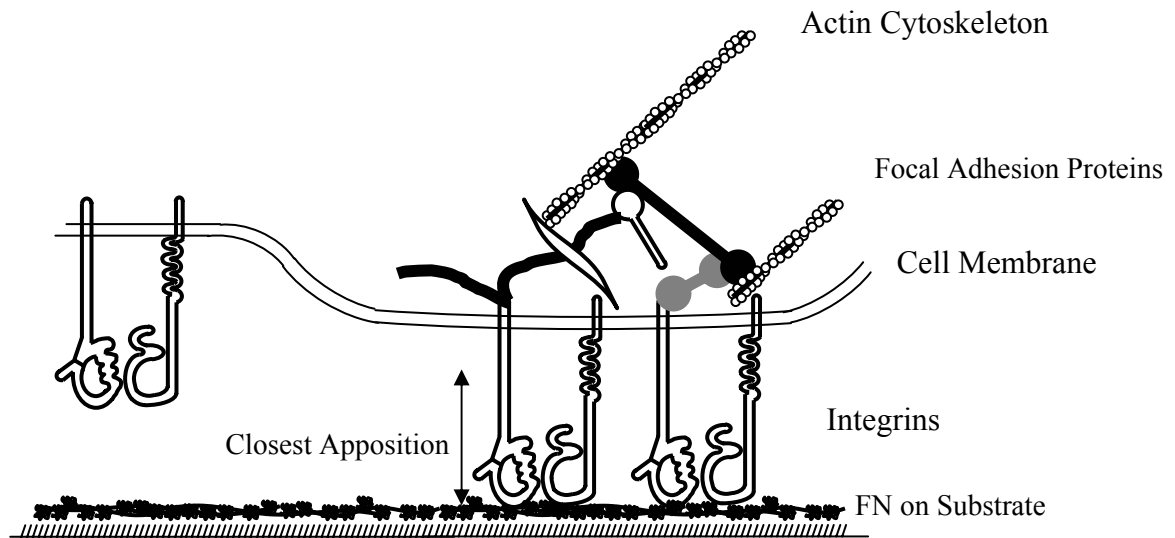


Figure 2.1. Diagram of a focal adhesion showing the clustering of integrins binding to surface-adsorbed FN. Focal adhesions are in close apposition to the substrate and the complex of structural and signaling molecules bridge receptors and actin cytoskeleton.

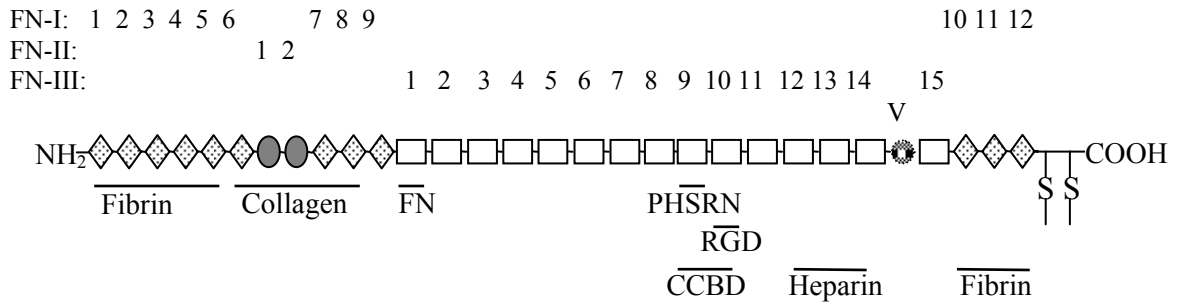


Figure 2.2. Schematic model of FN. This diagram illustrates the linear organization of repeating structural subunits I, II and III, the amine and carboxy termini as well as the disulfide-bridge site of dimerization. Shown are fibrin, collagen and FN (self-assembly) binding domains, as well as the central cell binding domain (CCBD) that includes the RGD binding motif and the PHSRN synergy site. Also shown are the heparin and fibrin binding domains and the variable region, V.

REFERENCES

1. American Academy of Orthopaedic Surgeons. Arthroplasty and Total Joint Replacement Procedures. National Center for Health Statistics, 1991 to 2000 National Hospital Survey. 2004.
2. Arthritis Foundation, CDC. National Arthritis Action Plan: A Public Health Strategy. 1999.
3. Finkemeier,C.G.: Bone-grafting and bone-graft substitutes. *J Bone Joint Surg Am.* **84**:454-464, 2002.
4. Bucholz,R.W.: Nonallograft osteoconductive bone graft substitutes. *Clin Orthop.* **395**:44-52, 2002.
5. Einhorn,T.A.: Clinically applied models of bone regeneration in tissue engineering research. *Clin Orthop.* **367** Suppl:S59-S67, 1999.
6. Bauer,T.W. and Schils,J.: The pathology of total joint arthroplasty. I. Mechanisms of implant fixation. *Skeletal Radiol.* **28**:423-432, 1999.
7. Bauer,T.W. and Schils,J.: The pathology of total joint arthroplasty.II. Mechanisms of implant failure. *Skeletal Radiol.* **28**:483-497, 1999.
8. Albrektsson,T., Branemark,P.I., Hansson,H.A., Kasemo,B., Larsson,K., Lundstorm,I., McQueen,D.H., and Skalak,R.: The interface zone of inorganic implants in vivo: Titanium implants in bone. *Annals Biomed.Eng.* **11**:1-27, 1983.
9. Ryd,L., Albrektsson,B.E., Carlsson,L., Dansgard,F., Herbert,P., Lindstrand,A., Regner,L., and Toksvig-Larsen,S.: Roentgen stereophotogrammetric analysis as a predictor of mechanical loosening of knee prostheses. *J Bone Joint Surg Br.* **77**:377-383, 1995.
10. Aspenberg, ., and Herbertsson,P.: Periprosthetic bone resorption. Particles versus movement. *J Bone Joint Surg Br.* **78**:641-646, 1996.
11. Lemons,J.E.: Ceramics: past, present, and future. *Bone* **19**:121S-128S, 1996.
12. Plenk,H., Jr.: Prosthesis-bone interface. *J.Biomed.Mater.Res.* **43**:350-355, 1998.
13. Engh,C.A., Hooten,J.P., Zettl-Schaffer,K.F., Ghaffarpour,M., McGovern,T.F., Macalino,G.E., and Zicat,B.A.: Porous-coated total hip replacement. *Clin Orthop.* **298**:89-96, 1994.
14. Collier,J.P., Mayor,M.B., Chae,J.C., Surprenant,V.A., Surprenant,H.P., and Dauphinais,L.A.: Macroscopic and microscopic evidence of prosthetic fixation with porous-coated materials. *Clin Orthop.* **235**:173-180, 1988.

15. Cook,S.D., Thomas,K.A., Barrack,R.L., and Whitecloud,T.S.: Tissue growth into porous-coated acetabular components in 42 patients. Effects of adjunct fixation. *Clin Orthop.* **283**:163-170, 1992.
16. Cook,S.D., Barrack,R.L., Thomas,K.A., and Haddad,R.J.: Quantitative analysis of tissue growth into human porous total hip components. *J Arthroplasty* **3**:249-262, 1988.
17. Sychterz,C.J., Claus,A.M., and Engh,C.A.: What we have learned about long-term cementless fixation from autopsy retrievals. *Clin Orthop.* **405**:91, 2002.
18. Wong,M., Eulenberger,J., Schenk,R., and Hunziker,E.: Effect of surface topology on the osseointegration of implant materials in trabecular bone. *J Biomed Mater Res.* **29**:1567-1575, 1995.
19. Sykaras,N., Iacopino,A.M., Marker,V.A., Triplett,R.G., and Woody,R.D.: Implant materials, designs, and surface topographies: their effect on osseointegration. A literature review. *Int J Oral Maxillofac Implants* **15**:675-690, 2000.
20. Havelin,L.I., Espehaug,B., Vollset,S.E., and Engesaeter,L.B.: Early aseptic loosening of uncemented femoral components in primary total hip replacement. A review based on the Norwegian Arthroplasty Register. *J Bone Joint Surg Br.* **77**:11-17, 1995.
21. Torchia,M.E., Klassen,R.A., and Bianco,A.J.: Total hip arthroplasty with cement in patients less than twenty years old. Long-term results. *J Bone Joint Surg Am.* **78**:995-1003, 1996.
22. Geesink,R.G.: Osteoconductive coatings for total joint arthroplasty. *Clin Orthop.* **395** :53-65, 2002.
23. Hench,L.L.: Bioceramics: From concept to clinic. *J.Am.Ceram.Soc.* **74**:1487-1510, 1991.
24. Ducheyne,P. and Cuckler,J.M.: Bioactive ceramic prosthetic coatings. *Clin.Orthop.* **276** :102-114, 1992.
25. Prolo,D.J. and Rodrigo,J.J.: Contemporary bone graft physiology and surgery. *Clin.Orthop.* **200**:322-342, 1985.
26. Khan,S.N., Tomin,E., and Lane,J.M.: Clinical applications of bone graft substitutes. *Orthop Clin North Am* **31**:389-398, 2000.
27. Yaszemski,M.J., Payne,R.G., Hayes,W.C., Langer,R., and Mikos,A.G.: Evolution of bone transplantation: molecular, cellular and tissue strategies to engineer human bone. *Biomaterials* **17**:175-185, 1996.

28. Damien,C.J. and Parsons,J.R.: Bone graft and bone graft substitutes: A review of current technology and applications. *J.Appl.Biomat.* **2**:187-208, 1991.
29. Moore,W.R., Graves,S.E., and Bain,G.I.: Synthetic bone graft substitutes. *ANZ.J.Surg.* **71**:354-361, 2001.
30. Turgeman,G., Zilberman,Y., Zhou,S., Kelly,P., Moutsatsos,I.K., Kharode,Y.P., Borella,L.E., Bex,F.J., Komm,B.S., Bodine,P.V., and Gazit,D.: Systemically administered rhBMP-2 promotes MSC activity and reverses bone and cartilage loss in osteopenic mice. *J Cell Biochem.* **86**:461-474, 2002.
31. Yoon,S.T. and Boden,S.D.: Osteoinductive molecules in orthopaedics: basic science and preclinical studies. *Clin Orthop.* **395**:33-43, 2002.
32. Friedlaender,G.E., Perry,C.R., Cole,J.D., Cook,S.D., Cierny,G., Muschler,G.F., Zych,G.A., Calhoun,J.H., LaForte,A.J., and Yin,S.: Osteogenic protein-1 (bone morphogenetic protein-7) in the treatment of tibial nonunions. *J Bone Joint Surg Am.* **83**:S159-S168, 2004.
33. Winn,S.R., Uludag,H., and Hollinger,J.O.: Carrier systems for bone morphogenetic proteins. *Clin Orthop* **S**:95-106, 1999.
34. Musgrave,D.S., Fu,F.H., and Huard,J.: Gene therapy and tissue engineering in orthopaedic surgery. *J Am Acad Orthop Surg.* **10**:6-15, 2002.
35. Winn,S.R., Hu,Y., Sfeir,C., and Hollinger,J.O.: Gene therapy approaches for modulating bone regeneration. *Adv.Drug Deliv.Rev.* **42**:121-138, 2000.
36. Fang,J., Zhu,Y.Y., Smiley,E., Bonadio,J., Rouleau,J.P., Goldstein,S.A., McCauley,L.K., Davidson,B.L., and Roessler,B.J.: Stimulation of new bone formation by direct transfer of osteogenic plasmid genes. *Proc.Natl.Acad.Sci.U.S.A.* **93**:5753-5758, 1996.
37. Franceschi,R.T., Wang,D., Krebsbach,P.H., and Rutherford,R.B.: Gene therapy for bone formation: in vitro and in vivo osteogenic activity of an adenovirus expressing BMP7. *J Cell Biochem* **78**:476-486, 2000.
38. Krebsbach,P.H., Gu,K., Franceschi,R.T., and Rutherford,R.B.: Gene therapy-directed osteogenesis: BMP-7-transduced human fibroblasts form bone in vivo. *Hum Gene Ther* **11**:1201-1210, 2000.
39. Laurencin,C.T., Attawia,M.A., Lu,L.Q., Borden,M.D., Lu,H.H., Gorum,W.J., and Lieberman,J.R.: Poly(lactide-co-glycolide)/hydroxyapatite delivery of BMP-2-producing cells: a regional gene therapy approach to bone regeneration. *Biomaterials* **22**:1271-1277, 2001.
40. Lieberman,J.R., Daluiski,A., Stevenson,S., Wu,L., McAllister,P., Lee,Y.P., Kabo,J.M., Finerman,G.A., Berk,A.J., and Witte,O.N.: The effect of regional gene

therapy with bone morphogenetic protein-2-producing bone-marrow cells on the repair of segmental femoral defects in rats. *J Bone Joint Surg Am* **81**:905-917, 1999.

41. Musgrave,D.S., Pruchnic,R., Bosch,P., Ziran,B.H., Whalen,J., and Huard,J.: Human skeletal muscle cells in ex vivo gene therapy to deliver bone morphogenetic protein-2. *J Bone Joint Surg Br.* **84**:120-127, 2002.
42. Rose,F.R. and Oreffo,R.O.: Bone tissue engineering: hope vs hype. *Biochem.Biophys.Res.Commun.* **292**:1-7, 2002.
43. Langer,R. and Vacanti,J.P.: Tissue engineering. *Science* **260**:920-926, 1993.
44. Yaszemski,M.J., Payne,R.G., Hayes,W.C., Langer,R., and Mikos,A.G.: Evolution of bone transplantation: molecular, cellular and tissue strategies to engineer human bone. *Biomaterials* **17**:175-185, 1996.
45. Ishaug-Riley,S.L., Crane-Kruger,G.M., Yaszemski,M.J., and Mikos,A.G.: Three-dimensional culture of rat calvarial osteoblasts in porous biodegradable polymers. *Biomaterials* **19**:1405-1412, 1998.
46. Ishaug,S.L., Crane,G.M., Miller,M.J., Yasko,A.W., Yaszemski,M.J., and Mikos,A.G.: Bone formation by three-dimensional stromal osteoblast culture in biodegradable polymer scaffolds. *J.Biomed.Mater.Res.* **36**:17-28, 1997.
47. Holy,C.E., Shoichet,M.S., and Davies,J.E.: Engineering three-dimensional bone tissue in vitro using biodegradable scaffolds: investigating initial cell-seeding density and culture period. *J Biomed Mater Res* **51**:376-382, 2000.
48. El-Ghannam,A., Ducheyne,P., and Shapiro,I.M.: A bioactive glass template for the in vitro synthesis of bone. *J.Biomed.Mater.Res.* **29**:359-370, 1995.
49. Shea,L.D., Wang,D., Franceschi,R.T., and Mooney,D.J.: Engineered bone development from a pre-osteoblast cell line on three-dimensional scaffolds. *Tissue Eng* **6**:605-617, 2000.
50. Ma,P.X., Zhang,R., Xiao,G., and Franceschi,R.: Engineering new bone tissue in vitro on highly porous poly(alpha-hydroxyl acids)/hydroxyapatite composite scaffolds. *J Biomed Mater Res* **54**:284-293, 2001.
51. Marra,K.G., Szem,J.W., Kumta,P.N., DiMilla,P.A., and Weiss,L.E.: In vitro analysis of biodegradable polymer blend/hydroxyapatite composites for bone tissue engineering. *J Biomed Mater Res* **47**:324-335, 1999.
52. Alsberg,E., Anderson,K.W., Albeiruti,A., Franceschi,R.T., and Mooney,D.J.: Cell-interactive alginate hydrogels for bone tissue engineering. *J Dent Res.* **80**:2025-2029, 2001.

53. Ishaug,S.L., Yaszemski,M.J., Bizios,R., and Mikos,A.G.: Osteoblast function on synthetic biodegradable polymers. *J.Biomed.Mater.Res.* **28**:1445-1453, 1994.
54. Ishaug-Riley,S.L., Crane-Kruger,G.M., Yaszemski,M.J., and Mikos,A.G.: Three-dimensional culture of rat calvarial osteoblasts in porous biodegradable polymers. *Biomaterials* **19**:1405-1412, 1998.
55. Wheeler,D.L., Chamberland,D.L., Schmitt,J.M., Buck,D.C., Brekke,J.H., Hollinger,J.O., Joh,S.P., and Suh,K.W.: Radiomorphometry and biomechanical assessment of recombinant human bone morphogenetic protein 2 and polymer in rabbit radius ostectomy model. *J.Biomed.Mater.Res.* **43**:365-373, 1998.
56. Puleo,D.A., Holleran,L.A., Doremus,R.H., and Bizios,R.: Osteoblast responses to orthopedic implant materials in vitro. *J.Biomed.Mater.Res.* **25**:711-723, 1991.
57. Ohgushi,H., Goldberg,V.M., and Caplan,A.I.: Heterotopic osteogenesis in porous ceramics induced by marrow cells. *J.Orthop.Res.* **7**:568-578, 1989.
58. Bruder,S.P., Kraus,K.H., Goldberg,V.M., and Kadiyala,S.: The effect of implants loaded with autologous mesenchymal stem cells on the healing of canine segmental bone defects. *J Bone Joint Surg Am.* **80**:985-996, 1998.
59. Breitbart,A.S., Grande,D.A., Kessler,R., Ryaby,J.T., Fitzsimmons,R.J., and Grant,R.T.: Tissue engineered bone repair of calvarial defects using cultured periosteal cells. *Plast.Reconstr.Surg.* **101**:567-574, 1998.
60. Bruder,S.P., Kurth,A.A., Shea,M., Hayes,W.C., Jaiswal,N., and Kadiyala,S.: Bone regeneration by implantation of purified, culture-expanded human mesenchymal stem cells. *J Orthop Res.* **16**:155-162, 1998.
61. Quarto,R., Mastrogiacomo,M., Cancedda,R., Kutepov,S.M., Mukhachev,V., Lavroukov,A., Kon,E., and Marcacci,M.: Repair of large bone defects with the use of autologous bone marrow stromal cells. *N.Engl.J.Med.* **344**:385-386, 2001.
62. Alsberg,E., Anderson,K.W., Albeiruti,A., Rowley,J.A., and Mooney,D.J.: Engineering growing tissues. *Proc.Natl.Acad.Sci.U.S.A* **99**:12025-12030, 2002.
63. Horwitz,E.M., Gordon,P.L., Koo,W.K., Marx,J.C., Neel,M.D., McNall,R.Y., Muul,L., and Hofmann,T.: Isolated allogeneic bone marrow-derived mesenchymal cells engraft and stimulate growth in children with osteogenesis imperfecta: Implications for cell therapy of bone. *Proc.Natl.Acad.Sci.U.S.A* **99**:8932-8937, 2002.
64. Moursi,A.M., Damsky,C.H., Lull,J., Zimmerman,D., Doty,S.B., Aota,S., and Globus,R.K.: Fibronectin regulates calvarial osteoblast differentiation. *J.Cell Sci.* **109**:1369-1380, 1996.

65. Dee,K.C., Rueger,D.C., Andersen,T.T., and Bizios,R.: Conditions which promote mineralization at the bone-implant interface: a model in vitro study. *Biomaterials* **17**:209-215, 1996.
66. Rezania,A. and Healy,K.E.: Biomimetic peptide surfaces that regulate adhesion, spreading, cytoskeletal organization, and mineralization of the matrix deposited by osteoblast-like cells. *Biotechnol.Prog.* **15**:19-32, 1999.
67. Eid,K., Chen,E., Griffith,L., and Glowacki,J.: Effect of RGD coating on osteocompatibility of PLGA-polymer disks in a rat tibial wound. *J.Biomed.Mater.Res.* **57**:224-231, 2001.
68. Lutolf,M.P., Weber,F.E., Schmoekel,H.G., Schense,J.C., Kohler,T., Muller,R., and Hubbell,J.A.: Repair of bone defects using synthetic mimetics of collagenous extracellular matrices. *Nat Biotechnol.* **21**:513-518, 2003.
69. Hynes,R.O.: Integrins: bidirectional, allosteric signaling machines. *Cell* **110**:673-687, 2002.
70. Grossmann,J.: Molecular mechanisms of “detachment-induced apoptosis—Anoikis”. *Apoptosis* **7**:247-260, 2002.
71. Giancotti,F.G. and Ruoslahti,E.: Integrin signaling. *Science* **285**:1028-1032, 1999.
72. Albelda,S.M.: Role of integrins and other cell adhesion molecules in tumor progression and metastasis. *Lab Invest* **68**:4-17, 1993.
73. Hubbell,J.A.: Bioactive biomaterials. *Curr.Opin.Biotechnol.* **10**:123-129, 1999.
74. Brash,J.L.: Exploiting the current paradigm of blood-material interactions for the rational design of blood-compatible materials. *J.Biomater.Sci.Polym.Ed* **11**:1135-1146, 2000.
75. Anderson,J.M.: Biological Responses to Materials. *Annual Review of Materials Research* **31**:81-110, 2001.
76. Young,B.R., Lambrecht,L.K., Albrecht,R.M., Mosher,D.F., Cooper,S.L.: Platelet-protein interactions at blood-polymer interfaces in the canine test model. *Trans. Am. Soc. Artif. Intern. Organs* **29**:442-447, 1983.
- 76a. Grinnell,F.: Fibroblast-collagen-matrix contraction: growth-factor signaling and mechanical loading. *Trends Cell Biol.* **10**:362-365, 2000.
77. Shen,M. and Horbett,T.A.: The effects of surface chemistry and adsorbed proteins on monocyte/macrophage adhesion to chemically modified polystyrene surfaces. *J.Biomed.Mater.Res.* **57**:336-345, 2001.

78. De Arcangelis,A. and Georges-Labousse,E.: Integrin and ECM functions- roles in vertebrate development. *Trends Genetics* **16**(9):389-395, 2000.
79. Ruoslahti,E. and Pierschbacher,M.D.: New perspectives in cell adhesion: RGD and integrins. *Science* **238**:491-497, 1987.
80. Nermut,M.V., Green,N.M., Eason,P., Yamada,S.S., and Yamada,K.M.: Electron microscopy and structural model of human fibronectin receptor. *EMBO J.* **7**:4093-4099, 1988.
81. LaFlamme,S.E., Akiyama,S.K., and Yamada,K.M.: Regulation of fibronectin receptor distribution. *J.Cell Biol.* **117**:437-447, 1992.
82. Vinogradova,O., Velyvis,A., Velyviene,A., Hu,B., Haas,T., Plow,E., and Qin,J.: A structural mechanism of integrin alpha(IIb)beta(3) "inside-out" activation as regulated by its cytoplasmic face. *Cell* **110**:587-597, 2002.
83. Takagi,J., Petre,B.M., Walz,T., and Springer,T.A.: Global conformational rearrangements in integrin extracellular domains in outside-in and inside-out signaling. *Cell* **110**:599-611, 2002.
84. Xiong,J.P., Stehle,T., Zhang,R., Joachimiak,A., Frech,M., Goodman,S.L., and Arnaout,M.A.: Crystal structure of the extracellular segment of integrin alpha(V)beta(3) complex with an Arg-Gly-Asp ligand. *Science* **296**:151-155, 2002.
85. Takagi,J., Strokovich,K., Springer,T.A., and Walz,T.: Structure of integrin alpha5beta1 in complex with fibronectin. *EMBO J.* **22**:4607-4615, 2003.
86. Menko,A.S. and Boettiger,D.: Occupation of the extracellular matrix receptor, integrin, is a control point for myogenic differentiation. *Cell* **51**:51-57, 1987.
87. Hynes,R.O.: Integrins: versatility, modulation, and signaling in cell adhesion. *Cell* **69**:11-25, 1992.
88. Burridge,K. and Chrzanowska-Wodnicka,M.: Focal adhesions, contractility, and signaling. *Annu.Rev.Cell Dev.Biol.* **12**:463-518, 1996.
89. Miyamoto,S., Teramoto,H., Coso,O.A., Gutkind,J.S., Burbelo,P.D., Akiyama,S.K., and Yamada,K.M.: Integrin function: molecular hierarchies of cytoskeletal and signaling molecules. *J.Cell Biol.* **131**:791-805, 1995.
90. Jockusch,B.M., Bubeck,P., Giehl,K., Kroemker,M., Moschner,J., Rothkegel,M., Rudiger,M., Schluter,K., Stanke,G., and Winkler,J.: The molecular architecture of focal adhesions. *Annu.Rev.Cell Dev.Biol.* **11**:379-416, 1995.

91. Kolega,J., Shure,M.S., Chen,W.T., and Young,N.D.: Rapid cellular translocation is related to close contacts formed between various cultured cells and their substrata. *J.Cell Sci.* **54**:23-34, 1982.
92. Sastry,S.K. and Burridge,K.: Focal adhesions: a nexus for intracellular signaling and cytoskeletal dynamics. *Exp.Cell Res.* **261**:25-36, 2000.
93. Geiger,B., Bershadsky,A., Pankov,R., and Yamada,K.M.: Transmembrane crosstalk between the extracellular matrix—cytoskeleton crosstalk. *Nat.Rev.Mol.Cell Biol.* **2**:793-805, 2001.
94. Johansson,S.: 3 Non-Collagenous Matrix Proteins, *In: Extracellular Matrix.* Ed. W.D.Comper. Harwood Academic Publishers, Netherlands, 1996.
95. Mosesson,M.W. and Umfleet,R.A.: The cold-insoluble globulin of human plasma. I. Purification, primary characterization, and relationship to fibrinogen and other cold- insoluble fraction components. *J.Biol.Chem.* **245**:5728-5736, 1970.
96. Hynes,R.O.: Fibronectins. Springer-Verlag, New York, 1990.
97. George,E.L., Georges-Labouesse,E.N., Patel-King,R.S., Rayburn,H., and Hynes,R.O.: Defects in mesoderm, neural tube and vascular development in mouse embryos lacking fibronectin. *Development* **119**:1079-1091, 1993.
98. Damsky,C.H., Moursi,A., Zhou,Y., Fisher,S.J., and Globus,R.K.: The solid state environment orchestrates embryonic development and tissue remodeling. *Kidney Int.* **51**:1427-1433, 1997.
99. Pierschbacher,M.D., Hayman,E.G., and Ruoslahti,E.: Location of the cell-attachment site in fibronectin with monoclonal antibodies and proteolytic fragments of the molecule. *Cell* **26**:259-267, 1981.
100. Alitalo,K., Hovi,T., and Vaheri,A.: Fibronectin is produced by human macrophages. *J.Exp.Med.* **151**:602-613, 1980.
101. Grinnell,F. and Feld,M.K.: Adsorption characteristics of plasma fibronectin in relationship to biological activity. *J.Biomed.Mater.Res.* **15**:363-381, 1981.
102. Grainger,D., Pavon-Djavid,G., Migonney,V., and Josefowicz,M.: Assessment of fibronectin conformation adsorbed to polytetrafluoroethylene surfaces from serum protein mixtures and correlation to support of cell attachment in culture. *J Biomater Sci Polym Ed.* **14**:973-988, 2003.
103. Sigal,G.B., Mrksich,M., and Whitesides,G.M.: Effect of Surface Wettability on the Adsorption of Proteins and Detergents. *J.Am.Chem.Soc.* **120**:3464-3473, 1998.

104. Scotchford,C.A., Ball,M.D., Winkelmann,M., Voros,J., Csucs,C., Brunette,D.M., Danuser,G., and Textor,M.: Chemically patterned, metal-oxide-based surfaces produced by photolithographic techniques for studying protein- and cell-interactions. II: Protein adsorption and early cell interactions. *Biomaterials* **24**:1147-1158, 2003.
105. Prime,K.L. and Whitesides,G.M.: Self-assembled organic monolayers: model systems for studying adsorption of proteins at surfaces. *Science* **252**:1164-1167, 1991.
106. Bergkvist,M., Carlsson,J., and Oscarsson,S.: Surface-dependent conformations of human plasma fibronectin adsorbed to silica, mica, and hydrophobic surfaces, studied with use of Atomic Force Microscopy. *J Biomed Mater Res.* **64A**:349-356, 2003.
107. Narasimhan,C. and Lai,C.S.: Conformational changes of plasma fibronectin detected upon adsorption to solid substrates: a spin-label study. *Biochemistry* **28**:5041-5046, 1989.
108. Pitt,W.G., Spiegelberg,S.H., and Cooper,S.L.: Adsorption of fibronectin to polyurethane surfaces: Fourier transform infrared spectroscopy studies., *In*: Proteins at Interfaces. Eds. T.A.Horbett and J.L.Brash. Washington, D.C., 1987, pp. 324-338.
109. Williams,E.C., Janmey,P.A., Ferry,J.D., and Mosher,D.F.: Conformational states of fibronectin. Effects of pH, ionic strength, and collagen binding. *J.Biol.Chem.* **257** :14973-14978, 1982.
110. Price,T.M., Rudee,M.L., Pierschbacher,M., and Ruoslahti,E.: Structure of fibronectin and its fragments in electron microscopy. *Eur.J.Biochem.* **129**:359-363, 1982.
111. Grinnell,F. and Feld,M.K.: Fibronectin adsorption on hydrophilic and hydrophobic surfaces detected by antibody binding and analyzed during cell adhesion in serum- containing medium. *J.Biol.Chem.* **257**:4888-4893, 1982.
112. Kowalczyńska,H.M., Nowak-Wyrzykowska,M., Dobkowski,J., Kolos,R., Kaminski,J., Makowska-Cynka,A., and Marciniak,E.: Adsorption characteristics of human plasma fibronectin in relationship to cell adhesion. *J Biomed Mater Res.* **61**:260-269, 2002.
113. Burmeister,J.S., Vraný,J.D., Reichert,W.M., and Truskey,G.A.: Effect of fibronectin amount and conformation on the strength of endothelial cell adhesion to HEMA/EMA copolymers. *J.Biomed.Mater.Res.* **30**:13-22, 1996.
114. Koenig,A.L., Gambillara,V., and Grainger,D.W.: Correlating fibronectin adsorption with endothelial cell adhesion and signaling on polymer substrates. *J Biomed Mater Res.* **64A**:20-37, 2003.

115. Garcia,A.J., Vega,M.D., and Boettiger,D.: Modulation of cell proliferation and differentiation through substrate- dependent changes in fibronectin conformation. *Mol.Biol.Cell* **10**:785-798, 1999.
- 115a. Stephansson,S.N., Byers,B.A., and Garcia,A.J.: Enhanced expression of the osteoblastic phenotype on substrates that modulate fibronectin conformation and integrin receptor binding. *Biomaterials* **23**:2527-2534, 2002.
116. Healy,K.E., Carson H.Thomas, Alireza Rezaia, Jung E.Kim, Patrick J.McKeown, Barbara Lom, and Philip E.Hockberger: Kinetics of bone cell organization and mineralization on materials with patterned surface chemistry. *Biomaterials* **17**:195-208, 1996.
117. Scotchford,C.A., Gilmore,C.P., Cooper,E., Leggett,G.J., and Downes,S.: Protein adsorption and human osteoblast-like cell attachment and growth on alkylthiol on gold self-assembled monolayers. *J.Biomed.Mater.Res.* **59**:84-99, 2002.
118. Hu,Y., Winn,S.R., Krajbich,I., and Hollinger,J.O.: Porous polymer scaffolds surface-modified with arginine-glycine-aspartic acid enhance bone cell attachment and differentiation in vitro. *J Biomed Mater Res.* **64A**:583-590, 2003.
119. Miao,H., Li,S., Hu,Y.L., Yuan,S., Zhao,Y., Chen,B.P., Puzon-McLaughlin,W., Tarui,T., Shyy,J.Y., Takada,Y., Usami,S., and Chien,S.: Differential regulation of Rho GTPases by beta1 and beta3 integrins: the role of an extracellular domain of integrin in intracellular signaling. *J Cell Sci.* **115**:2199-2206, 2002.
120. Gilbert,M., Giachelli,C.M., and Stayton,P.S.: Biomimetic peptides that engage specific integrin-dependent signaling pathways and bind to calcium phosphate surfaces. *J Biomed Mater Res.* **67A**:69-77, 2003.
121. Mostafavi-Pour,Z., Askari,J.A., Parkinson,S.J., Parker,P.J., Ng,T.T., and Humphries,M.J.: Integrin-specific signaling pathways controlling focal adhesion formation and cell migration. *J.Cell Biol.* **161**:155-167, 2003.

CHAPTER 3

QUANTITATIVE METHODS FOR ANALYSIS OF INTEGRIN BINDING AND FOCAL ADHESION FORMATION ON BIOMATERIAL SURFACES*

SUMMARY

Integrin binding and focal adhesion assembly are critical to cellular responses to biomaterial surfaces in biomedical and biotechnological applications. While immunostaining techniques to study focal adhesion assembly are well-established, a crucial need remains for quantitative methods for analyzing adhesive structures. We present simple yet robust approaches to quantify integrin binding and focal adhesion assembly on biomaterial surfaces. Integrin binding to fibronectin and a RGD-containing synthetic peptide was quantified by sequentially cross-linking integrin-ligand complexes via a water-soluble homo-bifunctional cross-linker, extracting bulk cellular components in detergent, and detecting bound integrins by ELISA. Focal adhesion components (vinculin, talin, α -actinin) localized to adhesion plaques were isolated from bulk cytoskeletal and cytoplasmic components by mechanical rupture at a plane close to the basal cell surface and quantified by Western blotting. These approaches represent simple and efficient methodologies to analyze structure-function relationships in cell-material interactions.

INTRODUCTION

Cell adhesion to biological and synthetic surfaces is critical to biomedical and biotechnological applications.¹⁻⁵ For example, adhesion to proteins adsorbed onto implant surfaces, including immunoglobulins, vitronectin, fibrinogen and fibronectin

* Keselowsky, B.G. and García, A.J. Biomaterials. (*in press*).

(FN), is important to host and cellular responses in biomaterial and tissue engineering applications.^{6,7} In many instances, cell adhesion to extracellular proteins is mediated by the integrin family of cell surface receptors. In addition to anchoring cells and supporting spreading and migration, integrins trigger signaling cascades that regulate cell survival, proliferation and differentiation.^{8,9} Upon binding their extracellular ligand, integrins cluster to form focal adhesions, complexes containing structural and signaling molecules that participate in both mechanical and signaling capacities crucial to the adhesion process.^{10,11} Over the last decade, it has become evident that the structure, composition, and distribution of focal adhesion components play central roles in the regulation of adhesive processes.¹² This is particularly important in the context of cell-biomaterial interactions as different materials elicit diverse adhesive interactions that modulate cell function.¹³⁻¹⁷ While immunostaining techniques to study focal adhesion assembly are well-established, a crucial need remains for quantitative methods for analyzing integrin binding and focal adhesion assembly. These methodologies are essential to structure-function analyses of cell-material interactions. In the present chapter, we describe two robust approaches to quantify integrin binding and focal adhesion assembly on biomaterial surfaces.

MATERIALS AND METHODS

Cells and reagents

Human plasma FN, Dulbecco's phosphate buffered saline (DPBS: 137 mM NaCl, 2.7 mM KCl, 4.3 mM Na₂HPO₄·7H₂O, 1.5 mM KH₂PO₄, 0.9 mM CaCl₂·2H₂O, 1 mM MgCl₂·6H₂O, pH 7.4) and other tissue culture reagents were obtained from Invitrogen

(Carlsbad, CA). Fetal bovine serum was purchased from Hyclone (Logan, UT). The cross-linkers bis(2-(sulfo-succinimidooxycarbonyloxy)ethyl)sulfone (sulfo-BSOCOES) and 3,3'-dithiobis(sulfosuccinimidylpropionate) (DTSSP) were acquired from Pierce Chemical (Rockford, IL). Monoclonal antibodies against paxillin (Z035) and vinculin (V284) were obtained from Zymed Laboratories (San Francisco, CA) and Upstate (Lake Placid, NY), respectively. Alexa Fluor 488-conjugated anti-rabbit and anti-mouse IgG antibodies were acquired from Molecular Probes (Eugene, OR), while biotinylated anti-rabbit IgG and alkaline phosphatase-conjugated anti-rabbit IgG antibodies were purchased from Jackson ImmunoResearch (West Grove, PA). Bovine serum albumin, Fibronectin-Like Engineered Protein Polymer (ProNectinTM), anti-talin (8D4) and anti- α -actinin (BM-75.2) monoclonal antibodies, alkaline phosphatase-conjugated anti-biotin antibody (BN-34), and all other chemical reagents were obtained from Sigma (St. Louis, MO).

MC3T3-E1 cells were obtained from the RIKEN Cell Bank (Tokyo, Japan). Prior to seeding on FN-coated substrates, MC3T3-E1 cells were maintained in α -modified Eagle's medium supplemented with 10% fetal bovine serum and 1% penicillin-streptomycin and passaged every 2 days using standard techniques.

Integrin binding analysis

Tissue culture-treated polystyrene 48-well plates were coated with a range of coating concentrations of either FN or ProNectinTM for 30 minutes and then blocked in 1% heat denatured-BSA (hd-BSA) for 30 minutes. Cells were detached from their

culture dishes with 0.5% trypsin + 0.53 mM EDTA for 3 min and resuspended in serum-containing media. After washing and resuspending in DPBS + 2 mM dextrose, cells were seeded onto substrates at 500 cells/mm² under serum-free conditions (2 mM dextrose in DPBS) for 1 hour. Sulfo-BSOCOES or DTSSP (in cold DPBS, 1mM final concentration) was then added for 30 minutes to cross-link integrins to their bound ligand. Unreacted cross-linker was quenched for 10 minutes by the addition of 50 mM Tris in 2 mM dextrose-DPBS. Uncross-linked cellular components were then extracted in 0.1% SDS + 350 µg/ml phenylmethylsulfonyl fluoride (PMSF) in cold DPBS.

Cross-linked integrins were quantified by ELISA. After rinsing three times with PBS, samples were incubated in blocking buffer (5% serum in DPBS) for 1 hour, and cross-linked integrins were probed with integrin-specific primary antibodies (2.5 µg/mL) in blocking buffer for 1 hour at 37°C. After washing, samples were incubated in alkaline phosphatase-conjugated secondary antibody (0.6 µg/mL) in blocking buffer for 1 hour at 37°C. After washing in DPBS and diethanolamine buffer (10 mM diethanolamine, 0.5 mM MgCl₂, pH 9.5), 5-methyl umbelliferyl phosphate (60 µg/ml in diethanolamine buffer + 50 mM Na₂CO₃, pH 9.5) was incubated for 45 minutes at 37°C in the dark. Reaction supernatants were transferred to clean black 96-well plates and the resulting fluorescence (365 nm excitation/450 nm emission) was read in a HTS 7000 Plus BioAssay microwell plate reader (Perkin Elmer, Norwalk, CT). For each sample, relative fluorescence intensity, which is proportional to the amount of antibody bound, was determined as a function of ligand density. In parallel samples, cross-linked integrins were visualized via immunofluorescence staining by incubating in Alexa Fluor 488-conjugated secondary antibody (10 µg/mL) instead of alkaline phosphatase-conjugated

antibody. Additional samples were processed for standard immunofluorescence staining for comparison to cross-linked samples. Cells were permeabilized for 5 min in 0.5% Triton X-100 in 50 mM Tris (pH 6.8), 50 mM NaCl, 150 mM sucrose, 3 mM MgCl₂ supplemented with protease inhibitors (10 µg/mL PMSF, leupeptin, and aprotinin) and then fixed in cold 3.6% formaldehyde (in DPBS) for 5 min. After blocking with 5% serum, cultures were incubated in primary and secondary antibodies for integrins as described above.

Focal adhesion assembly analysis

Tissue culture-treated polystyrene 35 mm dishes were coated with either 0.1 or 10 µg/mL FN (corresponding to 0.3 ng/cm² and 320 ng/cm² adsorbed FN) for 30 min and blocked with 1% hd-BSA for 30 min. Cells were detached as described above and seeded onto FN-coated substrates at 400 cells/mm² in 10% serum for 1 hour. After rinsing in DPBS, buffer was aspirated from cell cultures and a dry nitrocellulose sheet (PROTRAN BA85, Schleicher & Schuell) was overlaid onto the cells for 1 min. Cells were then cleaved by rapidly by lifting the nitrocellulose sheet with tweezers, and cleaved surfaces were rinsed in DPBS with protease inhibitors (10 µg/mL PMSF, leupeptin, and aprotinin) and scraped in Laemmli sample buffer (100 µl). Recovered proteins were analyzed by Western blotting as detailed previously.¹⁸ DNA was solubilized from corresponding nitrocellulose sheets and quantified by SYBR Green (Molecular Probes, OR) incorporation to normalize for cell numbers. Parallel plates were cleaved and examined by immunofluorescence staining as described above to corroborate Western

blotting analyses. For comparison with standard techniques, cells were permeabilized in Triton X-100 buffer, fixed in formaldehyde, and immunostained for focal adhesion proteins as detailed above.

RESULTS

Integrin binding analysis

Integrin binding to adsorbed adhesive proteins (FN or ProNectin™) was quantified using a modification of the cross-linking/extraction biochemical method developed by our group.^{13,18} This scheme (**Fig 3.1A**) uses a water-soluble, cell membrane-impermeable, homobifunctional cross-linker (equivalent results have been obtained for sulfo-BSOCOES [13Å spacer arm] and DTSSP [12Å spacer arm]) to couple primary amine groups in the integrin and adhesive ligand. Taking advantage of the fact that most adhesive matrix proteins, including FN, are resistant to mild detergent extraction, the bulk of cell components (including unbound receptors) is then extracted with 0.1% SDS, leaving behind matrix proteins adsorbed to the substrate and their associated integrins. Bound integrins can then be easily visualized by immunofluorescence staining or quantified by ELISA as shown here. Alternatively, bound integrins can be recovered by cleaving the cross-linking and quantified by Western blotting.^{13,18} Control experiments have previously demonstrated that these chemical reagents will specifically cross-link bound integrins. Only FN-binding integrins are detected when cells are seeded on FN, while only laminin-binding integrins are detected when cells are plated on laminin.¹⁹ Furthermore, only activated integrins, but not inactive

receptors, are cross-linked to FN,²⁰ demonstrating that the cross-linking is specific for bound integrins.

Immunofluorescence staining for integrin subunit α_5 on cells plated on FN-coated substrates was performed for samples prepared by conventional (TritonX-100 extracted/formaldehyde fixed) and cross-linking/extraction protocols (**Fig. 3.1B**). This analysis showed equivalent localization of $\alpha_5\beta_1$ integrin to focal adhesions for both treatments, demonstrating that the cross-linking/extraction method does not alter integrin distribution. Differences in staining intensity resulted from differences in antibody accessibility to the integrin. A clear advantage of the cross-linking/extraction method for immunofluorescence staining is the absence of non-specific nuclear staining, allowing visualization of receptor binding across the entire spread area.

In order to demonstrate the ability of this technique to quantify integrin binding, the relative levels of $\alpha_5\beta_1$ and $\alpha_v\beta_3$ integrin bound to adsorbed FN and ProNectinTM were measured by ELISA (**Fig. 3.2**). Both integrins bind to the RGD motif in the 10th type III repeat of FN, but $\alpha_5\beta_1$ binding also requires the PHSRN synergy site in the 9th type III repeat.^{21,22} ProNectinTM is a protein polymer presenting multiple RGD loop repeats that supports $\alpha_v\beta_3$, but not $\alpha_5\beta_1$, binding.²² Dose-dependent increases in $\alpha_5\beta_1$ binding to adsorbed FN were detected, while binding of $\alpha_v\beta_3$ was minimal. This result is consistent with antibody-blocking experiments demonstrating that $\alpha_5\beta_1$ provides the dominant adhesion mechanism in this cell model.¹⁴ In contrast, ProNectinTM-coated substrates supported high levels of $\alpha_v\beta_3$ integrin binding and background levels of $\alpha_5\beta_1$ integrin binding, in accordance with the requirement of the PHSRN site for $\alpha_5\beta_1$ integrin binding. Notably, dose-dependent increases in integrin binding follow the expected hyperbolic

relationship for a simple receptor-ligand interaction, thereby allowing estimation of effective binding affinity. These measurements can be used for rigorous comparisons among experimental treatments. For example, we have recently shown that changes in the structure of adsorbed FN modulate integrin binding affinity.¹⁴ Taken together, these results demonstrate the ability of this cross-linking/extraction technique to quantify integrin binding to adsorbed extracellular matrix proteins.

Focal adhesion assembly analysis

Quantification of focal adhesion components localized to adhesive plaques requires the isolation of these adhesive cell structures from bulk cellular components. We have modified the wet-cleaving technique developed by Brands and Feltkamp²³ to expose the cytoplasm of adherent cells in order to quantify focal adhesion assembly (**Fig. 3.3A**). A nitrocellulose sheet is overlaid onto cells to irreversibly bind protein and membrane components on the apical surface. After a specified overlay time, the nitrocellulose sheet is rapidly removed to mechanically rupture the cells, leaving basal cell structures anchored to the underlying extracellular matrix. These components can then be visualized by immunostaining or recovered for biochemical analyses. By controlling the cleaving conditions (overlay time and liquid volume present at the cell/membrane interface), cells can be ruptured at different planes relative to the underlying substrate. Using a dry nitrocellulose sheet and 1-min overlay time, spread cells are cleaved at a rupture point close to the adhesive substrate. These cleaving conditions produced similar results in spread fibroblasts (data not shown), but may have to be modified for other cell types or spreading conditions.

Immunostaining for vinculin, a marker of mature focal adhesions, demonstrated equivalent distribution and intensities of vinculin recruitment for samples prepared by conventional (Triton X-100 extraction/formaldehyde fixation) and wet-cleaving approaches (**Fig. 3.3B**). Similar results were obtained for other focal adhesion components, including integrin, talin, and α -actinin. These results demonstrate that the wet-cleaving technique isolates basal membranes containing focal adhesion structures without introducing mechanical/staining artifacts. In order to demonstrate the ability of this technique to quantify focal adhesion assembly, cells were plated on substrates coated with low or high FN densities, wet-cleaved, and immunostained for focal adhesion components (**Fig. 3.4A**). As expected, higher densities of vinculin, talin, and β_1 integrin subunit were detected on high FN substrates than on low FN substrates. These results were confirmed by Western blotting analyses on cleaved cells showing 2-, 1.3-, 5-, and 1.4-fold increases in vinculin, talin, β_1 integrin subunit, and α -actinin localization on high FN compared to low FN substrates, respectively (**Fig. 3.4B**). Taken together, these results validate this wet-cleaving protocol to quantify focal adhesion assembly.

DISCUSSION

Quantification of integrin binding and focal adhesion assembly is critical to structure-function analyses of cell-material interactions. While immunostaining techniques provide relatively easy approaches to visualize integrin binding and focal plaque assembly, these approaches are limited in their ability to quantify adhesive structures. In the present paper, we describe two robust yet simple protocols for the visualization and quantification of adhesive structures. These approaches provide

sensitive and reproducible measurements that can be used to examine functional relationships in cell adhesive interactions as shown here and other reports from our group.^{14,24} Furthermore, these techniques are applicable to analyses on a broad range of material substrates.

The cross-linking/extraction protocol was originally developed by Boettiger and colleagues to visualize bound integrins¹⁹ and subsequently modified by García and Boettiger to quantify integrin binding via Western blotting.^{13,18} In the present work, we extend this approach to ELISA-based detection to provide rapid, high-throughput, simple and sensitive detection of integrin binding. Furthermore, we demonstrate that this technique can be used to quantify integrins bound to natural (FN) and synthetic (ProNectinTM) ligands. This detection protocol offers considerable advantages over quantitative image analysis-based microscopy methods, which are significantly more time- and skill-intensive and require specialized equipment. Finally, it is important to note that this technique relies on a labile cross-linker of fixed spacer arm and chemical reactivity (primary amines) and, while we have demonstrated applicability to several integrin-ligand pairs, application of this technique to other adhesive systems requires careful validation. We strongly recommend using integrin binding to FN as a positive control or standard for comparison.

We also describe a modified wet-cleaving technique to quantify focal adhesion assembly. This method relies on mechanically rupturing the cell to isolate the basal cell membrane and associated focal adhesions from bulk cell components. To quantify focal adhesion components, Western blotting was chosen instead of ELISA-based detection methods to avoid antibody accessibility issues for components assembled into focal

plaque structures. This technique is straightforward compared to image-based microscopy analyses which involve considerable time and computational costs and sophisticated experimental systems. The wet-cleaving approach contrasts with conventional biochemical techniques that rely on sequential extraction with detergents of varying strength to segregate cytoskeletal components from the cytosolic fraction.²⁵ In fact, Plopper and Ingber demonstrated that wet-cleaving methods are more effective/selective than detergent extraction approaches in isolating focal adhesion components from bulk cell constituents.²⁶ These investigators also described a combined biochemical and mechanical isolation technique using ligand-coated magnetic microbeads.²⁶ This combined approach, however, is more time- and skill-intensive and is not easily applied to different material formulations. In contrast, the modified wet-cleaving method described here can be used on a variety of substrates. Finally, we recommend that this technique be used in combination with immunostaining to provide additional spatial information on focal adhesion distribution as well as experimental validation of the results.

ACKNOWLEDGMENT

This work was funded by the Whitaker Foundation and the Georgia Tech/Emory NSF ERC on the Engineering of Living Tissues (EEC-9731643). B.G.K. was supported by an NSF Graduate Research Fellowship.

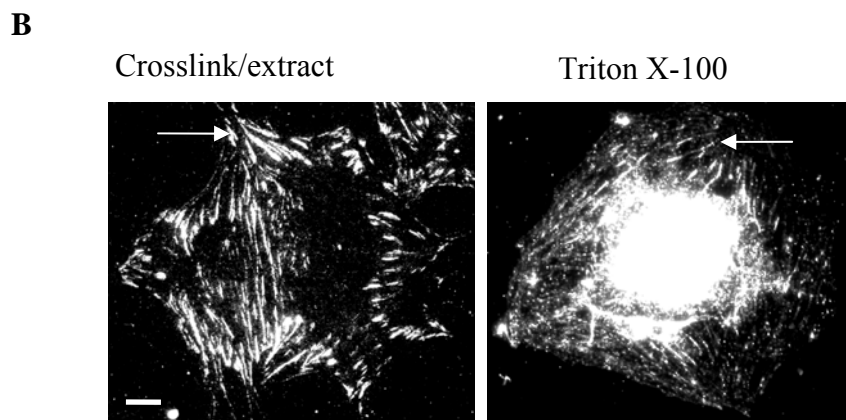
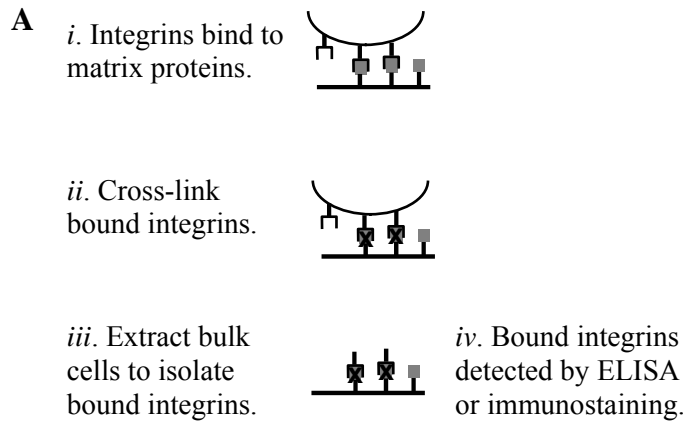


Figure 3.1. Analysis of integrin binding via cross-linking/extraction method. (A) Cross-linking/extraction scheme consisting of (i) integrin binding to adsorbed adhesive protein, (ii) cross-linking of bound integrins to the underlying matrix and (iii) detergent extraction to isolate bound integrins for (iv) detection by immunostaining or ELISA. (B) Comparison of cross-linking/extraction method to Triton X-100 permeabilization, showing similar $\alpha_5\beta_1$ integrin localization to focal adhesions (arrows), as well as demonstrating the greater accessibility of bound integrins to immunostaining with the cross-linking/extraction method. Scale bar (left panel) indicates 10 μm .

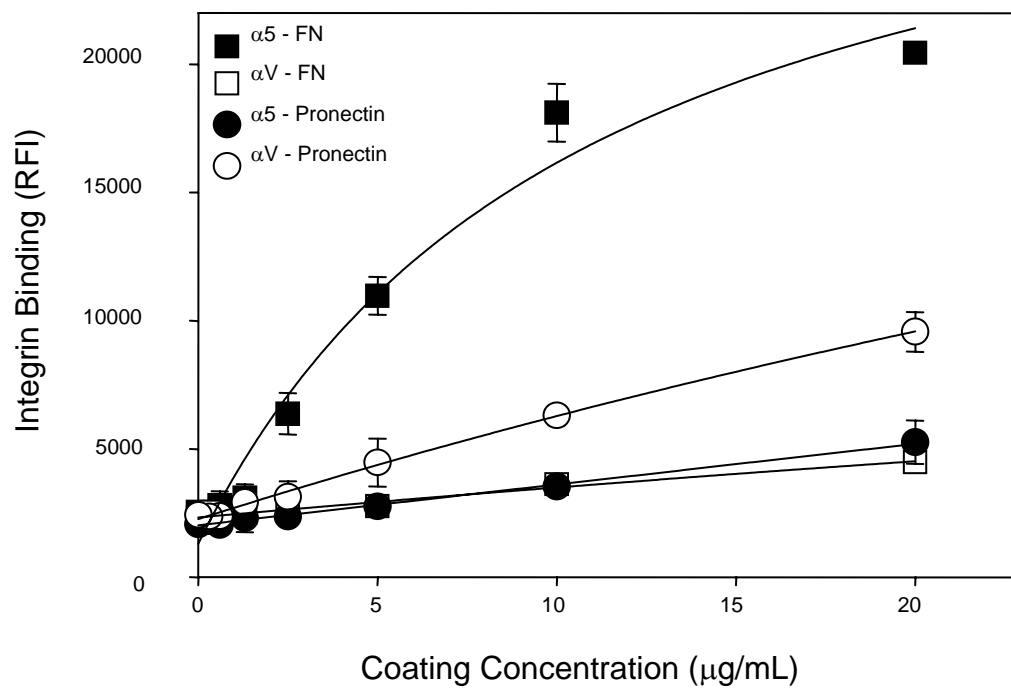
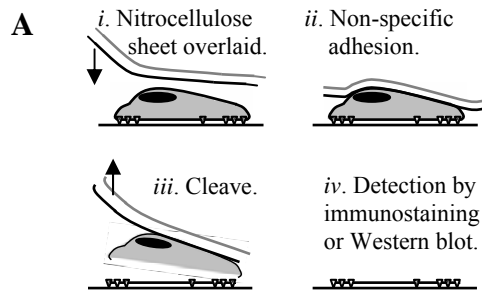


Figure 3.2. Quantitative analysis of integrin binding via cross-linking/extraction method. Bound integrins $\alpha_5\beta_1$ and $\alpha_V\beta_3$ plotted as a function of ligand coating concentration (FN or ProNectinTM), showing specificity for bound integrins and dose-dependent increases following the expected hyperbolic relationship.



B

Wet-cleaved

Triton X-100

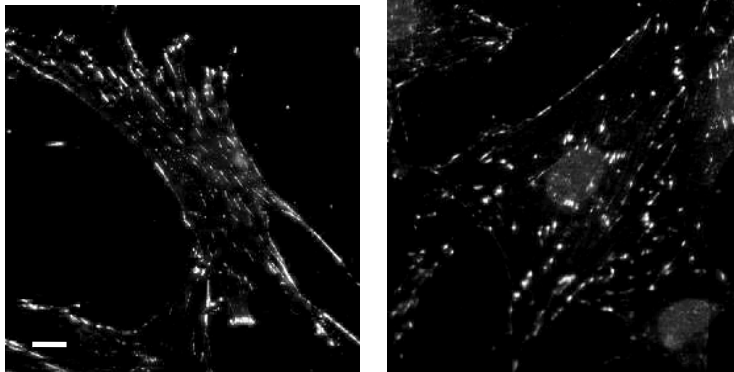
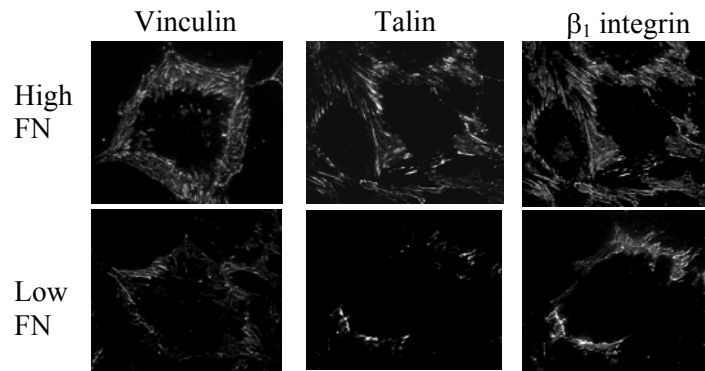


Figure 3.3. Analysis of focal adhesion formation by wet-cleaving method. (A) Wet-cleaving scheme, consisting of (*i*) overlaying nitrocellulose onto adherent cells, (*ii*) non-specific adhesion of membrane-bound proteins to the nitrocellulose, (*iii*) mechanical cleaving of cells in order to isolate focal adhesion complexes in a plane close to the underlying substrate and (*iv*) detection by immunostaining or Western blotting. (B) Comparison of wet-cleaving method to Triton X-100 permeabilization, showing similar localization of vinculin to focal adhesions (arrows). Scale bar (left panel) indicates 10 μm .

A



B

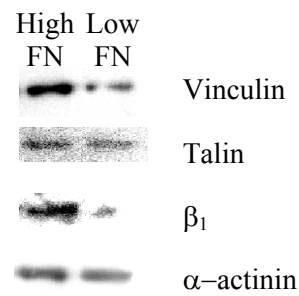


Figure 3.4. Quantification of focal adhesion assembly by wet-cleaving method, showing differences in vinculin, talin, β_1 integrin and α -actinin localization to focal plaques between low and high FN densities by (A) immunostaining and (B) Western blotting.

REFERENCES

1. Anderson, J.M.: Biological Responses to Materials. *Annual Review of Materials Research* **31**:81-110, 2001.
2. Hubbell, J.A.: Bioactive biomaterials. *Curr. Opin. Biotechnol.* **10**:123-129, 1999.
3. Garcia, A.J. and Keselowsky, B.G.: Biomimetic surfaces for control of cell adhesion to facilitate bone formation. *Crit Rev. Eukaryot. Gene Expr.* **12**:151-162, 2002.
4. Gorbet, M.B. and Sefton, M.V.: Leukocyte activation and leukocyte procoagulant activities after blood contact with polystyrene and polyethylene glycol-immobilized polystyrene beads. *J. Lab Clin. Med.* **137**:345-355, 2001.
5. Shen, M. and Horbett, T.A.: The effects of surface chemistry and adsorbed proteins on monocyte/macrophage adhesion to chemically modified polystyrene surfaces. *J. Biomed. Mater. Res.* **57**:336-345, 2001.
6. Anderson, J.M., Ziats, N.P., Azeez, A., Brunstedt, M.R., Stack, S., and Bonfield, T.L.: Protein adsorption and macrophage activation on polydimethylsiloxane and silicone rubber. *J. Biomater. Sci. Polym. Ed* **7**:159-169, 1995.
7. Hynes, R.O.: Integrins: bidirectional, allosteric signaling machines. *Cell* **110**:673-687, 2002.
8. Giancotti, F.G. and Ruoslahti, E.: Integrin signaling. *Science* **285**:1028-1032, 1999.
9. Sastry, S.K. and Burridge, K.: Focal adhesions: a nexus for intracellular signaling and cytoskeletal dynamics. *Exp. Cell Res.* **261**:25-36, 2000.
10. Geiger, B., Bershadsky, A., Pankov, R., and Yamada, K.M.: Transmembrane crosstalk between the extracellular matrix--cytoskeleton crosstalk. *Nat. Rev. Mol. Cell Biol.* **2**:793-805, 2001.
11. Geiger, B. and Bershadsky, A.: Assembly and mechanosensory function of focal contacts. *Curr. Opin. Cell Biol.* **13**:584-592, 2001.
12. Garcia, A.J., Vega, M.D., and Boettiger, D.: Modulation of cell proliferation and differentiation through substrate- dependent changes in fibronectin conformation. *Mol. Biol. Cell* **10**:785-798, 1999.
13. Keselowsky, B.G., Collard, D.M., and Garcia, A.J.: Surface chemistry modulates fibronectin conformation and directs integrin binding and specificity to control cell adhesion. *J. Biomed. Mater. Res.* **66A**:247-259, 2003.

14. Tziampazis,E., Kohn,J., and Moghe,P.V.: PEG-variant biomaterials as selectively adhesive protein templates: model surfaces for controlled cell adhesion and migration. *Biomaterials* **21**:511-520, 2000.
15. Allen,L.T., Fox,E.J., Blute,I., Kelly,Z.D., Rochev,Y., Keenan,A.K., Dawson,K.A., and Gallagher,W.M.: Interaction of soft condensed materials with living cells: phenotype/transcriptome correlations for the hydrophobic effect. *Proc.Natl.Acad.Sci.U.S.A* **100**:6331-6336, 2003.
16. Brodbeck,W.G., Patel,J., Voskerician,G., Christenson,E., Shive,M.S., Nakayama,Y., Matsuda,T., Ziats,N.P., and Anderson,J.M.: Biomaterial adherent macrophage apoptosis is increased by hydrophilic and anionic substrates in vivo. *Proc.Natl.Acad.Sci.U.S.A* **99**:10287-10292, 2003.
17. Garcia,A.J. and Boettiger,D.: Integrin-fibronectin interactions at the cell-material interface: initial integrin binding and signaling. *Biomaterials* **20**:2427-2433, 1999.
18. Enomoto-Iwamoto,M., Menko,A.S., Philp,N., and Boettiger,D.: Evaluation of integrin molecules involved in substrate adhesion. *Cell Adhes.Commun.* **1**:191-202, 1993.
19. Garcia,A.J., Takagi,J., and Boettiger,D.: Two-stage activation for alpha5beta1 integrin binding to surface- adsorbed fibronectin. *J.Biol.Chem.* **273**:34710-34715, 1998.
20. Aota,S., Nomizu,M., and Yamada,K.M.: The short amino acid sequence Pro-His-Ser-Arg-Asn in human fibronectin enhances cell-adhesive function. *J.Biol.Chem.* **269**:24756-24761, 1994.
21. Garcia,A.J., Schwarzbauer,J.E., and Boettiger,D.: Distinct activation states of alpha5beta1 integrin show differential binding to RGD and synergy domains of fibronectin. *Biochemistry* **41**:9063-9069, 2002.
22. Brands,R. and Feltkamp,C.A.: Wet cleaving of cells: a method to introduce macromolecules into the cytoplasm. Application for immunolocalization of cytosol-exposed antigens. *Exp.Cell Res.* **176**:309-318, 1988.
23. Keselowsky,B.G., Collard,D.M., and Garcia,A.J.: Surface chemistry modulates focal adhesion composition and signaling through changes in integrin binding. *Biomaterials* (in press).
24. Haimovich,B., Aneskievich,B.J., and Boettiger,D.: Cellular partitioning of beta-1 integrins and their phosphorylated forms is altered after transformation by Rous sarcoma virus or treatment with cytochalasin D. *Cell Regul.* **2**:271-283, 1991.
25. Plopper,G. and Ingber,D.E.: Rapid induction and isolation of focal adhesion complexes. *Biochem.Biophys.Res.Commun.* **193**:571-578, 1993.

CHAPTER 4

SURFACE CHEMISTRY MODULATES FIBRONECTIN CONFORMATION AND DIRECTS INTEGRIN BINDING AND SPECIFICITY TO CONTROL CELL ADHESION*

SUMMARY

Integrin-mediated cell adhesion to proteins adsorbed onto synthetic surfaces anchors cells and triggers signals that direct cell function. In the case of fibronectin (FN), adsorption onto substrates of varying properties alters its conformation/structure and its ability to support cell adhesion. In the present study, self-assembled monolayers (SAMs) of alkanethiols on gold were used as model surfaces to investigate the effects of surface chemistry on FN adsorption, integrin binding and cell adhesion. SAMs presenting terminal CH₃, OH, COOH and NH₂ functionalities modulated adsorbed FN conformation as determined through differences in the binding affinities of monoclonal antibodies raised against the central cell-binding domain (OH > COOH = NH₂ > CH₃). Binding of $\alpha_5\beta_1$ integrin to adsorbed FN was controlled by SAM surface chemistry in a manner consistent with antibody binding (OH > COOH = NH₂ > CH₃), while α_v integrin binding followed the trend: COOH >> OH = NH₂ = CH₃, demonstrating $\alpha_5\beta_1$ integrin specificity for FN adsorbed onto the NH₂ and OH SAMs. Cell adhesion strength to FN-coated SAMs correlated with $\alpha_5\beta_1$ integrin binding (OH > COOH = NH₂ > CH₃), and experiments with function-perturbing antibodies demonstrated that this receptor provides the dominant adhesion mechanism in this cell model. This work establishes an experimental framework to analyze adhesive mechanisms controlling cell-surface interactions and provides a general strategy of surface-directed control of adsorbed

* Keselowsky, B.G., Collard, D.M. and García, A.J. J Biomed Mat Res. 66A:247-259. (2003).

protein activity to manipulate cell function in biomaterial and biotechnological applications.

INTRODUCTION

Cell adhesion to synthetic surfaces is critical to numerous biomedical and biotechnological applications.^{1,2} Cell adhesion to proteins adsorbed onto implant surfaces is particularly important to host responses in biomaterial and tissue engineering applications.^{1,3,4} Many proteins, including immunoglobulins, vitronectin, fibrinogen and fibronectin (FN), adsorb onto implant surfaces immediately upon contact with physiological fluids and modulate subsequent inflammatory responses.⁵⁻⁷ For example, adsorbed adhesive proteins mediate the attachment and activation of neutrophils, macrophages and other inflammatory cells.^{8,9} For *in vitro* applications such as tissue-engineered constructs, bioreactors and cell culture supports, cell adhesion to pre-adsorbed proteins, proteins adsorbed from serum-containing media, endogenous proteins secreted by the cells, or engineered bioadhesive motifs, provides mechanical coupling to the underlying substrate and triggers signals that direct subsequent cellular responses including proliferation and differentiation.¹⁰⁻¹² Consequently the engineering of surfaces to control cell adhesion represents an active area of biomaterials research.

Because of the central role of protein adsorption in inflammation, clotting and cell adhesion, extensive research efforts have focused on the analysis of protein adsorption to synthetic surfaces. These studies have shown that the type, quantity and conformation (activity) of adsorbed proteins are influenced by the underlying substrate. Surface properties that influence protein adsorption and subsequent cell adhesion include surface

energy, roughness and chemistry.¹³⁻¹⁸ For example, FN adsorption to different surfaces alters the structure of the protein and influences cell adhesion, spreading and migration.^{13,19,20} Although these studies have provided insights into the relationships between surface properties and protein adsorption, many of these experimental systems suffer either from a lack of surface homogeneity or indeterminable surface properties. For instance, polymeric surfaces can undergo conformational rearrangements in response to environmental conditions and can exhibit differences in surface roughness and topology depending on processing or surface modifications.^{21,22} These factors can obscure correlations between biological markers (e.g. protein adsorption, cell spreading) and surface properties, thus complicating interpretation of these fundamental interactions. To address these limitations, recent work has focused on model substrates with well-controlled properties.^{23,24,60} In particular, self-assembled monolayers (SAMs) of alkanethiols on gold have provided a useful model system to systematically investigate the effects of surface chemistry without altering other surface properties such as roughness. Long-chain, functionally-terminated alkanethiols ($\text{HS}-(\text{CH}_2)_n\text{-X}$, $n \geq 10$) adsorb from solution onto gold surfaces through gold-sulfur coordination at the chain head and the alkyl chains pack together to form stable, well-packed and ordered monolayers.²⁵⁻²⁷ Once assembled, the end group X comprises a uniform interface of designated surface chemistry (**Figure 4.1A**). SAMs of alkanethiols on gold, therefore, represent a versatile and robust model system to study protein adsorption and cell adhesion.

Recent studies using alkanethiol SAMs have demonstrated that surface chemistry can modulate cell adhesion, spreading and adhesion strength.^{15,28-32} However, the

underlying mechanisms controlling these cell-protein-surface interactions remain poorly understood, especially in terms of the adhesion receptors mediating the observed cellular responses. A fundamental understanding of these adhesive interactions is critical to the rational design of surfaces, as recent work has shown that modulation of specific adhesive interactions directs cell signaling to control higher order cellular programs such as proliferation and differentiation.^{33,34}

Cell adhesion to extracellular matrix proteins is primarily mediated by the integrin family of cell-surface receptors.¹⁰ Integrins not only anchor cells, supporting cell spreading and migration, but also trigger signals that regulate survival, proliferation and differentiation.^{33,35-40} In the present work, using SAMs presenting well-defined chemistries, we demonstrate that surface-dependent conformational differences in adsorbed FN modulate integrin binding to potentiate cell adhesion. These results contribute to our understanding of mechanisms controlling cell-surface interactions.

MATERIALS AND METHODS

Reagents

Human plasma FN and other tissue culture reagents were obtained from Life Technologies (Grand Island, NY). Fetal bovine serum was purchased from Hyclone (Logan, UT). Bovine serum albumin, 5-methyl umbelliferyl phosphate, and all other chemical reagents were obtained from Sigma Chemical (St. Louis, MO). Bis(2-(sulfosuccinimidooxycarbonyloxy)ethyl)sulfone (sulfo-BSOCOES) cross-linker was purchased from Pierce Chemical (Rockford, IL). Mouse monoclonal HFN7.1 and MAB88916 clone 3E3 antibodies directed against human plasma FN were obtained from

the Developmental Studies Hybridoma Bank (Iowa City, IA) and Chemicon (Temecula, CA), respectively. Rabbit polyclonal antibodies against murine integrin subunits were purchased from Chemicon. Calcein-AM and Alexa Fluor 488-conjugated goat anti-rabbit IgG antibody were acquired from Molecular Probes (Eugene, OR), while alkaline phosphatase-conjugated donkey anti-rabbit IgG antibody was purchased from Jackson ImmunoResearch (West Grove, PA). Bolton-Hunter Reagent for FN iodination was purchased from NEN Life Science Products (Boston, MA).

Alkanethiols and Self-Assembled Monolayers

Alkanethiols 1-dodecanethiol ($\text{CH}_3\text{-(CH}_2\text{)}_{11}\text{-SH}$), 11-mercapto-1-undecanol ($\text{HO-(CH}_2\text{)}_{11}\text{-SH}$) and 11-mercaptoundecanoic acid ($\text{HOOC-(CH}_2\text{)}_{10}\text{-SH}$) were purchased from Aldrich Chemical (Milwaukee, WI) and used as received. The amine-terminated alkanethiol, 12-amino-1-mercaptododecane ($\text{H}_2\text{N-(CH}_2\text{)}_{12}\text{-SH}$) was synthesized and purified following the scheme of Sayre and Collard⁴¹, and validated by ¹H NMR. Assembled SAMs of their respective alkanethiols are referred to hereafter as CH_3 , OH, COOH and NH_2 SAMs, respectively. Gold-coated glass coverslips were used as SAM substrates for SAM characterization, FN adsorption studies, and immunofluorescence staining of integrins. Gold-coated glass chamber slides (16-well Lab-Tek Chamber Slides, Nalge Nunc International, Naperville, IL) were used as SAM substrates for FN conformation, integrin binding quantification, and cell adhesion studies. Both gold-coated substrates were prepared by sequential deposition of optically transparent films of titanium (10 nm) and gold (20 nm) onto clean glass supports. An electron beam evaporator (CVC Products/Veeco, Rochester, NY) was used for metal deposition at a

chamber base-pressure between $1-2 \times 10^{-6}$ torr with a deposition rate of $2 \text{ \AA}/\text{second}$. Freshly prepared gold surfaces were immersed in ethanolic alkanethiol solutions (1 mM in absolute ethanol), and SAMs were allowed to assemble for 12 hours. Before use, SAMs were rinsed in ethanol, dried with N_2 , and allowed to equilibrate in Dulbecco's phosphate buffered saline (DPBS: 137 mM NaCl, 2.7 mM KCl, 4.3 mM $\text{Na}_2\text{HPO}_4 \cdot 7\text{H}_2\text{O}$, 1.5 mM KH_2PO_4 , 0.9 mM $\text{CaCl}_2 \cdot 2\text{H}_2\text{O}$, 1 mM $\text{MgCl}_2 \cdot 6\text{H}_2\text{O}$, pH = 7.4) for 15 minutes prior to incubation in FN solutions.

Surfaces were characterized by contact angle and X-ray photoelectron spectroscopy (XPS) measurements. Ambient air-water-substrate contact angle measurements (5 μL pure, de-ionized H_2O) were taken with a Rame-Hart (Mountain Lakes, NJ) model # 100-00 goniometer fitted with a digital camera and analyzed using in-house image analysis software. Multi-angle XPS data was obtained at 30° and 70° , measured from the plane of the substrate, using a PHI Model ESCA 1600 system operating below 5×10^{-9} torr with a 350 W monochromatic $\text{Al}_{k\alpha}$ source of 1486.7 eV. Electron pass energy of 11.75 eV was used to analyze the regions of interest and curve fitting was performed on each spectral region to calculate atomic percentages.

FN Adsorption to SAMs

FN adsorption onto SAMs was quantified as a function of FN coating concentration using ^{125}I -FN. FN was iodinated with the Bolton-Hunter Reagent as described previously.⁴² Briefly, the Bolton-Hunter Reagent benzene solvent was evaporated with a gentle stream of N_2 and 100 μg FN (10 $\mu\text{g}/\mu\text{l}$ in 0.1 M sodium borate, pH = 8.5) was added to the reaction vessel and incubated overnight at 4°C . The coupling

reaction was stopped with 50 μ l of 0.2 M glycine in 0.1 M sodium borate (pH = 8.5). Labeled FN (125 I-FN) was separated from glycine conjugate and hydrolysis products by size exclusion chromatography in a Sephadex G-25 column (Sephadex column was blocked in 1% bovine serum albumin overnight prior to use). Fractions were collected and examined for radioactive counts. Fractions containing 125 I-FN were pooled and stored at 4°C. Specific activity (1.5×10^6 cpm/ μ g) of 125 I-FN was determined using a COBRA II Auto Gamma counter (Packard Bioscience, Meriden, CT), in conjunction with the NanoOrange Protein Quantification Kit (Molecular Probes). Control adsorption experiments with different ratios of labeled to unlabeled FN demonstrated that the iodination procedure did not alter FN adsorption behavior.

SAMs were coated for 30 minutes at room temperature with 125 I-FN mixed with unlabeled FN and diluted in Dulbecco's phosphate-buffered saline (DPBS) to a range (1-20 μ g/ml) of coating concentrations and subsequently blocked for 30 minutes in 1% heat-denatured bovine serum albumin (hd-BSA). Adsorbed 125 I-FN was quantified and radioactive counts (cpm) were converted to adsorbed FN surface densities (ng/cm²).

FN Conformation on SAMs

The conformation of FN adsorbed onto SAMs was examined over a range of FN surface densities using monoclonal antibodies, 3E3 and HFN7.1, in a normalized enzyme-linked immunosorbent assay (ELISA).³³ SAMs were coated with FN for 30 minutes, blocked in 1% hd-BSA for 30 minutes, and incubated with FN-specific antibodies (3E3: 1/4000 dilution; HFN7.1: 1/10,000 dilution) in blocking buffer (DPBS + 0.25% BSA + 0.05% Tween-20) for 1 hour at 37 °C. After washing three times in blocking buffer, SAMs

were incubated in alkaline phosphatase-conjugated anti-mouse IgG antibody (1/1000 dilution) in blocking buffer for 1 hour at 37 °C. After three washes in blocking buffer, 5-methyl umbelliferyl phosphate (60 µg/ml in diethanolamine, pH = 9.5) was incubated for 45 minutes at 37 °C in the dark. Reaction supernatants were transferred to clean black 96-well plates and the resulting fluorescence (365 nm excitation/450 nm emission) was read in a HTS 7000 Plus BioAssay microwell plate reader (Perkin Elmer, Norwalk, CT). For each antibody, relative fluorescence intensity, which is proportional to the amount of antibody bound, was determined as a function of FN surface density.

Cell Model to Examine Adhesive Interactions

We chose the MC3T3-E1 osteoblast-like cell line to investigate the effects of surface chemistry on integrin binding. This immature osteoblast-like cell line expresses multiple FN-binding integrins, including $\alpha_5\beta_1$ and $\alpha_v\beta_3$, and previous work in our group has shown that integrin binding to FN is critical for osteoblastic gene expression and matrix mineralization in these cells.³⁴ Cells were obtained from the RIKEN Cell Bank (Tokyo, Japan). Prior to seeding on FN-coated SAMs, MC3T3-E1 cells were maintained in α -Modified Eagle's Medium supplemented with 10% fetal bovine serum and 1% penicillin-streptomycin and subcultured every 2 days using standard techniques.

Integrin Binding Analyses

Integrin binding to FN adsorbed onto SAMs was quantified using a cross-linking/extraction biochemical method developed by our group^{33,40} and modified to quantify bound integrins via ELISA. In addition, immunofluorescence staining for integrin

subunits was carried out to validate biochemical quantification and examine bound integrin localization. For biochemical quantification, SAMs were coated with a range of FN surface densities for 30 minutes, then blocked in 1% hd-BSA for 30 minutes. MC3T3-E1 cells were seeded at 500 cells/mm² under serum-free conditions (2 mM dextrose in DPBS) for either 30 or 90 minutes. Cold sulfo-BSOCOES (1mM in DPBS) was then added for 30 minutes. Unreacted cross-linker was quenched for 10 minutes by the addition of 50 mM Tris in 2 mM dextrose-DPBS. Uncross-linked cellular components were then extracted in 0.1% SDS + 350 µg/ml phenylmethylsulfonyl fluoride (protease inhibitor) in DPBS. Cross-linked integrins were probed with integrin-specific antibodies and either quantified by ELISA using an alkaline phosphatase-conjugated antibody (1/1000 dilution) as described above or visualized by immunofluorescence staining using a fluorescence probe-conjugated antibody (1/200 dilution) as described previously.³⁴

Cell Adhesion Assay

Cell adhesion to SAMs was measured using a centrifugation assay to apply well-controlled detachment forces. SAMs were coated with a range of FN surface densities for 30 minutes and blocked in 1% hd-BSA or 0.1% non-fat dry milk for 30 minutes to prevent non-specific adhesion to the substrate. MC3T3-E1 cells were labeled with 2 µg/mL calcein-AM, a membrane permeable fluorescent dye, and seeded at 200 cells/mm² in 2 mM dextrose-DPBS into reassembled chamber slides for 30 minutes at room temperature. Initial fluorescence intensity was measured to quantify the number of adherent cells prior to application of centrifugal force. After filling the wells with media and sealing with transparent adhesive tape, substrates were spun at a fixed speed in a

centrifuge (Beckman Allegra 6, GH 3.8 rotor) to apply a specified centrifugal force (46g). This detachment force was chosen because it resulted in a sigmoidal adhesion profile providing sufficient resolution to discriminate among FN surface densities. After centrifugation, media was exchanged and fluorescence intensity was read to measure remaining adherent cells. For each well, adherent cell fraction was calculated as the ratio of post-spin to pre-spin fluorescence readings.

Curve-Fits and Statistics

Non-linear regression was used to curve-fit experimental data to selected models using SigmaPlot 5.0 (SPSS, Chicago, IL), yielding R^2 values of 0.90 or better. Results were analyzed by one-way ANOVA using SYSTAT 8.0 (SPSS). If treatments were determined to be significant, pair-wise comparisons were performed using Tukey post-hoc test. A 95% confidence level was considered significant.

RESULTS

Model Surfaces with Well-Defined Chemistry

Four functional end groups X ($X = \text{CH}_3, \text{OH}, \text{COOH}, \text{NH}_2$) were chosen to examine a wide range of surface chemistries. The CH_3 SAM presents a non-polar hydrophobic surface, while the OH SAM provides a neutral hydrophilic surface. At the experimental physiological pH of 7.4, the COOH SAM presents a negatively charged surface (COO^-), while the NH_2 SAM displays a positively charged surface (NH_3^+). Surface properties were verified by advancing contact angle measurements (**Figure 4.1B**) and XPS (**Table 4.1**). Ambient air-water-substrate contact angle measurements provided

information on wettability and surface energy, and the values obtained are in agreement with those reported in literature.^{23,30,45} Variable-angle XPS was used to obtain information on SAM composition and assembled alkanethiol orientation. Values obtained are in agreement with theoretical compositions, within the sensitivity of the instrument. Comparing atomic percentages at multiple depths of analysis indicated that SAMs were oriented correctly, with the sulfur atom at the greatest depth from the surface and the functional tail groups being closest to the surface. Taken together, these analyses confirmed the expected surface characteristics for each of the four SAMs.

FN Adsorption onto SAMs

FN adsorption onto SAMs was measured as a function of FN coating concentration using radiolabeled FN. **Figure 4.2** shows adsorption profiles exhibiting a linear adsorption regime at low coating concentrations and a saturation plateau at higher concentrations, as expected for single component adsorption.⁶ These results are in agreement with previous results on FN adsorption onto several synthetic substrates.^{33,46} Results for adsorbed FN density (FN_{ads}) vs. coating concentration ($[FN]$) were curve-fit to a simple hyperbola ($FN_{ads} = FN_{sat} * [FN] / ([FN] + [FN]_{50})$) to obtain estimates for the saturation density (FN_{sat}) and the FN concentration for half-maximal adsorption ($[FN]_{50}$) (**Table 4.2**). Analysis of curve-fit parameters revealed significant differences in saturation density ($p < 0.000012$) and the concentration for half-maximal adsorption ($p < 0.013$) among SAMs. FN adsorption onto OH SAM was lower than adsorption onto the other functionalities, consistent with other work reporting differences in protein adsorption as a function of surface wettability.²³ Although there were no differences in

FN adsorption among NH₂, COOH, and CH₃ SAMs at low coating concentrations, adsorption saturated at higher levels for the positively charged NH₂ SAM compared to the negatively charged COOH.

SAM-dependent Changes in Adsorbed FN Conformation

An antibody-based assay was used to examine differences in the structure or conformation of FN adsorbed onto different surface chemistries. This approach has been previously used by several groups to study substrate-induced changes in adsorbed proteins.^{13,20,30,33} We used monoclonal antibodies that block adhesion to the central cell-binding domain of FN to examine the sensitivity of this functional region to adsorption onto different surface chemistries. 3E3 maps to the 10th type III repeat⁴³ while HFN7.1 maps to the flexible linker between the 9th and 10th type III repeats.^{44,58} For each SAM, antibody binding increased in a sigmoidal fashion with FN surface density, displaying a toe-in region at low FN surface densities, a transition region at intermediate densities, and a saturation regime at higher FN surface densities (**Figures 4.3** and **4.4**). The antibody binding profile is strongly dependent on the binding affinity of the antibody for the adsorbed FN and left-right shifts in the binding profile reflect differences in binding affinity to adsorbed FN. These changes in antibody binding affinity reflect substrate-dependent differences in the functional presentation of FN, which includes differences in the adsorbed structure and orientation. As demonstrated in **Figures 4.3** and **4.4**, antibody binding profiles exhibited significant shifts among SAMs. The bound antibody (AB_{bound}) vs. FN surface density (FN_{ads}) profiles were curve-fit to a symmetric sigmoid ($AB_{\text{bound}} = AB_{\text{bkgd}} + AB_{\text{sat}} / [1 + \exp\{-(FN_{\text{ads}} - FN_{\text{AB-50}})/b\}]$) to obtain estimates for the FN density

for half-maximal antibody binding (FN_{AB-50}) (**Tables 4.3** and **4.4**). The parameters AB_{bkgd} and AB_{sat} represent the background and saturation levels of bound antibody, respectively, while b corresponds to the slope of the curve at the inflection point. Importantly, the FN_{AB-50} parameter represents the inverse of the antibody binding affinity and is characteristic for a particular antibody-adsorbed FN pair. For instance, a leftward shift in binding profile reflects enhanced ability of the antibody to bind adsorbed FN at lower surface densities, representing a higher binding affinity and a smaller FN_{AB-50} . Analysis of FN_{AB-50} parameters revealed significant differences in binding affinity among SAMs – HFN7.1 antibody ($p < 0.000023$): $OH > COOH = NH_2 > CH_3$; 3E3 antibody ($p < 8 \times 10^{-7}$): $OH > COOH > CH_3 = NH_2$. These results indicate significant differences in the functional presentation of the central cell-binding domain of FN upon adsorption to different surface chemistries.

Integrin Binding to FN-coated SAMs

We quantified integrin binding to FN adsorbed onto SAMs via a cross-linking and extraction biochemical method that uses a water-soluble, cell membrane-impermeable, homobifunctional cross-linker (sulfo-BSOCOES) to cross-link integrins to their bound ligands.³³ This method takes advantage of the fact that many extracellular matrix proteins, including FN, are resistant to mild detergent extraction. After cross-linking, the bulk of cell components was extracted, leaving behind the FN adsorbed on the surface with their bound integrins. Control experiments with non-activated integrins have shown cross-linker specificity for integrins bound to their extracellular matrix ligand, without cross-linking unbound receptors.^{33,48} After cross-linking integrins and extracting

unbound receptors, bound integrins were quantified via ELISA using antibodies specific for the α_5 integrin subunit. Since the α_5 subunit only dimerizes with the β_1 subunit, measurements of α_5 binding directly reflect binding of the $\alpha_5\beta_1$ integrin, the classic fibronectin receptor. This analysis revealed significant differences in α_5 -integrin binding to FN adsorbed onto SAMs as demonstrated by shifts in bound α_5 vs. FN density profiles among SAMs (**Figure 4.5**). To quantitatively compare the effects of surface chemistry on integrin binding to FN-coated SAMs, measurements of bound integrin (α_5 _{bound}) as a function of adsorbed FN density (FN_{ads}) were curve-fit to a symmetrical sigmoid (α_5 _{bound} = α_5 _{bkgd} + α_5 _{sat} / [1 + exp{-(FN_{ads} - FN _{α_5 -50})/d}]}) to obtain values for the FN density required for half-maximal integrin binding (FN _{α_5 -50}) (**Table 4.5**). The parameters α_5 _{bkgd} and α_5 _{sat} correspond to background and saturation levels of bound integrin, respectively, while d is the slope of the curve at the inflection point. In a manner analogous to the antibody binding analysis described above, FN _{α_5 -50} is inversely proportional to integrin binding affinity for adsorbed FN. Analysis of FN _{α_5 -50} revealed significant differences in integrin binding affinity among SAMs (p < 0.0014) following the pattern OH > COOH = NH₂ > CH₃.

Integrin binding to FN-coated SAMs was also investigated by immunofluorescence staining of cells plated onto equivalent FN surface densities (40 ng/cm²) for 90 min and cross-linked and extracted as before. In excellent agreement with the biochemical quantification, immunofluorescence staining for α_5 integrin subunit demonstrated substrate-dependent differences in $\alpha_5\beta_1$ integrin binding to adsorbed FN (**Figure 4.6**). Furthermore, cell spreading and, more importantly, clustering of $\alpha_5\beta_1$ integrin exhibited substrate-dependent differences. While cells on the CH₃ SAM showed

low levels of bound $\alpha_5\beta_1$ integrin, cells on the other surface functionalities exhibited significant assembly of $\alpha_5\beta_1$ integrin-containing complexes and showed differences in the localization and distribution of these $\alpha_5\beta_1$ integrin clusters. The COOH SAM displayed robust integrin clusters throughout the entire spread area of the cell, while cells on the OH SAM featured fewer integrin clusters at the center of the spread area but maintained intense receptor clustering at the cell periphery. Interestingly, cells on the NH_2 SAM showed localization of integrin clustering at the periphery of the cell but absent in the center of the spread area. Finally, although excellent agreement was observed between both methods to examine integrin binding, it is important to point out that the biochemical method provides quantitative measures of total $\alpha_5\beta_1$ integrin bound, while immunofluorescent staining is biased to detect clustered receptors. Nonetheless, these two approaches revealed substrate-dependent differences in $\alpha_5\beta_1$ integrin binding to adsorbed FN.

Immunofluorescence staining also revealed SAM-dependent differences in the binding of α_V integrin subunit to adsorbed FN (**Figure 4.6**), most likely reflecting differences in $\alpha_V\beta_3$ integrin binding. While the CH_3 , OH, and NH_2 SAMs exhibited little binding of α_V above non-specific staining of remaining nuclear material, the COOH surface displayed punctate clusters containing α_V integrin. Of particular importance, this analysis revealed that FN-coated SAMs exhibited integrin specificity – the COOH surface supported both $\alpha_5\beta_1$ and $\alpha_V\beta_3$ integrin binding, while the OH and NH_2 functionalities selectively recruited $\alpha_5\beta_1$. Biochemical quantification of bound α_V integrin showed slight differences among SAMs but due to higher background levels (as evidenced in **Figure 4.6**) the analysis could not be reliably performed. Nevertheless,

analysis of integrin binding to FN-coated SAMs revealed differences in integrin binding affinity and specificity among surface chemistries.

Cell Adhesion to FN-coated SAMs

We used a centrifugation assay to apply controlled and reproducible forces to adherent cells in order to quantify MC3T3-E1 cell adhesion to SAMs as a function of FN density. For a fixed centrifugal force, the fraction of adherent cells increased in a sigmoidal fashion with FN surface density (**Figure 4.7**). Shifts in the adhesion profile (adherent fraction vs. FN density) reflect differences in adhesion strength. For instance, a leftward shift indicates higher adhesion levels at lower FN densities, reflecting an increase in adhesion strength. Considerable differences were observed in adhesion profiles among SAMs. The OH SAM showed the greatest level of cell adhesion at lower FN densities, while the COOH and NH₂ SAMs had comparable levels of adhesion at intermediate FN densities, and the CH₃ SAM demonstrated equivalent levels of adhesion only at the highest FN surface density. Profiles for adherent fraction (f) as a function of FN density (FN_{ads}) were curve-fit to a symmetric sigmoid ($f = f_{sat} / [1 + \exp\{-(FN_{ads} - FN_{ADH-50})/g\}]$) to obtain estimates for the FN density for half-maximal adhesion (FN_{ADH-50}) (**Table 4.6**). The parameters f_{sat} and g represent the maximum adhesive fraction and the slope of the curve at the inflection point, respectively. The parameter FN_{ADH-50} represents the surface density of FN required for 50% maximal adhesion and was used as a measure of adhesion strength. This analysis revealed significant differences in adhesion strength among FN-coated SAMs ($p < 2 \times 10^{-8}$) following the trend: OH > COOH > NH₂ > CH₃. This pattern of adhesion strength correlates with the $\alpha_5\beta_1$ integrin

binding profile. Blocking experiments with function-perturbing antibodies demonstrated that cell adhesion to adsorbed FN was mediated by $\alpha_5\beta_1$ integrin as antibodies against the α_5 or β_1 integrin subunit or human plasma FN completely abrogated cell adhesion for all SAMs.

DISCUSSION

A fundamental understanding of substrate-directed control of cell function is critical to the rational design of surfaces relevant to biomaterials, tissue engineering scaffolds, and in vitro culture supports for biotechnological applications. In the present work, using model substrates with well-controlled surface properties, we demonstrate that surface chemistry modulates the functional presentation of adsorbed FN to direct integrin binding and specificity, thereby controlling cell adhesion. Our results reveal quantitative differences in the functional presentation of the major integrin-binding domain of FN, $\alpha_5\beta_1$ integrin binding, and cell adhesion among FN-coated SAMs (**Table 4.7**), as well as differences in the composition and localization of integrins to focal adhesion complexes. These surface chemistry-dependent changes in integrin binding and adhesion may provide a versatile strategy to control downstream cellular activities such as proliferation and expression of tissue-specific phenotypes, for various biomedical and biotechnological applications.

Antibody-based measurements using monoclonal antibodies revealed differences in antibody affinity for FN adsorbed onto different chemistries. These differences in antibody binding affinity reflect alterations in the functional presentation of the particular domain examined. These findings are consistent with earlier work by Grinnell and

others^{13,20,49} and, more recently, McClary and colleagues who demonstrated changes in adsorbed FN conformation between CH₃ and COOH SAMs.³⁰ In the present work, the central cell-binding domain of FN, spanning the 9th and 10th type III repeats of the molecule, was particularly sensitive to adsorption onto different chemistries as determined by changes in the binding affinities of the HFN7.1 and 3E3 antibodies. Structural alterations in this region of FN may have significant consequences for downstream cellular activities because this region contains critical binding domains for several integrins, including the RGD recognition site. Notably, binding of $\alpha_5\beta_1$ integrin to fibronectin requires both the PHSRN sequence in the 9th type III repeat and the RGD motif in the 10th type III repeat of the molecule.⁵⁰ Each domain independently contributes little to binding, but in combination, they synergistically bind to the integrin to produce significant increases in adhesion strength.^{51,52} Furthermore, the structural orientation of these binding domains is crucial to the synergistic effects as increases in the relative distance between the PHSRN and RGD sites completely abrogate $\alpha_5\beta_1$ binding, cell spreading, and integrin-mediated signaling.⁵³ Adsorption-induced changes in the structural orientation of these two binding domains may explain the observed substrate-dependent differences in integrin binding and cell adhesion.

These substrate-dependent differences in functional presentation among SAMs motivated us to investigate whether a minimum “active” or functional FN density exists independently of surface chemistry. Using antibody binding as a metric of functional presentation, cell adhesion was plotted as a function of HFN7.1 binding (**Figure 4.8**). When normalized by antibody binding, the adhesion profiles for all SAMs collapse into a single curve exhibiting a minimum functional FN density (approximately 8,000 RFI) for

maximum cell adhesion. This concept of a minimum active FN density is consistent with the findings of Massia and Hubbell, who reported a minimum ligand density of tethered RGD peptide required for cell spreading and focal adhesion assembly.⁶¹ Notably, HFN7.1 antibody proved to be an effective probe for the presentation of integrin binding sites in FN adsorbed onto different supports.

A significant contribution of this work is the rigorous analysis of integrin binding to FN adsorbed onto different surface chemistries. Using biochemical and immunostaining methods, we demonstrate significant substrate-dependent differences in integrin binding, localization, and specificity for adsorbed FN, providing new information on the mechanisms controlling cell-substrate interactions. The substantial differences in integrin $\alpha_5\beta_1$ binding among FN-coated SAMs correlate strongly with, and most likely result from, the observed substrate-dependent differences in the structure of the central cell-binding domain of FN. The differences in integrin binding among SAMs control subsequent differences in cell adhesion as demonstrated by blocking with function-perturbing antibodies. To further investigate this relationship, adhesion strength (FN_{ADH-50}) for each SAM was plotted vs. the FN density required for half-maximal integrin binding (FN_{α_5-50}) (**Figure 4.9**). While a general correlation between FN_{α_5-50} and FN_{ADH-50} exists, it is not necessarily linear, supporting contributions to cell adhesion strength from other factors including cell spreading, integrin clustering, and integrin-FN specific bond strength.^{54,46}

The differences in integrin binding, specificity, and localization among varying surface chemistries are particularly important to the understanding of cell-substrate interactions and concomitant engineering of surfaces to control cell function. In addition

to modulating short-term adhesive responses such as attachment and spreading, differences in integrin binding may differentially regulate integrin-mediated signaling and high order cellular activities, including proliferation and tissue-specific gene expression. For instance, we have previously shown that differential integrin binding between $\alpha_5\beta_1$ and $\alpha_v\beta_3$ triggers intracellular signals that control switching between proliferation and differentiation.³³ Differences in integrin clustering may also regulate the composition of structural and signaling proteins localizing to focal adhesion complexes, modulating downstream gene and protein activities. Moreover, integrin distribution along the cell-substrate interface is critical in controlling the distribution of forces throughout the cell and influences overall adhesion strength.⁵⁴

Our results indicate graded increases in accessibility of binding domains in FN, integrin binding, and cell adhesion as a function of underlying surface chemistry following the trend $\text{OH} > \text{COOH} = \text{NH}_2 > \text{CH}_3$. These findings are consistent with previous reports showing enhanced cell adhesion and spreading on COOH and OH SAMs compared to CH_3 SAMs.^{30,55,32} Scotchford et al. reported higher levels of cell attachment and clustered $\alpha_5\beta_1$ and $\alpha_v\beta_3$ integrins ($\text{COOH} > \text{CH}_3$).⁵⁵ In contrast to the present work, Scotchford and colleagues reported higher levels of attachment on COOH compared to OH SAMs. However, this study did not control for the density of adsorbed FN, which for the same coating concentration is greater for the COOH than the OH monolayer (**Figure 4.2**). Tidwell et al. also reported poor adhesion and cell growth on OH SAMs compared to CH_3 and COOH SAMs, but these substrates were incubated in serum-containing solutions that resulted in differences in protein adsorption.³²

Adsorption of FN onto the non-polar CH₃ SAM essentially destroyed $\alpha_5\beta_1$ integrin binding and cell adhesion for most FN surface densities, while the OH functionality resulted in the highest levels of integrin affinity and cell adhesion. These results are consistent with previous studies suggesting that hydrophobic surfaces strongly denature adsorbed proteins.^{13,20,33,49,23,59,60} For instance, Wertz and Santore demonstrated higher rates of interfacial relaxation or partial unfolding for proteins adsorbing to CH₃ surfaces compared to OH monolayers. Lower rates of protein unfolding on the OH monolayer compared to the CH₃ surface are consistent with our observations of enhanced functional presentation and cell activities. Finally, the present work provides an experimental framework to analyze adhesive mechanisms controlling cell-surface interactions and our findings contribute to the general understanding of cell-protein-surface interactions. However, detailed structure-function analyses, including molecular modeling of the adsorption process⁵⁷, are required to provide a more complete understanding of mechanisms directing cellular responses to synthetic surfaces.

In conclusion, using model substrates with well-controlled surface properties, we demonstrate that surface chemistry alters the functional presentation of the major integrin-binding domain of adsorbed FN and modulates integrin binding, localization, and specificity. These differences in integrin receptor binding control subsequent cell adhesion activities, providing new insights on mechanisms regulating cell-substrate interactions. Furthermore, substrate-directed control of adsorbed protein activity to manipulate integrin binding represents a versatile approach to elicit specific cellular responses in biomaterial applications.

ACKNOWLEDGMENT

This work was funded by the Whitaker Foundation and the Georgia Tech/Emory NSF ERC on the Engineering of Living Tissues (EEC-9731643). B.G.K. was supported by an NSF Graduate Research Fellowship. The authors gratefully acknowledge Kristi Chavez, Tazrien Kamal and Dennis Hess for XPS analysis of SAMs and Kristin Michael for assistance with contact angle measurements. HFN7.1 monoclonal antibody was obtained from the Developmental Studies Hybridoma Bank developed under the auspices of the NICHD and maintained by the University of Iowa, Dept. of Biological Sciences, Iowa City, IA 52242.

	Angle	C1s (%)	O1s (%)	N1s (%)	S2p (%)
CH ₃	30°	97.6	-	-	2.4
	75°	96.0	-	-	4.0
	theoretical	92.3	-	-	7.7
OH	30°	83.2	13.3	-	3.5
	75°	85.2	10.6	-	4.1
	theoretical	84.6	7.7	-	7.7
COOH	30°	79.4	18.9	-	1.8
	75°	80.1	17.8	-	2.2
	theoretical	79.0	14.0	-	7.0
NH ₂	30°	86.6	-	11.9	1.5
	75°	90.1	-	6.3	3.8
	theoretical	86.0	-	7.0	7.0

Table 4.1. Variable-angle XPS measurements of self-assembled monolayers of alkanethiols on gold. Angle is measured from the plane of the surface. Excellent agreement between measured and expected (theoretical) atomic compositions is indicated.

	Adsorption Parameters		Tukey Pair-Wise Comparison for FN _{sat}		
	FN _{sat} (ng/cm ²)	[FN] ₅₀ (μg/mL)	OH	COOH	NH ₂
CH ₃	360 ± 76	14 ± 4.6	p < 0.00007	n.s.	n.s.
OH	110 ± 83	7.2 ± 2.4	-	p < 0.004	p < 0.00002
COOH	280 ± 43	12 ± 1.5	-	-	p < 0.032
NH ₂	410 ± 72	18 ± 5.2	-	-	-

Table 4.2. Hyperbolic curve-fit parameters for FN adsorption showing differences among SAMs (n.s.-not significant). Data presented as mean ± standard deviation (three separate runs, in duplicate).

	FN _{AB-50} (ng/cm ²)	Tukey Pair-Wise Comparison		
		OH	COOH	NH ₂
CH ₃	210 ± 12	p < 0.000028	p < 0.023	n.s.
OH	32 ± 6.5	-	p < 0.00076	p < 0.000072
COOH	150 ± 29	-	-	n.s.
NH ₂	180 ± 20	-	-	-

Table 4.3. HFN7.1 monoclonal antibody FN_{AB-50} values for FN-coated SAMs obtained from sigmoidal curve-fits, demonstrating significant differences in antibody binding affinity among SAMs (n.s.-not significant). FN_{AB-50} values are mean ± standard deviation (three separate runs, in duplicate).

	FN _{AB-50} (ng/cm ²)	Tukey Pair-Wise Comparison		
		OH	COOH	NH ₂
CH ₃	160 ± 48	p < 0.0000063	p < 0.028	n.s.
OH	24 ± 13	-	p < 0.00016	p < 0.000011
COOH	110 ± 44	-	-	n.s.
NH ₂	170 ± 76	-	-	-

Table 4.4. 3E3 monoclonal antibody FN_{AB-50} values for FN-coated SAMs obtained from sigmoidal curve-fits demonstrating significant differences in antibody binding affinity among SAMs (n.s.-not significant). FN_{AB-50} values are mean ± standard deviation (three separate runs, in duplicate).

	FN _{α5-50} (ng/cm ²)	Tukey Pair-Wise Comparison		
		OH	COOH	NH ₂
CH ₃	150 ± 48	p < 0.00079	p < 0.043	p < 0.048
OH	15 ± 8.0	-	p < 0.047	p < 0.042
COOH	84 ± 12	-	-	n.s.
NH ₂	86 ± 13	-	-	-

Table 4.5. FN _{α 5-50} values for MC3T3-E1 cells on FN-coated SAMs obtained from sigmoidal curve-fits demonstrating significant differences in $\alpha_5\beta_1$ integrin binding among SAMs (n.s.-not significant). FN _{α 5-50} values are mean ± standard deviation (three separate runs, in duplicate).

	FN _{ADH-50} (ng/cm ²)	Tukey Pair-Wise Comparison		
		OH	COOH	NH ₂
CH ₃	240 ± 43	p < 0.0000084	p < 0.0000084	p < 0.0000084
OH	19 ± 8.1	-	p < 0.0027	p < 0.000093
COOH	56 ± 9.5	-	-	p < 0.015
NH ₂	82 ± 6.6	-	-	-

Table 4.6. FN_{ADH-50} values for MC3T3-E1 adhesion to FN-coated SAMs demonstrating differences in cell adhesion among SAMs. Values are mean ± standard deviation (three separate runs, in duplicate) obtained from sigmoidal curve-fits.

FN Conformation / α_5 Binding / Adhesion			
	OH	COOH	NH ₂
CH ₃	+ / + / +	+ / + / +	- / + / +
OH	-	+ / + / +	+ / + / +
COOH	-	-	- / - / +

Table 4.7. Summary of FN conformation/integrin binding/cell adhesion results showing pair-wise comparisons (+: significant, -: not significant).

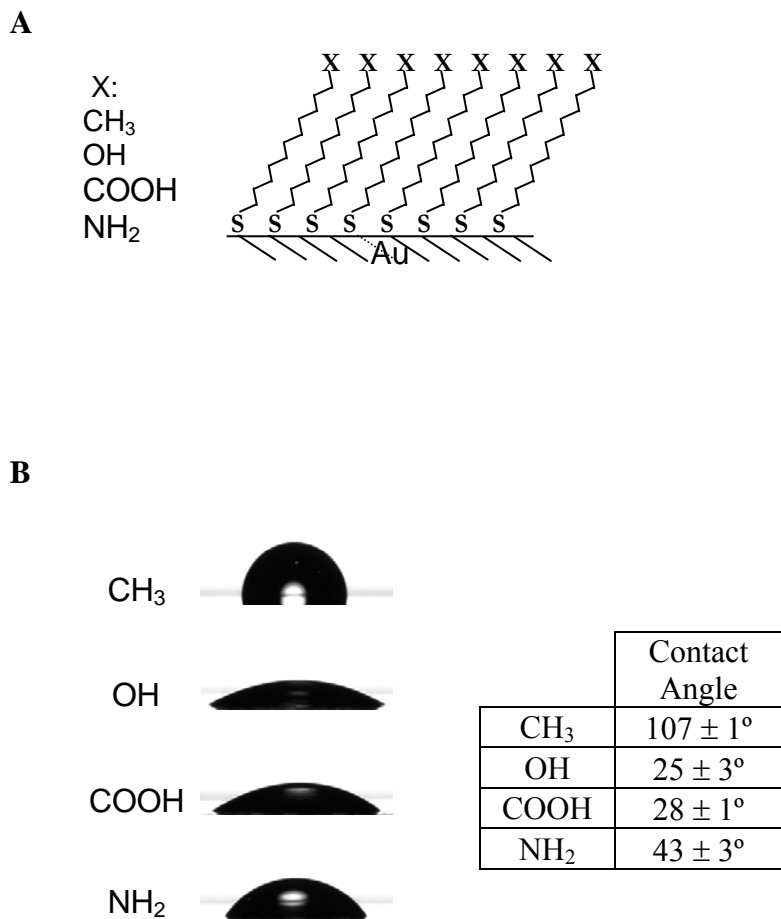


Figure 4.1. SAM structure and characterization by contact angle. A. Functionalized alkanethiol SAMs on Au presenting tail group X. B. Shown are drop profiles and contact angle measurements (mean ± standard deviation) using 5 µL water-drops on SAMs at ambient conditions. 3-4 drops were analyzed with contact angles measured on both sides of the drop.

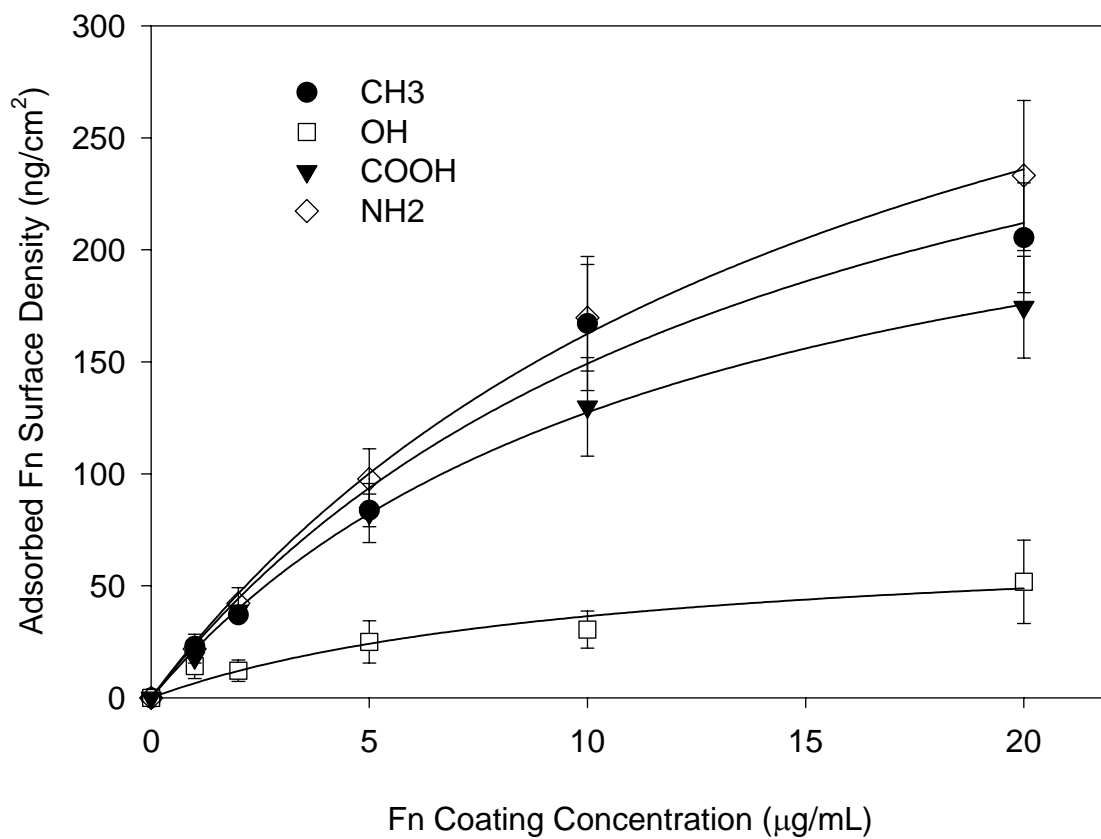


Figure 4.2. FN adsorption on SAMs as a function of coating concentration showing differences among SAMs. Data is plotted as mean \pm standard deviation (three separate runs, in duplicate) with hyperbolic curve fits.

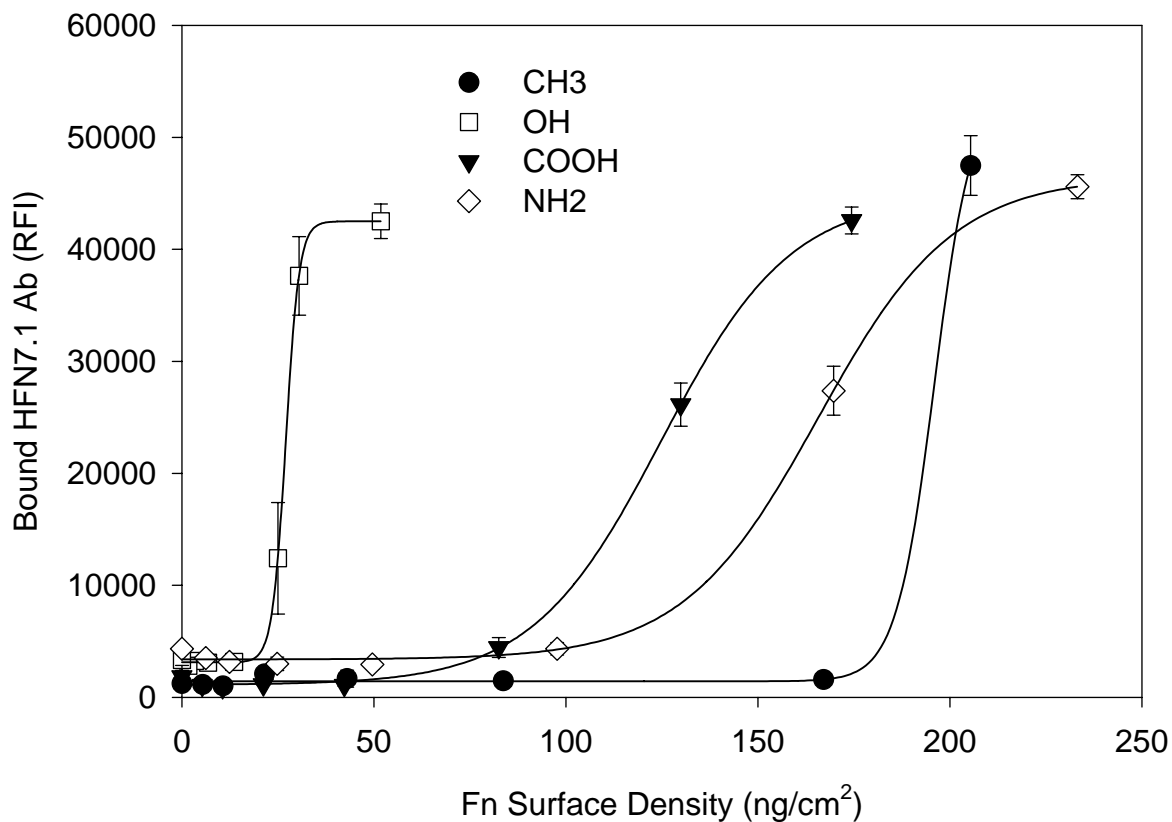


Figure 4.3. Bound HFN7.1 monoclonal antibody (relative fluorescence intensity), as a function of FN surface density demonstrating substrate-dependent differences in antibody binding affinity among SAMs. Shown are representative data (mean \pm standard deviation) and sigmoidal curve-fits for one experimental run.

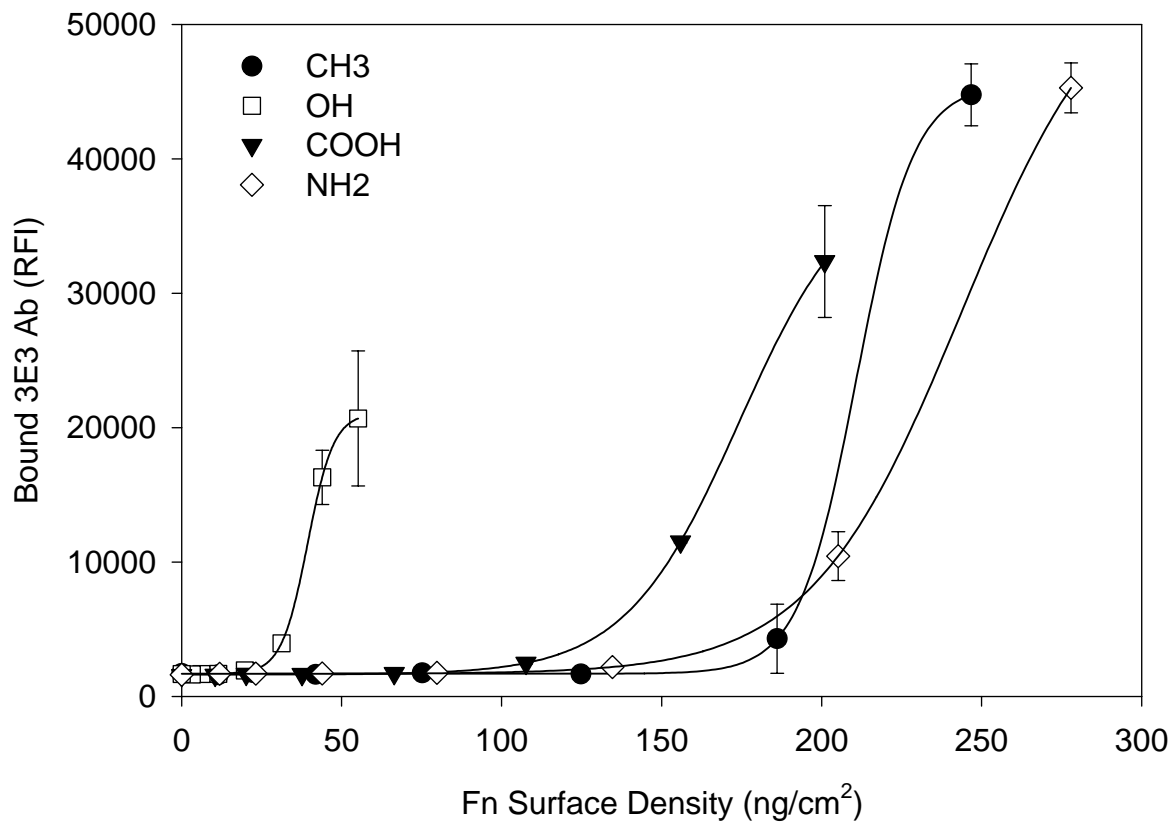


Figure 4.4. Bound 3E3 monoclonal antibody (relative fluorescence intensity) as a function of FN surface density demonstrating substrate-dependent changes in antibody binding affinity among SAMs. Shown are representative data (mean \pm standard deviation) and sigmoidal curve-fits for one experimental run.

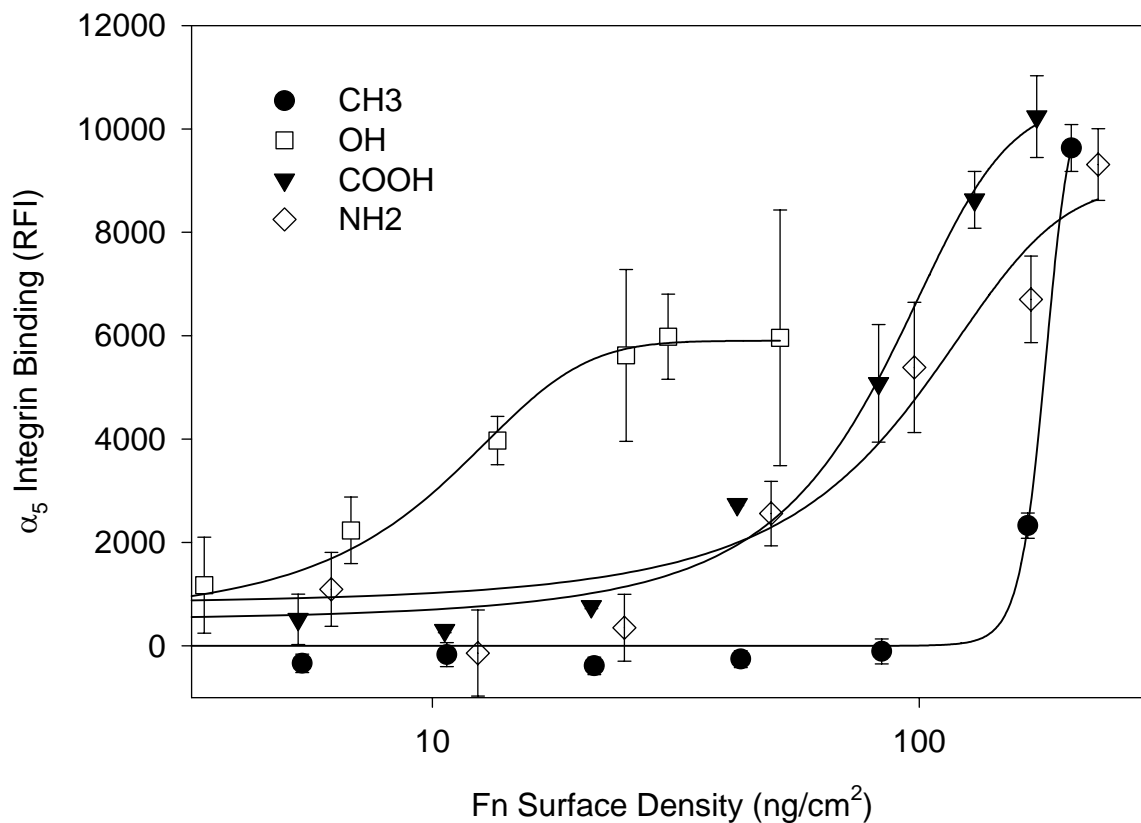


Figure 4.5. $\alpha_5\beta_1$ integrin binding as a function of FN surface density demonstrating differences in integrin binding of MC3T3-E1 cells seeded on FN-coated SAMs. Shown are representative data (mean \pm standard deviation) and sigmoidal curve-fits for one experimental run.

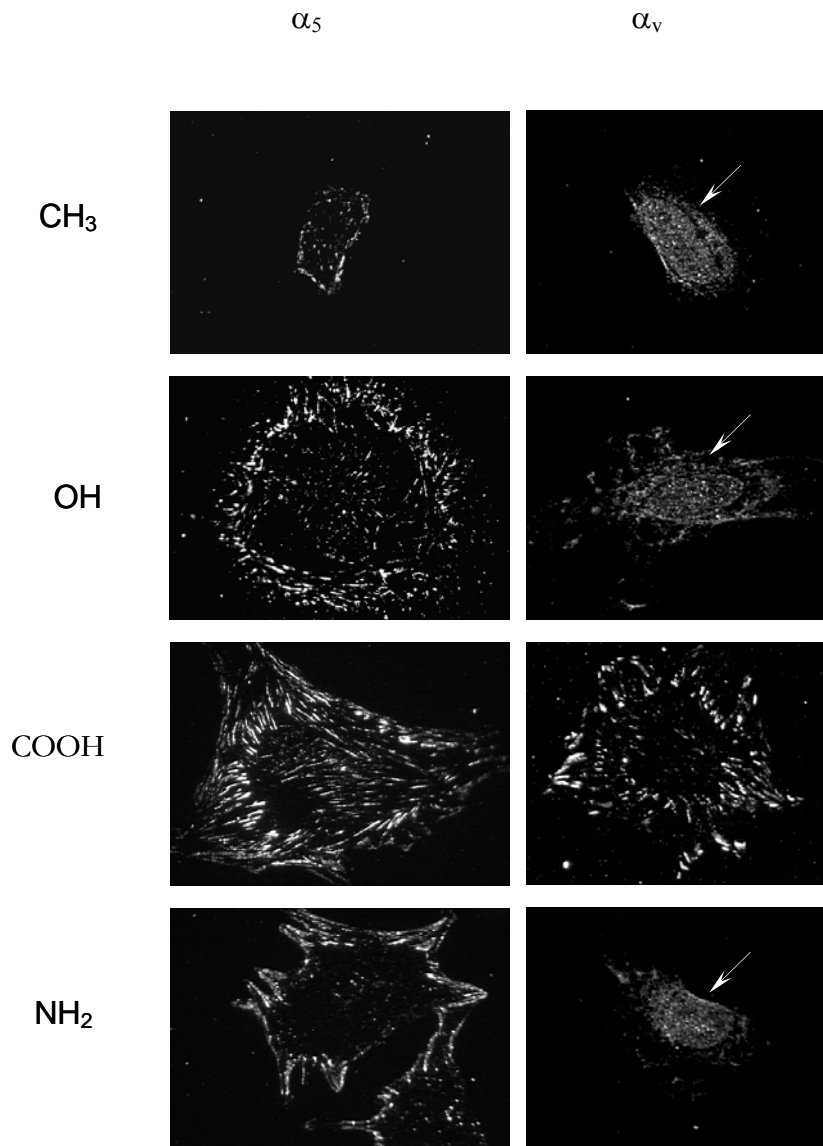


Figure 4.6. Immunofluorescence staining for α_5 and α_v integrin subunits on MC3T3-E1 cells (one cell per frame) seeded serum-free for 90 min on FN (40 ng/cm²) demonstrating differences in clustering and localization among surface chemistries. Focal adhesion complexes display characteristic discrete spear-like structures. Arrows indicate residual nuclear background staining.

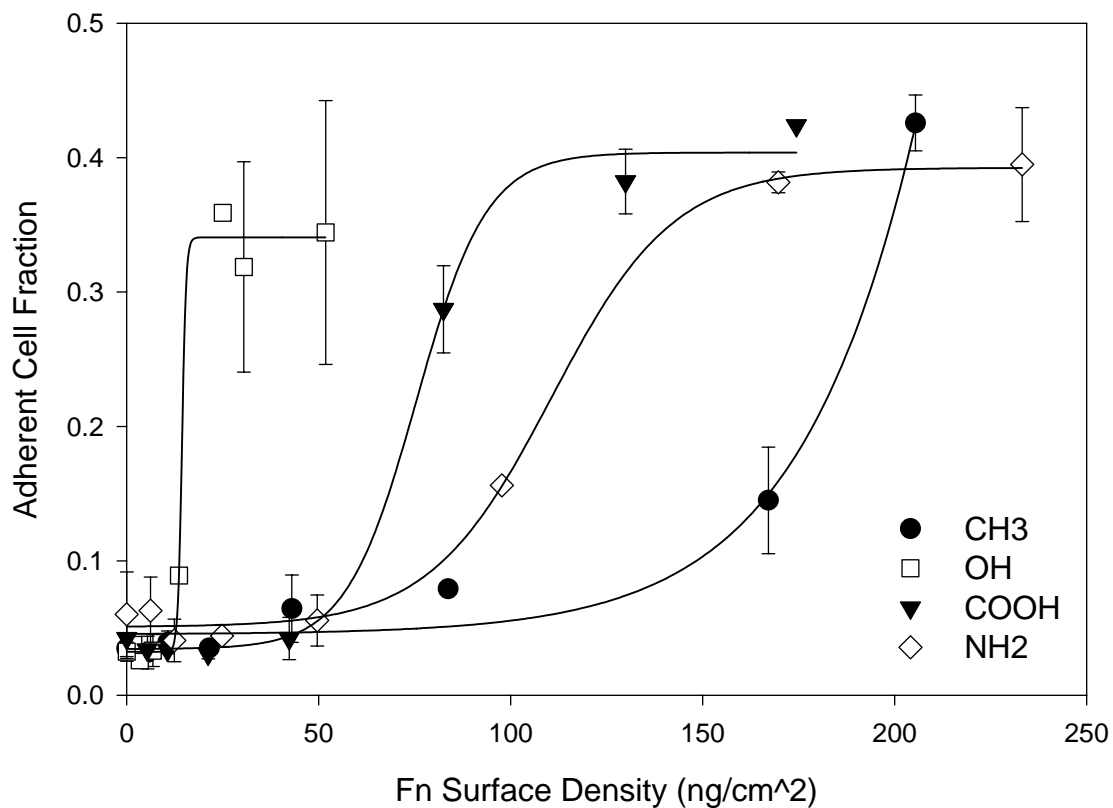


Figure 4.7. Adherent fraction of MC3T3-E1 cells seeded on FN-coated SAMs, as a function of FN surface density demonstrating differences in cell adhesion among SAMs. Shown is representative data (mean \pm standard deviation) and sigmoidal curve-fits for one experimental run.

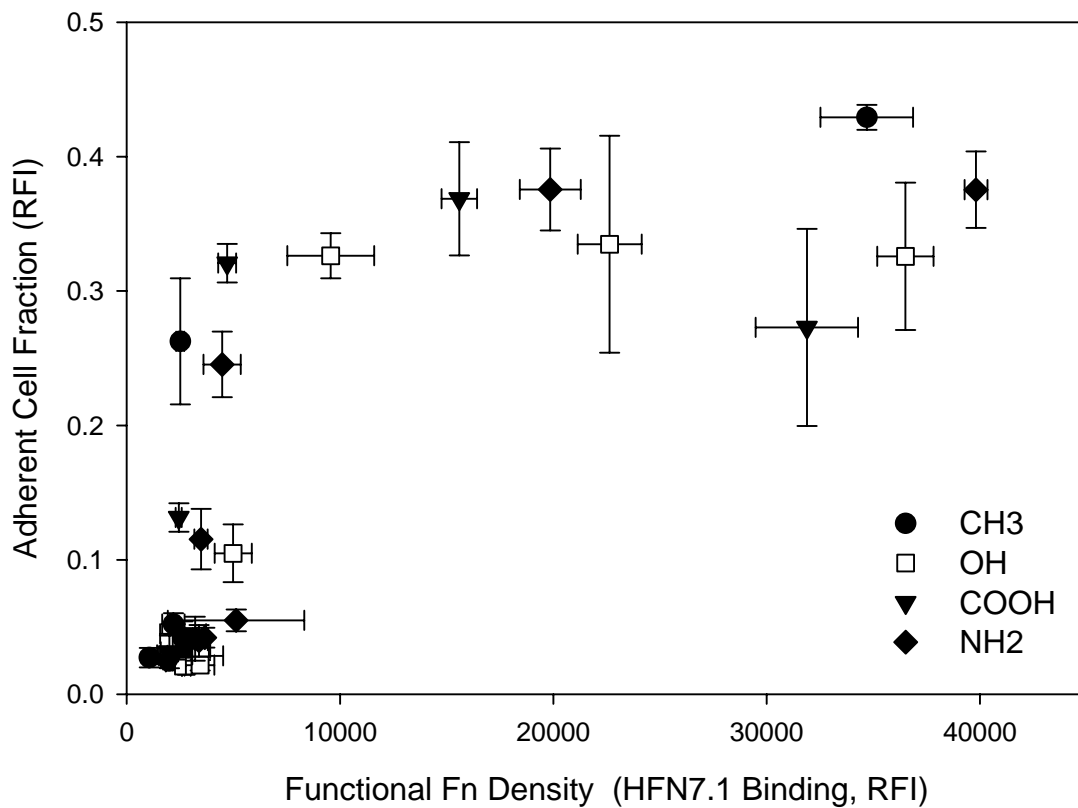


Figure 4.8. Adherent fraction of MC3T3-E1 cells seeded on FN-coated SAMs, as a function of functional FN surface density, as measured by HFN7.1 antibody binding (in RFI), demonstrating a minimum “active” FN surface density to produce maximum cell adhesion. Data is plotted as mean \pm standard error (average of three separate runs).

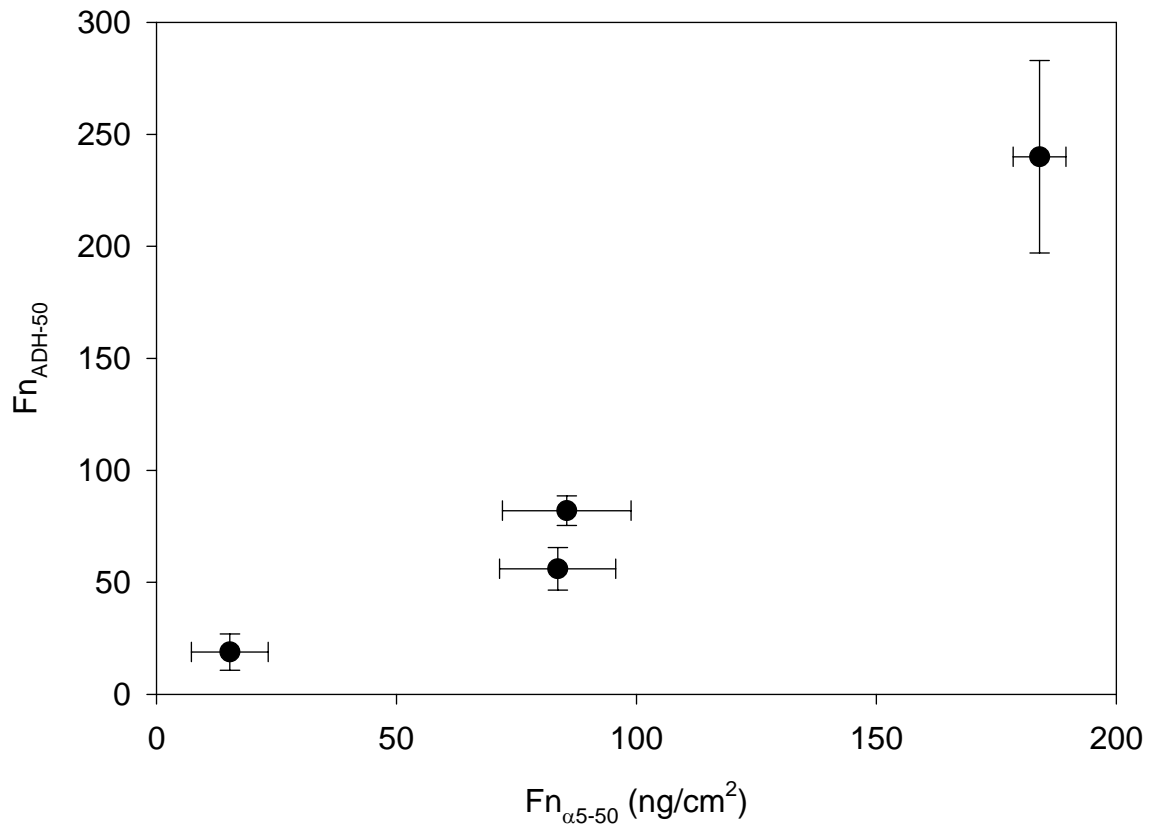


Figure 4.9. Relationship between $FN_{\alpha 5-50}$ and FN_{ADH-50} showing positive correlation between $\alpha_5\beta_1$ integrin binding and cell adhesion strength.

REFERENCES

1. Park PK, Jarrell BE, Williams SK, Carter TL, Rose DG, Martinez-Hernandez A, and Carabasi RA, III.: Thrombus-free, human endothelial surface in the midregion of a Dacron vascular graft in the splanchnic venous circuit-observations after nine months of implantation. *J. Vasc. Surg.* **11**:468-475, 1990.
2. Sharma SK and Mahendroo PP.: Affinity chromatography of cells and cell membranes. *J. Chromatogr.* **184**:471-499, 1980.
3. Anderson JM.: Inflammatory response to implants. *ASAIO Trans.* **34**:101-107, 1988.
4. Langer R and Vacanti JP.: Tissue engineering. *Science* **260**:920-926, 1993.
5. Baier RE.: The role of surface energy in thrombogenesis. *Bull. N. Y. Acad. Med.* **48**:257-272, 1972.
6. Andrade JD and Hlady V. V.: Protein adsorption and materials biocompatibility: A tutorial review and suggested hypotheses. *Adv. Polym. Sci.* **79**:1-63, 1986.
7. Brash JL.: Protein adsorption at the solid-solution interface in relation to blood-material interactions. Horbett TA and Brash JL, editors. *Proteins at Interfaces*. Washington, DC: American Chemical Society. 490-506, 1987.
8. Shen M and Horbett TA.: The effects of surface chemistry and adsorbed proteins on monocyte/macrophage adhesion to chemically modified polystyrene surfaces. *J. Biomed. Mater. Res.* **57**:336-345, 2001.
9. Anderson JM, Ziats NP, Azeez A, Brunstedt MR, Stack S, and Bonfield TL.: Protein adsorption and macrophage activation on polydimethylsiloxane and silicone rubber. *J. Biomater. Sci. Polym. Ed.* **7**:159-169, 1995.
10. Hynes RO.: Integrins: versatility, modulation, and signaling in cell adhesion. *Cell.* **69**:11-25, 1992.
11. Ruoslahti E and Pierschbacher MD.: New perspectives in cell adhesion: RGD and integrins. *Science* **238**:491-497, 1987.
12. Hubbell JA.: Bioactive biomaterials. *Curr. Opin. Biotechnol.* **10**:123-129, 1999.
13. Grinnell F and Feld MK.: Adsorption characteristics of plasma fibronectin in relationship to biological activity. *J. Biomed. Mater. Res.* **15**:363-381, 1981.
14. Prime KL and Whitesides GM.: Self-assembled organic monolayers: model systems for studying adsorption of proteins at surfaces. *Science* **252**:1164-1167, 1991.

15. Tegoulia VA and Cooper SL.: Leukocyte adhesion on model surfaces under flow: effects of surface chemistry, protein adsorption, and shear rate. *J. Biomed. Mater. Res.* **50**:291-301, 2000.
16. Lewandowska K, Pergament E, Sukenik CN, and Culp LA.: Cell-type-specific adhesion mechanisms mediated by fibronectin adsorbed to chemically derivatized substrata. *J. Biomed. Mater. Res* **26**:1343-1363, 1992.
17. Martin JY, Schwartz Z, Hummert TW, Schraub DM, Simpson J, Lankford J, Jr., Dean DD, Cochran DL, and Boyan BD.: Effect of titanium surface roughness on proliferation, differentiation, and protein synthesis of human osteoblast-like cells (MG63). *J. Biomed. Mater. Res.* **29**:389-401, 1995.
18. Thomas CH, McFarland CD, Jenkins ML, Rezanian A, Steele JG, and Healy KE. : The role of vitronectin in the attachment and spatial distribution of bone-derived cells on materials with patterned surface chemistry. *J. Biomed. Mater. Res.* **37**:81-93, 1997.
19. Iuliano DJ, Saavedra SS, and Truskey GA.: Effect of the conformation and orientation of adsorbed fibronectin on endothelial cell spreading and the strength of adhesion. *J. Biomed. Mater. Res.* **27**:1103-1113, 1993.
20. Pettit DK, Hoffman AS, and Horbett TA.: Correlation between corneal epithelial cell outgrowth and monoclonal antibody binding to the cell binding domain of adsorbed fibronectin. *J. Biomed. Mater. Res.* **28**:685-691, 1994.
21. Tyler BJ, Ratner BD, Castner DG, and Briggs D.: Variations between Biomer lots. I. Significant differences in the surface chemistry of two lots of a commercial poly(ether urethane). *J. Biomed. Mater. Res.* **26**:273-289, 1992.
22. Silver JH, Lewis KB, Ratner BD, and Cooper SL.: Effect of polyol type on the surface structure of sulfonate-containing polyurethanes. *J. Biomed. Mater. Res.* **27**:735-745, 1993.
23. Sigal GB, Mrksich M, and Whitesides GM.: Effect of Surface Wettability on the Adsorption of Proteins and Detergents. *J. Am. Chem. Soc.* **120**:3464-3473, 1998.
24. Vogler EA, Graper JC, Harper GR, Sugg HW, Lander LM, and Brittain WJ.: Contact activation of the plasma coagulation cascade. I. Procoagulant surface chemistry and energy. *J. Biomed. Mater. Res.* **29**:1005-1016, 1995.
25. Porter MD, Bright TB, Allara DL, and Chidsey CED.: Spontaneously Organized Molecular Assemblies. 4. Structural Characterization of *n*-Alkyl Thiol Monolayers on Gold by Optical Ellipsometry, Infrared Spectroscopy, and Electrochemistry. *J. Am. Chem. Soc.* **109**:3559-3568, 1987.
26. Ulman A, Eilers JE, and Tillman N.: Packing and molecular-orientation of alkanethiol monolayers on gold surfaces. *Langmuir* **5**:1147-1152, 1989.

27. Bain CD, Evall J, and Whitesides GM.: Formation of monolayers by the coadsorption of thiols on gold: Variation in the head group, tail group and solvent. *J. Am. Chem. Soc.* **111**:7155-7164, 1989.
28. Singhvi R, Kumar A, Lopez GP, Stephanopoulos GN, Wang DI, Whitesides GM, and Ingber DE.: Engineering cell shape and function. *Science* **264**:696-698, 1994.
29. Franco M, Nealey PF, Campbell S, Teixeira AI, and Murphy CJ.: Adhesion and proliferation of corneal epithelial cells on self- assembled monolayers. *J. Biomed. Mater. Res.* **52**:261-269, 2000.
30. McClary KB, Ugarova T, and Grainger DW.: Modulating fibroblast adhesion, spreading, and proliferation using self- assembled monolayer films of alkylthiolates on gold. *J. Biomed. Mater. Res.* **50**:428-439, 2000.
31. Scotchford CA, Cooper E, Leggett GJ, and Downes S.: Growth of human osteoblast-like cells on alkanethiol on gold self- assembled monolayers: the effect of surface chemistry. *J. Biomed. Mater. Res.* **41**:431-442, 1998.
32. Tidwell CD, Ertel SI, and Ratner BD.: Endothelial Cell Growth and Protein Adsorption on Terminally Functionalized, Self-Assembled Monolayers of Alkanethiolates on Gold. *Langmuir* **13**:3404-3413, 1997.
33. García AJ, Vega MD, and Boettiger D.: Modulation of cell proliferation and differentiation through substrate- dependent changes in fibronectin conformation. *Mol. Biol. Cell* **10**:785-798, 1999.
34. Stephansson SN, Byers BA, and García AJ.: Enhanced expression of the osteoblastic phenotype on substrates that modulate fibronectin conformation and integrin receptor binding. *Biomaterials* **23**:2527-2534, 2002.
35. Menko AS and Boettiger D.: Occupation of the extracellular matrix receptor, integrin, is a control point for myogenic differentiation. *Cell* **51**:51-57, 1987.
36. Werb Z, Tremble PM, Behrendtsen O, Crowley E, and Damsky CH.: Signal transduction through the fibronectin receptor induces collagenase and stromelysin gene expression. *J. Cell Biol.* **109**:877-889, 1989.
37. Adams JC and Watt FM.: Changes in keratinocyte adhesion during terminal differentiation: reduction in fibronectin binding precedes alpha 5 beta 1 integrin loss from the cell surface. *Cell* **63**:425-435, 1990.
38. Streuli CH, Bailey N, and Bissell MJ.: Control of mammary epithelial differentiation: basement membrane induces tissue-specific gene expression in the absence of cell-cell interaction and morphological polarity. *J. Cell Biol.* **115**:1383-1395, 1991.

39. Zhu X, Ohtsubo M, Bohmer RM, Roberts JM, and Assoian RK.: Adhesion-dependent cell cycle progression linked to the expression of cyclin D1, activation of cyclin E-cdk2, and phosphorylation of the retinoblastoma protein. *J. Cell Biol.* **133**:391-403, 1996.
40. García AJ and Boettiger D.: Integrin-fibronectin interactions at the cell-material interface: initial integrin binding and signaling. *Biomaterials* **20**:2427-2433, 1999.
41. Sayre CN and Collard DM.: Electrooxidative Deposition of polypyrrole and polyaniline on self-assembled monolayer modified electrodes. *Langmuir* **13**:714-722, 1997.
42. García AJ, Huber F, and Boettiger D. Force required to break alpha5beta1 integrin-fibronectin bonds in intact adherent cells is sensitive to integrin activation state. *J. Biol. Chem.* **273**:10988-10993, 1998.
43. Pierschbacher MD, Hayman EG, and Ruoslahti E.: Location of the cell-attachment site in fibronectin with monoclonal antibodies and proteolytic fragments of the molecule. *Cell* **26**:259-267, 1981.
44. Schoen RC, Bentley KL, and Klebe RJ.: Monoclonal antibody against human fibronectin which inhibits cell attachment. *Hybridoma* **1**:99-108, 1982.
45. Tanahashi M and Matsuda T.: Surface functional group dependence on apatite formation on self- assembled monolayers in a simulated body fluid. *J. Biomed. Mater. Res.* **34**:305-315, 1997.
46. García AJ, Ducheyne P, and Boettiger D.: Effect of surface reaction stage on fibronectin-mediated adhesion of osteoblast-like cells to bioactive glass. *J. Biomed. Mater. Res.* **40**:48-56, 1998.
47. Hynes, R. O.: Fibronectins. New York: Springer-Verlag 1990.
48. Enomoto-Iwamoto M, Menko AS, Philp N, and Boettiger D.: Evaluation of integrin molecules involved in substrate adhesion. *Cell Adhes. Commun.* **1**:191-202, 1993.
49. Underwood PA, Steele JG, and Dalton BA.: Effects of polystyrene surface chemistry on the biological activity of solid phase fibronectin and vitronectin, analysed with monoclonal antibodies. *J. Cell Sci.* **104**:793-803, 1993.
50. Aota S, Nomizu M, and Yamada KM.: The short amino acid sequence Pro-His-Ser-Arg-Asn in human fibronectin enhances cell-adhesive function. *J. Biol. Chem.* **269**:24756-24761, 1994.
51. Redick SD, Settles DL, Briscoe G, and Erickson HP.: Defining fibronectin's cell adhesion synergy site by site-directed mutagenesis. *J Cell Biol.* **149**:521-527, 2000.

52. García AJ, Schwarzbauer JE, and Boettiger D.: Distinct activation states of $\alpha_5\beta_1$ integrin show differential binding to RGD and synergy domains of fibronectin. *Biochemistry* **41**:9063-9069, 2002.
53. Grant RP, Spitzfaden C, Altroff H, Campbell ID, and Mardon HJ.: Structural requirements for biological activity of the ninth and tenth FIII domains of human fibronectin. *J. Biol. Chem.* **272**:6159-6166, 1997.
54. Gallant ND, Capadona JR, Frazier AB, Collard DM, and García AJ.: Micropatterned surfaces to engineer focal adhesions for analysis of cell adhesion strengthening. *Langmuir* **18**:5579-5584, 2002.
55. Scotchford CA, Gilmore CP, Cooper E, Leggett GJ, and Downes S.: Protein adsorption and human osteoblast-like cell attachment and growth on alkylthiol on gold self-assembled monolayers. *J. Biomed. Mater. Res.* **59**:84-99, 2002.
56. Grinnell F and Feld MK.: Fibronectin adsorption on hydrophilic and hydrophobic surfaces detected by antibody binding and analyzed during cell adhesion in serum-containing medium. *J. Biol. Chem.* **257**:4888-4893, 1982.
57. Latour R, Jr. and Rini CJ.: Theoretical analysis of adsorption thermodynamics for hydrophobic peptide residues on SAM surfaces of varying functionality. *J. Biomed. Mater. Res.* **60**:564-577, 2002.
58. Bowditch RD, Halloran CE, Aota S, Obara M, Plow EF, Yamada KM, and Ginsberg MH.: Integrin alpha IIb beta 3 (platelet GPIIb-IIIa) recognizes multiple sites in fibronectin. *J. Biol. Chem.* **266**:23323-23328, 1991.
59. Wertz CF and Santore MM.: Adsorption and Relaxation Kinetics of Albumin and Fibrinogen on Hydrophobic Surfaces: Single Species and Competitive Behavior. *Langmuir* **15**:8884-8894, 1999.
60. Wertz CF and Santore MM.: Effect of Surface Hydrophobicity on Adsorption and Relaxation Kinetics of Albumin and Fibrinogen: Single-Species and Competitive Behavior. *Langmuir* **17**:3006-3016, 2001.
61. Massia SP and Hubbell JA.: An RGD spacing of 440 nm is sufficient for integrin alpha v beta 3-mediated fibroblast spreading and 140 nm for focal contact and stress fiber formation. *J. Cell Biol.* **114**:1089-1100, 1991.

CHAPTER 5

SURFACE CHEMISTRY MODULATES FOCAL ADHESION COMPOSITION AND SIGNALING THROUGH CHANGES IN INTEGRIN BINDING*

SUMMARY

Biomaterial surface properties influence protein adsorption and elicit diverse cellular responses in biomedical and biotechnological applications. However, the molecular mechanisms directing cellular activities remain poorly understood. Using a model system with well-defined chemistries (CH₃, OH, COOH, NH₂) and a fixed density of the single adhesive ligand fibronectin, we investigated the effects of surface chemistry on focal adhesion assembly and signaling. Surface chemistry strongly modulated integrin binding and specificity – $\alpha_5\beta_1$ integrin binding affinity followed the pattern OH > NH₂ = COOH > CH₃, while integrin $\alpha_v\beta_3$ displayed the relationship COOH > NH₂ >> OH = CH₃. Immunostaining and biochemical analyses revealed that surface chemistry modulates the structure and molecular composition of cell-matrix adhesions as well as FAK signaling. The neutral hydrophilic OH functionality supported the highest levels of recruitment of talin, α -actinin, paxillin, and tyrosine-phosphorylated proteins to adhesive structures. The positively charged NH₂ and negatively charged COOH surfaces exhibited intermediate levels of recruitment of focal adhesion components, while the hydrophobic CH₃ substrate displayed the lowest levels. These patterns in focal adhesion assembly correlated well with integrin $\alpha_5\beta_1$ binding. Phosphorylation of specific tyrosine residues in FAK also showed differential sensitivity to surface chemistry. These differences in focal adhesion assembly

* Keselowsky, B.G., Collard, D.M. and García, A.J. Biomaterials. (*in press*).

and signaling provide a potential mechanism for the diverse cellular responses elicited by different material properties.

INTRODUCTION

Cell adhesion to synthetic surfaces is crucial to many biomedical and biotechnological applications.¹⁻⁶ In addition to anchoring cells, adhesive interactions activate various intracellular signaling pathways that direct cell viability, proliferation, and differentiation.^{7,8} In many instances, cell adhesion to biomaterial surfaces is mediated by a layer of adsorbed proteins, such as immunoglobulins, vitronectin, fibrinogen and fibronectin (FN).^{9,10} Numerous studies have shown that the type, quantity and activity of adsorbed proteins are influenced by the underlying substrate properties, including chemistry and hydrophobicity.^{9,11-16} These substrate-dependent differences in protein adsorption have profound effects on cellular activities, including integrin receptor binding and subsequent cell adhesive events.¹⁷⁻²³ Several studies have demonstrated diverse cellular responses to substrates with different surface chemistries. For instance, Allen et al. showed differential gene expression for several cell types on surfaces of varying hydrophobicity.²⁴ Similarly, Brodbeck and colleagues demonstrated increased in vivo apoptosis and reduced foreign body giant cell formation on hydrophilic and anionic surfaces compared to hydrophobic and cationic substrates.²⁵ While these studies highlight the importance of biomaterial surface properties in modulating cellular behaviors, the underlying mechanisms responsible for generating dissimilar cell responses among different substrates remain poorly understood.

Using model substrates with well-controlled surface properties, we recently reported that surface chemistry alters the adsorption kinetics and structure of adsorbed FN.²⁶ Furthermore, we demonstrated that surface chemistry modifies the functional presentation of the major integrin binding domain of FN, alters integrin binding, and potentiates cell adhesion strength.²³ In the present work, we analyzed the effects of surface chemistry on focal adhesion assembly and signaling. Focal adhesions are specialized adhesive complexes containing structural and signaling molecules that regulate cell migration, survival, cell cycle progression, and differentiation.^{27,28} We demonstrate that surface chemistry modulates focal adhesion composition and signaling. These findings provide a potential mechanism for the diverse cellular responses to biomaterial surfaces and offer design criteria for the engineering of surfaces that elicit specific cellular responses.

MATERIALS AND METHODS

Cells and reagents

Human plasma FN and other tissue culture reagents were obtained from Invitrogen (Carlsbad, CA). Fetal bovine serum was purchased from Hyclone (Logan, UT). Bovine serum albumin, anti-talin (clone 8D4) and anti- α -actinin (BM-75.2) monoclonal antibodies, alkaline phosphatase-conjugated anti-biotin antibody (BN-34), and all other chemical reagents were obtained from Sigma Chemical (St. Louis, MO). Bis(2-(sulfo-succinimidooxycarbonyloxy)ethyl)sulfone (sulfo-BSOCOES) cross-linker was purchased from Pierce Chemical (Rockford, IL). Anti-paxillin (Z035) and anti-phosphotyrosine (PY20) antibodies were obtained from Zymed Laboratories (San

Francisco, CA). Anti-vinculin (V284) and anti-FAK antibodies were purchased from Upstate (Lake Placid, NY). Antibodies against phosphotyrosine FAK, pFAK Tyr-576, pFAK Tyr-397 and pFAK Tyr-861, were obtained from Biosource International (Camarillo, CA). HFN7.1 monoclonal antibody directed against human plasma FN was obtained from the Developmental Studies Hybridoma Bank (Iowa City, IA). Rabbit antibodies against mouse integrin subunits were purchased from Chemicon (Temecula, CA). Alexa Fluor 488-conjugated anti-rabbit and anti-mouse IgG antibodies were acquired from Molecular Probes (Eugene, OR), while biotinylated anti-rabbit IgG and alkaline phosphatase-conjugated anti-rabbit IgG antibodies were purchased from Jackson ImmunoResearch (West Grove, PA).

MC3T3-E1 cells, an immature osteoblast-like cell line, were obtained from the RIKEN Cell Bank (Tokyo, Japan). Prior to seeding on FN-coated substrates, MC3T3-E1 cells were maintained in α -Modified Eagle's Medium supplemented with 10% fetal bovine serum and 1% penicillin-streptomycin and passaged every 2 days using standard techniques.

Model surfaces with well-defined chemistries

Self-assembled monolayers (SAMs) of alkanethiols on gold were used as model substrates with well-defined chemistries.²⁹⁻³¹ Alkanethiols 1-dodecanethiol (HS-(CH₂)₁₁-CH₃), 11-mercapto-1-undecanol (HS-(CH₂)₁₁-OH) and 11-mercaptoundecanoic acid (HS-(CH₂)₁₀-COOH) were purchased from Aldrich Chemical (Milwaukee, WI) and used as received. The amine-terminated alkanethiol, 12-amino-1-mercaptododecane (SH-(CH₂)₁₂-NH₂), was synthesized and purified as described previously.²³ SAMs of their

respective alkanethiols are referred to hereafter as CH₃, OH, COOH and NH₂ SAMs. Gold-coated substrates were prepared by sequential deposition of optically transparent films of titanium (10 nm) and gold (20 nm) onto clean glass coverslips or tissue culture dishes via electron beam evaporation (Thermionics Laboratories, Hayward, CA) at 1-2 x 10⁻⁶ torr with 2 Å/s deposition rate. Freshly prepared gold surfaces were immersed in alkanethiol solutions (1.0 mM in absolute ethanol), and SAMs were allowed to assemble for 12 hr. Surfaces were characterized by contact angle and X-ray photoelectron spectroscopy (XPS).^{23,26} XPS analyses revealed surface compositions within 5% of the theoretical values. Prior to FN coating, SAMs were rinsed in ethanol, dried with N₂, and allowed to equilibrate in Dulbecco's phosphate buffered saline (DPBS: 137 mM NaCl, 2.7 mM KCl, 4.3 mM Na₂HPO₄·7H₂O, 1.5 mM KH₂PO₄, 0.9 mM CaCl₂·2H₂O, 1 mM MgCl₂·6H₂O, pH 7.4) for 15 min. SAMs were coated for 30 min with different FN concentrations and blocked for 30 min in 1% heat-denatured serum albumin. Adsorbed FN densities were previously quantified with ¹²⁵I-labeled FN.²³

Cell adhesion assay

Cell adhesion was quantified using a centrifugation assay.³² This assay applies a single detachment force and allows estimation of cell adhesion strength. Calcein-labeled cells were seeded on FN-coated SAMs for 30 min and subjected to a 46g detachment force using a Beckman GS-6R centrifuge with a swinging bucket rotor. Adherent cell fraction (post-spin to pre-spin readings) vs. FN density was curve-fit to a sigmoid to obtain estimates of the FN surface density required for 50% detachment. This parameter provides a robust measure of effective cell adhesion strength.

Integrin binding and focal adhesion assembly assays

Integrin binding to FN-coated SAMs was quantified using a cross-linking/extraction biochemical method that selectively isolates bound integrins.^{33,23} MC3T3-E1 cells were seeded at 500 cells/mm² under serum-free conditions for 30 min. Ligated integrins were cross-linked with sulfo-BSOCOES (1mM) and uncross-linked cellular components were extracted in 0.1% SDS + 350 µg/ml phenylmethanesulfonyl fluoride (PMSF). Cross-linked integrins were quantified by ELISA.

For immunostaining of focal adhesions, cells were seeded on FN-coated (40 ng/cm²) SAMs at 3,000 cells/cm² for 1 hr under serum-free conditions. Cells were then permeabilized for 5 min in 0.5% Triton X-100 in 50 mM Tris (pH 6.8), 50 mM NaCl, 150 mM sucrose, 3 mM MgCl₂ supplemented with 10 µg/mL PMSF, leupeptin, aprotinin, and 10mM Na₃VO₄, and fixed in cold 3.6% formaldehyde for 5 min. After blocking with 5% serum, cultures were incubated with primary and secondary antibodies.²³

Focal adhesion proteins localized to adhesive complexes were isolated and quantified by a modified wet-cleaving technique.^{34,35} Briefly, cells were seeded at 400 cells/mm² on FN-coated (40 ng/cm²) SAMs for 1 hr under serum-free conditions. Cells were washed with DPBS, and a nitrocellulose sheet (PROTRAN BA85, Schleicher & Schuell) was overlaid on the cells for 1 min. Cells were then cleaved by rapidly lifting the nitrocellulose sheet, and cleaved surfaces were rinsed in DPBS and scraped in Laemmli sample buffer. Recovered proteins were analyzed by Western blotting.^{36,33} DNA was solubilized from corresponding nitrocellulose sheets and quantified by SYBR Green (Molecular Probes, OR) incorporation to normalize for cell numbers. Parallel

plates were cleaved and examined by immunofluorescence staining to corroborate Western blotting analyses.

FAK phosphorylation

Cells were gently agitated in serum-free suspension for 45 min to reduce background signaling, and seeded at 400 cells/mm² for 1 hr on FN-coated SAMs. After rinsing in DPBS, cells were lysed in RIPA buffer (1% Triton X-100, 1% deoxycholate, 0.1% SDS, 150 mM Tris (pH 7.2), 10 µg/mL PMSF, leupeptin, aprotinin, and 10 mM Na₃VO₄). Total protein was quantified using micro-BCA (Pierce, IL), and equal amounts of total protein were analyzed by Western blotting and image analysis. Phosphorylated FAK levels were normalized to total FAK.

Statistical analyses

Results were analyzed by mixed-model ANOVA using SYSTAT 8.0 (SPSS Inc., IL). For treatments that were determined to be significant, pair-wise comparisons were performed using Tukey post-hoc test. A 95% confidence level was considered significant.

RESULTS

Surface chemistry modulates integrin binding and cell adhesion

Ordered and well-packed SAMs of ω-functionalized alkanethiols on gold were used to present four chemistries: (i) CH₃ (hydrophobic), (ii) OH (neutral hydrophilic), (iii) COOH (negatively charged at pH 7.4), and (iv) NH₂ (positively charged at pH 7.4). Prior

to cell seeding, surfaces were coated with a specified FN density and blocked with non-adhesive albumin to prevent adsorption of additional proteins which may influence cell behaviors. Surfaces densities were characterized following coating and washing steps and reflect tightly adsorbed proteins. This model provides a well-defined system with controlled densities of a single adhesive ligand and allows rigorous analysis of the effects of surface chemistry on cell adhesion. Using this system, we recently demonstrated that surface chemistry alters the structure and functional presentation of the major integrin binding domain in FN.^{23,26} This system, however, does not prevent long-term, cell-mediated extracellular matrix reorganization.

Surface chemistry strongly modulated integrin binding and specificity to adsorbed FN (**Fig. 5.1**). Binding of $\alpha_5\beta_1$ integrin exhibited surface chemistry-dependent differences following the pattern in binding affinity $\text{OH} > \text{NH}_2 = \text{COOH} > \text{CH}_3$. Integrin $\alpha_v\beta_3$ displayed high affinity to COOH SAM, intermediate values to the NH_2 surface, and negligible binding to OH and CH_3 SAMs. A fixed FN density (40 ng/cm^2) was selected to provide for equivalent ligand densities among surfaces for further analyses. This value represents the saturation density for the OH SAM and is the lowest saturation density of all SAMs examined.²³ For this FN density, the OH and NH_2 surfaces displayed high levels of bound $\alpha_5\beta_1$ integrin, while the COOH SAM supported high binding of both $\alpha_5\beta_1$ and $\alpha_v\beta_3$, and the CH_3 surface poorly bound both integrins. Cell adhesion strength to adsorbed FN also displayed SAM-dependent differences (**Fig. 5.2**), correlating well with integrin binding. Function-perturbing antibodies directed against human FN or integrin subunits completely blocked adhesion to these surfaces, demonstrating that the

adsorbed FN, not proteins adsorbed from solution or deposited by the cells, provided the primary adhesion mechanism in this model.

Surface chemistry alters focal adhesion assembly

Since integrin binding and clustering control focal adhesion assembly, we investigated the localization of specific structural (vinculin, talin, α -actinin) and signaling (paxillin, tyrosine-phosphorylated proteins) components to adhesion plaques on FN-coated SAMs. Analysis of focal adhesion assembly by complementary biochemical and immunofluorescence staining approaches revealed SAM-dependent modulation of the molecular composition and structure of cell-FN adhesions (**Table 5.1, Fig. 5.3 and Fig. 5.4**). Vinculin localized to large ($> 3 \mu\text{m}$ long), highly oriented complexes on the NH_2 and COOH SAMs, while forming a high number of smaller, more punctate clusters on the OH functionality, and fewer and poorly defined structures on the CH_3 surface (**Fig. 5.3**). In excellent agreement with immunofluorescence staining observations, wet-cleaving/biochemical quantification of assembled focal adhesions displayed significant differences among surface chemistries ($\text{NH}_2 = \text{COOH} > \text{OH} > \text{CH}_3$, $p < 0.0001$, **Fig. 5.3**). In contrast to vinculin, talin clustered into robust adhesive structures in the cell periphery on the OH and COOH SAMs, but displayed less and smaller clusters on the NH_2 surface, and even fewer and less mature complexes on the CH_3 substrate (**Fig. 5.4**). These observations were confirmed biochemically ($\text{OH} > \text{COOH} > \text{NH}_2 = \text{CH}_3$, $p < 0.0002$, **Fig. 5.4**). Similar to talin, α -actinin localized to adhesive plaques following the pattern $\text{OH} = \text{COOH} > \text{NH}_2 > \text{CH}_3$ (**Table 5.1**). Paxillin and tyrosine-phosphorylated proteins, components associated with signaling events, also exhibited differential recruitment to

focal adhesions, showing high levels on the OH functionality, intermediate amounts on COOH and NH₂ surfaces, and lowest levels on the CH₃ substrate (**Table 5.1**). These results demonstrate surface chemistry-dependent differences in the composition and organization of focal adhesions.

Surface chemistry modulates site-specific FAK phosphorylation

Focal adhesion kinase (FAK) localizes to focal adhesions to activate multiple signaling pathways that regulate cell migration, survival, proliferation, and differentiation.³⁸⁻⁴² Because of the multi-functional activities of FAK, we examined the effects of surface chemistry on the phosphorylation of three important tyrosine residues using site-specific antibodies. Phosphorylation of tyrosine-576, located in the FAK catalytic loop and essential for maximal kinase activity, was reduced on the CH₃ substrate compared to the other surface chemistries ($p < 0.05$, **Fig. 5.5A**). More importantly, tyrosine-397 (autophosphorylation site and SH2-binding site) and tyrosine-861 (SH2-binding site) exhibited differential phosphorylation following the pattern NH₂ > OH = COOH > CH₃ ($p < 0.05$, **Fig. 5.5B, 5.5C**). These results demonstrate differential phosphorylation of specific sites in FAK as a function of underlying surface chemistry.

DISCUSSION

Biomaterial surface properties play critical roles in controlling cellular behaviors in host responses to implanted devices, tissue engineering scaffolds and artificial organs, biosensors, and cell culture supports and bioreactors. Although it is generally accepted

that diverse cellular responses to synthetic surfaces arise from differences in protein adsorption, the molecular mechanisms directing cellular activities are not well understood. Because focal adhesions function in mechanical and biochemical capacities, these specialized structures represent putative transducers of biomaterial properties. In the present work, we used a model experimental system consisting of well-defined surface chemistries and a fixed density of a single adhesive ligand to analyze focal adhesion assembly as a function of surface chemistry. We demonstrate that surface chemistry, through modulation of integrin binding, regulates focal adhesion assembly, composition and signaling. This is a significant finding in the context of biomaterials because it provides a putative mechanism for signal transduction of biomaterial properties to cellular activities (e.g., adhesion and spreading, proliferation, differentiation) and demonstrates that differences in integrin binding differentially regulate specific intracellular signaling pathways. To our knowledge, this is the first report of surface chemistry-dependent, integrin-mediated differences on focal adhesion composition and signaling. The differences in focal adhesion assembly most likely result from surface chemistry-dependent differences in the functional presentation of adsorbed FN.²³ Using monoclonal antibodies as structural probes, we demonstrated that, upon adsorption onto these surfaces, FN undergoes significant structural changes.²³ The major integrin-binding RGD domain in FN was particularly sensitive to the underlying chemistry and presentation of this motif (as determined by antibody binding) followed the pattern OH > NH₂ = COOH > CH₃. These changes in FN structure, in turn, modulated integrin binding. These surface chemistry-dependent differences in integrin binding and specificity most likely result in the differences in focal adhesion composition

and signaling. Indeed, blocking antibodies against FN or integrin subunits completely abolish adhesive interactions on these substrates. Finally, it is important to note that the present analysis was performed on substrates with a well-defined pre-adsorbed protein layer to isolate the effects of surface chemistry from other factors influencing cell adhesion, such as differences in protein adsorption (e.g., multiple proteins, adsorbed density) and matrix deposition. These other mechanisms may influence cellular behaviors in other experimental systems, including the case of uncoated substrates exposed to serum- or plasma-containing solutions.

Analysis of focal adhesion assembly by two independent methods revealed that surface chemistry modulates the structure and molecular composition of cell-matrix adhesions as well as FAK signaling. In general, the neutral hydrophilic OH functionality supported the highest levels of recruitment to adhesive structures for talin, α -actinin, paxillin, and tyrosine-phosphorylated proteins. The NH_2 and COOH moieties, which present positively and negatively charged surfaces, respectively, exhibited intermediate levels of recruitment of focal adhesion components. The hydrophobic CH_3 substrate displayed the lowest levels of focal adhesion components. These patterns in focal adhesion assembly correlate well with integrin $\alpha_5\beta_1$ binding. The trends in integrin binding and focal adhesion assembly are in excellent agreement with differences in cell adhesion strength, consistent with the anchoring functions of these structural components.^{36,33,45-48} On the other hand, vinculin recruitment exhibited higher levels on the charged surfaces compared to the OH SAM and did not follow the same relationship with surface chemistry as other focal adhesion components. This is not surprising given

the tremendous complexity and inter-relationships involved in focal adhesion assembly and regulation.⁴⁹

Phosphorylation of FAK also showed differential sensitivity to surface chemistry. Phosphorylation of tyrosine-576 in the catalytic loop of FAK exhibited a binary response with negligible activation on the CH₃ SAM and high levels on all other surfaces. Notably, both tyrosine-397, the autophosphorylation site in FAK and a binding site for src and PI-3 kinase,^{50,51} and tyrosine-861 exhibited highest phosphorylation on the NH₂ surface, intermediate levels on the OH and COOH functionalities, and minimal activation on the CH₃ SAM. Because of the important roles of these SH2-binding sites on the activation of signaling pathways,⁵² these findings suggest a mechanism for differential activation of signaling cascades as a function of surface chemistry.

We propose a model in which surface chemistry-dependent differences in integrin binding, both in terms of bound numbers as well as integrin specificity, differentially regulate focal adhesion assembly and signaling which, in turn, modulate cellular functions (e.g., cell adhesion strength, matrix mineralization). This model is consistent with recent observations detailing integrin-specific differences in focal adhesion assembly and signaling.^{17,57-59} The present findings, however, differ from these previous reports in the mechanisms giving rise to differences in integrin binding and focal adhesion composition. In the present study, surface chemistry-dependent differences in focal adhesion assembly and signaling provide a mechanism for the differential cellular responses elicited by different material properties. These results contribute to the development of design principles for the engineering of surfaces that direct cell adhesion for biomedical and biotechnology applications.

ACKNOWLEDGMENT

This work was funded by the Whitaker Foundation and the Georgia Tech/Emory NSF ERC on the Engineering of Living Tissues (EEC-9731643). B.G.K. was supported by an NSF Graduate Research Fellowship.

	vinculin	talin	α -actinin	paxillin	p-Tyr
CH ₃	+	+	+	+	+
OH	++	+++	+++	+++	+++
COOH	+++	++	+++	++	++
NH ₂	+++	+	++	++	++

Table 5.1: Surface chemistry differentially alters recruitment and organization of structural and signaling components to focal adhesions. MC3T3-E1 cells were seeded serum-free for 1 hr on SAMs coated with equivalent FN surface densities (40 ng/cm²), fixed and immunostained. Scoring of relative immunostaining intensity for focal adhesion components localized to adhesive plaques (+ present, ++ strong, +++ very strong).

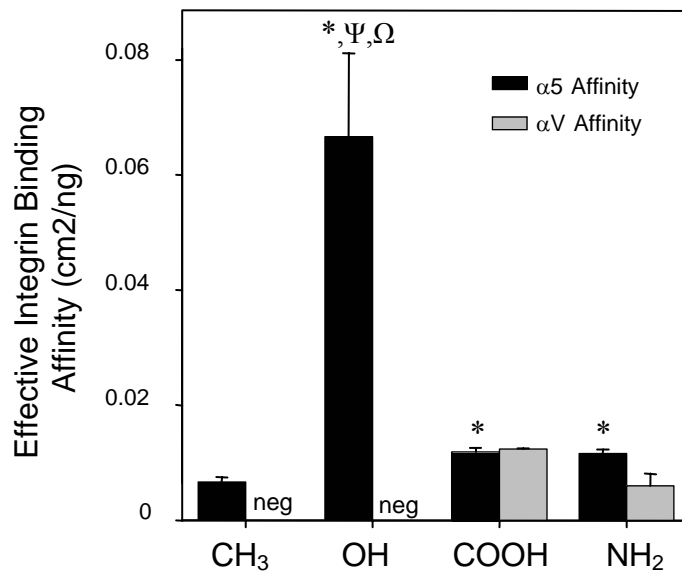


Figure 5.1: Surface chemistry modulates integrin binding affinity. MC3T3-E1 cells were seeded serum-free for 1 hr on FN-coated SAMs. Plotted are effective α_5 and α_V integrin binding affinities to adsorbed FN as quantified via cross-linking and extraction. α_V binding to CH₃ and OH FN-coated SAMs was negligible (neg). Pair-wise comparison showed significant differences between surface chemistries (* vs. CH₃; Ψ vs. COOH; Ω vs. NH₂; $p < 0.05$).

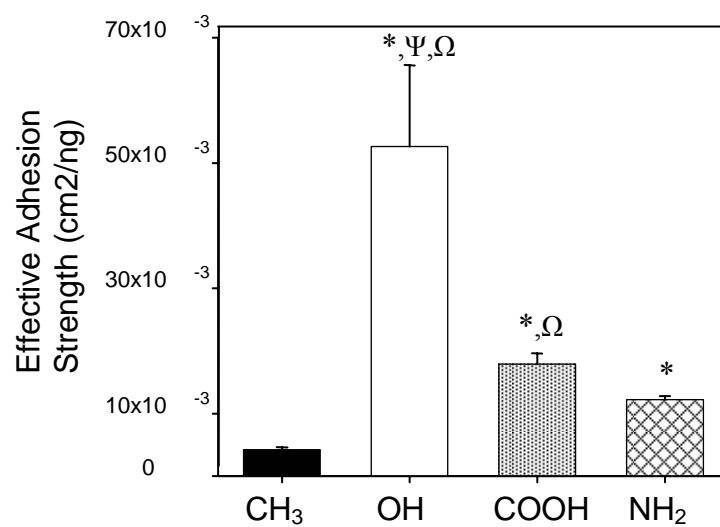


Figure 5.2: Surface chemistry modulates cell adhesion strength. MC3T3-E1 cells were seeded serum-free for 1 hr on FN-coated SAMs. Shown is effective cell adhesion strength to FN-coated SAMs. Pair-wise comparison showed significant differences between surface chemistries (* vs. CH₃; Ψ vs. COOH; Ω vs. NH₂; p < 0.05).

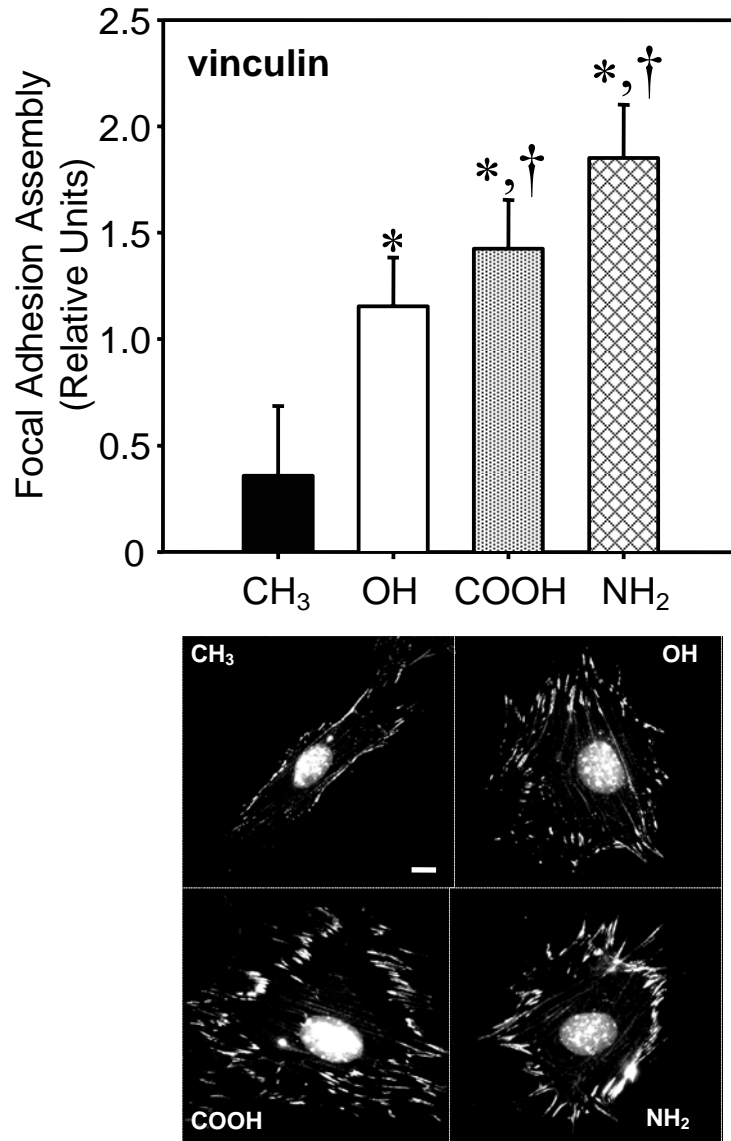


Figure 5.3: Surface chemistry differentially alters recruitment and organization of structural component, vinculin, to focal adhesions. MC3T3-E1 cells were seeded serum-free for 1 hr on SAMs coated with equivalent FN surface densities (40 ng/cm²). Wet-cleaving/biochemical and immunolabeling analysis of vinculin recruitment to focal adhesions demonstrating differences in localization and composition (scale bar 10 μm).

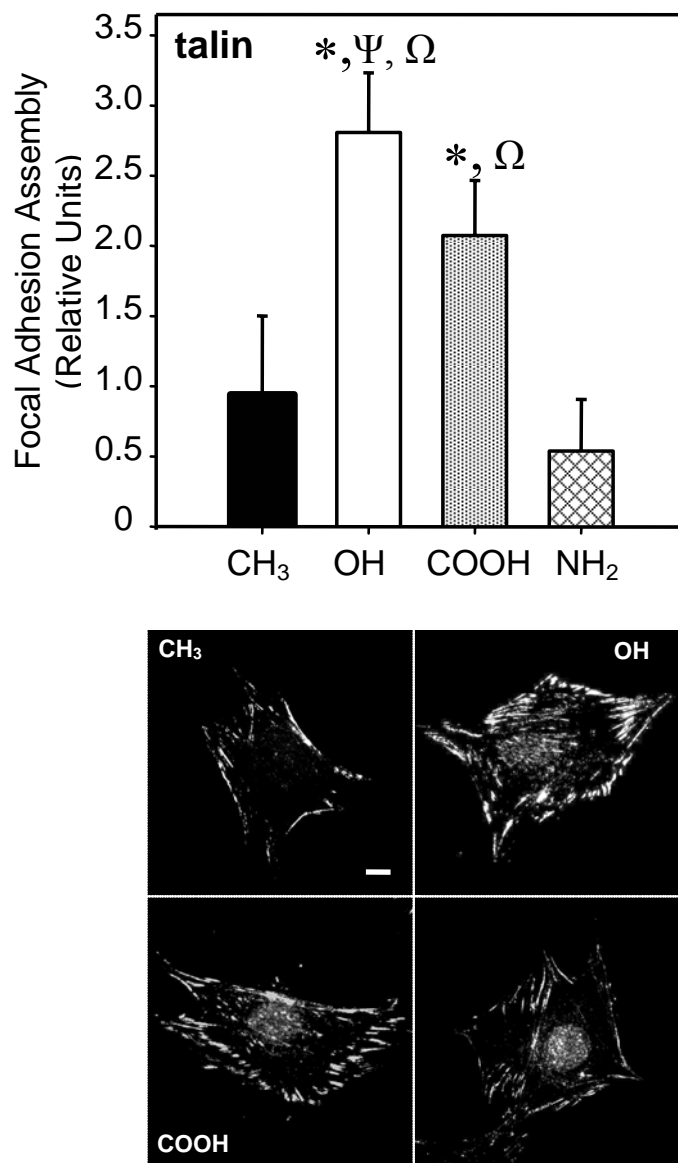


Figure 5.4: Surface chemistry differentially alters recruitment and organization of focal adhesion component, talin. MC3T3-E1 cells were seeded serum-free for 1 hr on SAMs coated with equivalent FN surface densities (40 ng/cm²). Wet-cleaving/biochemical and immunolabeling analysis of talin recruitment to focal adhesions demonstrating differences in localization and composition (scale bar 10 μm).

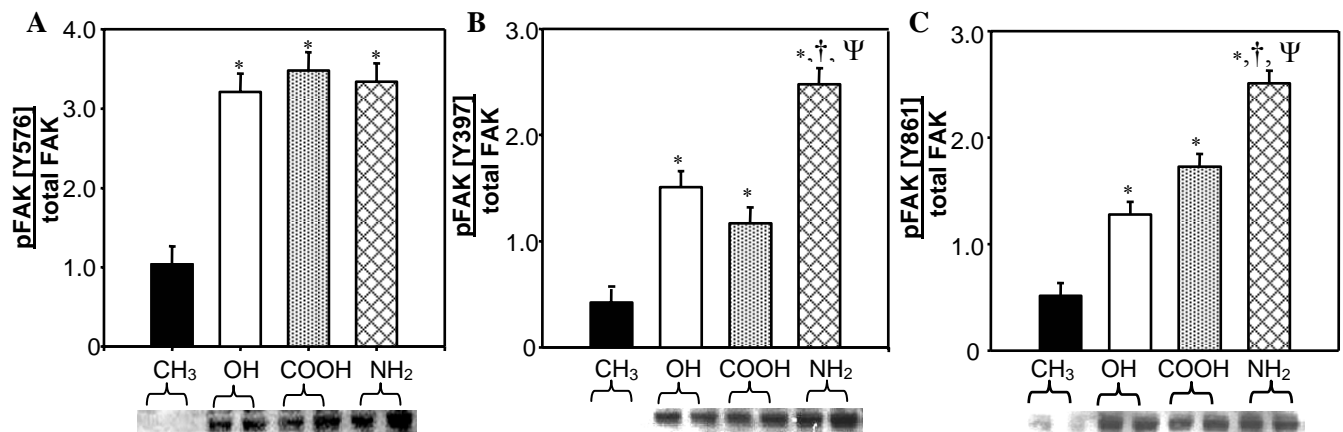


Figure 5.5: Surface chemistry modulates site-specific phosphorylation of FAK. Cells were seeded on SAMs coated with 40 ng/cm² FN, lysed, and analyzed by Western blotting using phosphotyrosine-specific antibodies. (A) Representative Western blot for phosphorylated tyrosine residues on FAK. (B) Quantification of Western blots (n = 6). Pair-wise comparison showed significant differences between surface chemistries (* vs. CH₃, p < 0.05; † vs. OH, p < 0.05; Ψ vs. COOH, p < 0.05).

REFERENCES

1. Langer, R. and Vacanti, J.P.: Tissue engineering. *Science* **260**:920-926, 1993.
2. Anderson, J.M.: Biological Responses to Materials. *Annual Review of Materials Research* **31**:81-110, 2001.
3. Hubbell, J.A.: Bioactive biomaterials. *Curr. Opin. Biotechnol.* **10**:123-129, 1999.
4. Hench, L.L. and Polak, J.M.: Third-generation biomedical materials. *Science* **295**:1014-1017, 2002.
5. Jung, D.R., Kapur, R., Adams, T., Giuliano, K.A., Mrksich, M., Craighead, H.G., and Taylor, D.L.: Topographical and Physicochemical Modification of Material Surface to Enable Patterning of Living Cells. *Critical Reviews in Biotechnology* **21**:111-154, 2001.
6. Garcia, A.J. and Keselowsky, B.G.: Biomimetic surfaces for control of cell adhesion to facilitate bone formation. *Crit Rev. Eukaryot. Gene Expr.* **12**:151-162, 2002.
7. Hynes, R.O.: Integrins: bidirectional, allosteric signaling machines. *Cell* **110**:673-687, 2002.
8. Giancotti, F.G. and Ruoslahti, E.: Integrin signaling. *Science* **285**:1028-1032, 1999.
9. Brash, J.L.: Protein adsorption at the solid-solution interface in relation to blood-material interactions., *In: Proteins at Interfaces.* Eds. T.A. Horbett and J.L. Brash. American Chemical Society, Washington, DC, 1987, pp. 490-506.
10. Grinnell, F., Feld, M., and Minter, D.: Fibroblast adhesion to fibrinogen and fibrin substrata: requirement for cold-insoluble globulin (plasma fibronectin). *Cell* **19**:517-525, 1980.
11. McClary, K.B. and Grainger, D.W.: RhoA-induced changes in fibroblasts cultured on organic monolayers. *Biomaterials* **20**:2435-2446, 1999.
12. McClary, K.B., Ugarova, T., and Grainger, D.W.: Modulating fibroblast adhesion, spreading, and proliferation using self-assembled monolayer films of alkylthiolates on gold. *J. Biomed. Mater. Res.* **50**:428-439, 2000.
13. Scotchford, C.A., Gilmore, C.P., Cooper, E., Leggett, G.J., and Downes, S.: Protein adsorption and human osteoblast-like cell attachment and growth on alkylthiol on gold self-assembled monolayers. *J. Biomed. Mater. Res.* **59**:84-99, 2002.
14. Mrksich, M. and Whitesides, G.M.: Using self-assembled monolayers to understand the interactions of man-made surfaces with proteins and cells. *Annu. Rev. Biophys. Biomol. Struct.* **25**:55-78, 1996.

15. Tengvall,P., Lundstrom,I., and Liedberg,B.: Protein adsorption studies on model organic surfaces: an ellipsometric and infrared spectroscopic approach. *Biomaterials* **19**:407-422, 1998.
16. Brash,J.L.: Exploiting the current paradigm of blood-material interactions for the rational design of blood-compatible materials. *J.Biomater.Sci.Polym.Ed* **11**:1135-1146, 2000.
17. Garcia,A.J., Vega,M.D., and Boettiger,D.: Modulation of cell proliferation and differentiation through substrate- dependent changes in fibronectin conformation. *Mol.Biol.Cell* **10**:785-798, 1999.
18. Tziampazis,E., Kohn,J., and Moghe,P.V.: PEG-variant biomaterials as selectively adhesive protein templates: model surfaces for controlled cell adhesion and migration. *Biomaterials* **21**:511-520, 2000.
19. Bonfield,T.L., Colton,E., Marchant,R.E., and Anderson,J.M.: Cytokine and growth factor production by monocytes/macrophages on protein preadsorbed polymers. *J.Biomed.Mater.Res.* **26**:837-850, 1992.
20. Merwin,J.R., Anderson,J.M., Kocher,O., Van Itallie,C.M., and Madri,J.A.: Transforming growth factor beta 1 modulates extracellular matrix organization and cell-cell junctional complex formation during in vitro angiogenesis. *J.Cell Physiol* **142**:117-128, 1990.
21. Gorbet,M.B. and Sefton,M.V.: Leukocyte activation and leukocyte procoagulant activities after blood contact with polystyrene and polyethylene glycol-immobilized polystyrene beads. *J.Lab Clin.Med.* **137**:345-355, 2001.
22. Shen,M. and Horbett,T.A.: The effects of surface chemistry and adsorbed proteins on monocyte/macrophage adhesion to chemically modified polystyrene surfaces. *J.Biomed.Mater.Res.* **57**:336-345, 2001.
23. Keselowsky,B.G., Collard,D.M., and Garcia,A.J.: Surface chemistry modulates fibronectin conformation and directs integrin binding and specificity to control cell adhesion. *J.Biomed.Mater.Res.* **66A**:247-259, 2003.
24. Allen,L.T., Fox,E.J., Blute,I., Kelly,Z.D., Rochev,Y., Keenan,A.K., Dawson,K.A., and Gallagher,W.M.: Interaction of soft condensed materials with living cells: phenotype/transcriptome correlations for the hydrophobic effect. *Proc.Natl.Acad.Sci.U.S.A* **100**:6331-6336, 2003.
25. Brodbeck,W.G., Patel,J., Voskerician,G., Christenson,E., Shive,M.S., Nakayama,Y., Matsuda,T., Ziats,N.P., and Anderson,J.M.: Biomaterial adherent macrophage apoptosis is increased by hydrophilic and anionic substrates in vivo. *Proc.Natl.Acad.Sci.U.S.A* **99**:10287-10292, 2003.

26. Michael, K.E., Vernekar, V.N., Keselowsky, B.G., Meredith, J.C., Latour, R., Jr., and Garcia, A.J.: Adsorption-Induced Conformational Changes in Fibronectin Due to Interactions with Well-Defined Surface Chemistries. *Langmuir* **19**:8033-8040, 2003.
27. Sastry, S.K. and Burridge, K.: Focal adhesions: a nexus for intracellular signaling and cytoskeletal dynamics. *Exp. Cell Res.* **261**:25-36, 2000.
28. Geiger, B., Bershadsky, A., Pankov, R., and Yamada, K.M.: Transmembrane crosstalk between the extracellular matrix--cytoskeleton crosstalk. *Nat.Rev.Mol.Cell Biol.* **2**:793-805, 2001.
29. Porter, M.D., Bright, T.B., Allara, D.L., and Chidsey, C.E.D.: Spontaneously Organized Molecular Assemblies. 4. Structural characterization of *n*-alkyl thiol monolayers on gold by optical ellipsometry, infrared spectroscopy, and electrochemistry. *J.Am.Chem.Soc.* **109**:3559-3568, 1987.
30. Ulman, A., Eilers, J.E., and Tillman, N.: Packing and molecular-orientation of alkanethiol monolayers on gold surfaces. *Langmuir* **5**:1147-1152, 1989.
31. Bain, C.D., Troughton, E.B., Tao, Y.T., Evall, J., Whitesides, G.M., and Nuzzo, R.G.: Formation of monolayer films by the spontaneous assembly of organic thiols from solution onto gold. *J.Am.Chem.Soc.* **111**:321-335, 1989.
32. Reyes CD, G.A.: A centrifugation cell adhesion assay for high-throughput screening of biomaterial surfaces. *J Biomed Mater Res.* **67A**:328-333, 2003.
33. Garcia, A.J. and Boettiger, D.: Integrin-fibronectin interactions at the cell-material interface: initial integrin binding and signaling. *Biomaterials* **20**:2427-2433, 1999.
34. Brands, R. and Feltkamp, C.A.: Wet cleaving of cells: a method to introduce macromolecules into the cytoplasm. Application for immunolocalization of cytosol-exposed antigens. *Exp. Cell Res.* **176**:309-318, 1988.
35. Keselowsky, B.G. and Garcia, A.J.: Quantitative methods for analysis of integrin receptor binding and focal adhesion formation. *Biomaterials* (in press).
36. Garcia, A.J., Huber, F., and Boettiger, D.: Force required to break alpha5beta1 integrin-fibronectin bonds in intact adherent cells is sensitive to integrin activation state. *J.Biol.Chem.* **273**:10988-10993, 1998.
37. Ilic, D., Furuta, Y., Kanazawa, S., Takeda, N., Sobue, K., Nakatsuji, N., Nomura, S., Fujimoto, J., Okada, M., and Yamamoto, T.: Reduced cell motility and enhanced focal adhesion contact formation in cells from FAK-deficient mice. *Nature* **377**:539-544, 1995.

38. Cary,L.A., Chang,J.F., and Guan,J.L.: Stimulation of cell migration by overexpression of focal adhesion kinase and its association with Src and Fyn. *J.Cell Sci.* **109** :1787-1794, 1996.
39. Frisch,S.M., Vuori,K., Ruoslahti,E., and Chan-Hui,P.Y.: Control of adhesion-dependent cell survival by focal adhesion kinase. *J.Cell Biol.* **134**:793-799, 1996.
40. Zhao,J.H., Reiske,H., and Guan,J.L.: Regulation of the cell cycle by focal adhesion kinase. *J.Cell Biol.* **143**:1997-2008, 1998.
41. Thannickal,V.J., Lee,D.Y., White,E.S., Cui,Z., Larios,J.M., Chacon,R., Horowitz,J.C., Day,R.M., and Thomas,P.E.: Myofibroblast differentiation by transforming growth factor-beta1 is dependent on cell adhesion and integrin signaling via focal adhesion kinase. *J.Biol.Chem.* **278**:12384-12389, 2003.
42. Lotz,M.M., Burdsal,C.A., Erickson,H.P., and McClay,D.R.: Cell adhesion to fibronectin and tenascin: quantitative measurements of initial binding and subsequent strengthening response. *J.Cell Biol.* **109**:1795-1805, 1989.
43. Coll,J.L., Ben Ze'ev,A., Ezzell,R.M., Rodriguez Fernandez,J.L., Baribault,H., Oshima,R.G., and Adamson,E.D.: Targeted disruption of vinculin genes in F9 and embryonic stem cells changes cell morphology, adhesion, and locomotion. *Proc.Natl.Acad.Sci.U.S.A* **92**:9161-9165, 1995.
44. Priddle,H., Hemmings,L., Monkley,S., Woods,A., Patel,B., Sutton,D., Dunn,G.A., Zicha,D., and Critchley,D.R.: Disruption of the talin gene compromises focal adhesion assembly in undifferentiated but not differentiated embryonic stem cells. *J.Cell Biol.* **142**:1121-1133, 1998.
45. Gallant,N.D., Capadona,J.R., Frazier,A.B., Collard,D.M., and Garcia,A.J.: Micropatterned Surfaces to Engineer Focal Adhesions for Analysis of Cell Adhesion Strengthening. *Langmuir* **18**:5579-5584, 2002.
46. Zamir,E. and Geiger,B.: Molecular complexity and dynamics of cell-matrix adhesions. *J.Cell Sci.* **114**:3583-3590, 2001.
47. Schaller,M.D., Hildebrand,J.D., Shannon,J.D., Fox,J.W., Vines,R.R., and Parsons,J.T.: Autophosphorylation of the focal adhesion kinase, pp125FAK, directs SH2-dependent binding of pp60src. *Mol.Cell Biol.* **14**:1680-1688, 1994.
48. Reiske,H.R., Kao,S.C., Cary,L.A., Guan,J.L., Lai,J.F., and Chen,H.C.: Requirement of phosphatidylinositol 3-kinase in focal adhesion kinase-promoted cell migration. *J.Biol.Chem.* **274**:12361-12366, 1999.
49. Parsons,J.T.: Focal adhesion kinase: the first ten years. *J.Cell Sci.* **116**:1409-1416, 2003.

50. Sastry,S.K., Lakonishok,M., Wu,S., Truong,T.Q., Huttenlocher,A., Turner,C.E., and Horwitz,A.F.: Quantitative changes in integrin and focal adhesion signaling regulate myoblast cell cycle withdrawal. *J.Cell Biol.* **144**:1295-1309, 1999.
51. Katz,B.Z., Zamir,E., Bershadsky,A., Kam,Z., Yamada,K.M., and Geiger,B.: Physical state of the extracellular matrix regulates the structure and molecular composition of cell-matrix adhesions. *Mol.Biol.Cell* **11**:1047-1060, 2000.
52. Mostafavi-Pour,Z., Askari,J.A., Parkinson,S.J., Parker,P.J., Ng,T.T., and Humphries,M.J.: Integrin-specific signaling pathways controlling focal adhesion formation and cell migration. *J.Cell Biol.* **161**:155-167, 2003.

CHAPTER 6

SURFACE CHEMISTRY DIRECTS OSTEOBLASTIC DIFFERENTIATION

SUMMARY

Cell adhesion to proteins adsorbed onto synthetic surfaces anchors cells and triggers signals that direct cell function. Using self-assembled monolayers (SAMs) of alkanethiols on gold presenting terminal CH₃, OH, COOH and NH₂ functionalities, we have shown that surface chemistry-dependent differences in FN adsorption induce differences in integrin binding, focal adhesion assembly and signaling, and cell adhesion strength. In the present work, we extend this mechanistic study by examining the effects of surface chemistry on osteoblast cell responses. While cell proliferation and alkaline phosphatase activity were relatively insensitive to underlying surface chemistry, osteoblast-specific gene expression and matrix mineralization exhibited significant differences among surface functionalities. In particular, FN-coated OH and NH₂ surfaces supported high levels of these markers of osteoblastic differentiation. Functional antibody blocking of the central cell-binding domain of pre-adsorbed FN completely inhibited mineralization, underscoring the importance of binding to FN to expression of the osteoblastic phenotype. These results contribute to the development of design principles for the engineering of surfaces that direct cell adhesion for biomedical and biotechnology applications.

INTRODUCTION

Substrate-mediated control of cell function has been shown to be an effective means to direct cell response in many model systems.¹⁻⁵ Surface chemistry is a tunable parameter that has been demonstrated to be a useful modulator of cell response through specific interactions of cell-surface receptors with adsorbed adhesive proteins.⁶⁻¹⁰ Specifically, osteoblast function has been shown to be sensitive to surface properties using polymers,^{11,12} metals^{13,14} and metal oxides,^{15,16} ceramics,¹⁷ and bioactive glasses.¹⁸⁻²¹ Similarly, *in vivo* studies have shown osseointegration of implant surfaces to be surface chemistry-dependent.^{22,23} Although these studies have provided insight into relationships between surface properties and osteoblast cell function and osseointegration, other variables such as surface roughness, have not been well controlled. For example, polymeric surfaces can undergo conformational rearrangements in response to environmental conditions and can exhibit differences in surface roughness and topology depending on processing or surface modifications.^{24,25} These factors can obscure correlations and complicate interpretation of these data. To address these limitations, self-assembled monolayers (SAMs) of alkanethiols on gold have been used as a useful model system to systematically investigate the effects of well-defined surface chemistry without altering other surface properties such as roughness. Long-chain, functionally-terminated alkanethiols ($\text{HS}-(\text{CH}_2)_n\text{-X}$, $n \geq 10$) adsorb from solution onto gold surfaces through gold-sulfur coordination at the chain head and the alkyl chains pack together to form stable, well-packed and ordered monolayers.²⁶⁻²⁸ Once assembled, the end group, X, comprises a uniform interface of designated surface chemistry. SAMs of alkanethiols on gold, therefore, create a versatile and robust model system to study the surface-

protein-cell interface. Recent studies using SAMs of alkanethiols on gold have demonstrated surface chemistry-dependent modulation of osteoblast cell functions of adhesion, growth and migration.^{6,7,29,30}

The present study is an extension of previous work by our group to isolate the effects of surface chemistry on osteoblast cell function, as mediated through the adhesive protein fibronectin (FN). Using SAMs of alkanethiols on gold with different surface chemistries (CH₃, OH, COOH, NH₂) and a fixed density of a single adhesive ligand FN, we have previously shown surface-dependent differences in the adsorbed conformation of FN, resulting in modulation of integrin receptor binding.^{6,7} These results are significant because cell adhesion to extracellular matrix proteins is primarily mediated by the integrin family of cell-surface receptors.³¹ Integrins not only anchor cells, supporting cell spreading and migration, but also trigger signals that regulate survival, proliferation and differentiation.^{31,32} Binding of integrins to the extracellular matrix protein fibronectin (FN) is critical for osteoblastic differentiation.³³ Furthermore, we have shown that these surface chemistry-dependent differences in FN conformation and integrin binding give rise to differences in focal adhesion assembly, FAK activation and adhesion strength of an immature osteoblastic cell line.⁶ These findings provide a putative mechanism for surface-dependent differences in early cell response.³⁴ In the present work, using this same model system, we investigated long-term effects of surface chemistry on osteoblastic cell function. We show that, for the model cell line used, proliferation was relatively insensitive to surface chemistry, while large differences in markers of osteoblastic differentiation were exhibited. Taken together, these results provide a mechanistic analysis of substrate-dependent control of cell function, potentially

advancing the development of engineering principles for the rational design of biomaterial surfaces.

MATERIALS AND METHODS

Cells and Reagents

Human plasma FN and other tissue culture reagents were obtained from Invitrogen (Carlsbad, CA). Fetal bovine serum was purchased from Hyclone (Logan, UT), bovine serum albumin and all other chemical reagents were obtained from Sigma Chemical (St. Louis, MO), while alamarBlue™ was purchased from BioSource International (Camarillo, CA). HFN7.1 monoclonal antibody directed against human plasma FN was obtained from the Developmental Studies Hybridoma Bank (Iowa City, IA). MC3T3-E1 cells, an immature osteoblast-like cell line, were obtained from the RIKEN Cell Bank (Tokyo, Japan). Prior to seeding on FN-coated substrates, MC3T3-E1 cells were maintained in α -Modified Eagle's Medium supplemented with 10% fetal bovine serum and 1% penicillin-streptomycin and passaged every 2 days using standard techniques.

Model Surfaces with Well-Defined Chemistries

Self-assembled monolayers (SAMs) of alkanethiols on gold were used as model substrates with well-defined chemistries. Alkanethiols 1-dodecanethiol (HS-(CH₂)₁₁-CH₃), 11-mercapto-1-undecanol (HS-(CH₂)₁₁-OH) and 11-mercaptoundecanoic acid (HS-(CH₂)₁₀-COOH) were purchased from Aldrich Chemical (Milwaukee, WI) and used as received. The amine-terminated alkanethiol, 12-amino-1-mercaptododecane (HS-

(CH₂)₁₂-NH₂), was synthesized and purified as described previously.⁶ SAMs of their respective alkanethiols are referred to hereafter as CH₃, OH, COOH and NH₂ SAMs. Gold-coated glass coverslips were prepared by sequential deposition of optically transparent films of titanium (100 Å) and gold (200 Å) onto clean glass via an electron beam evaporator (Thermionics Laboratories, Hayward, CA) operating at 2×10^{-6} torr with a deposition rate of 2 Å/s. Freshly prepared gold surfaces were immersed in ethanolic alkanethiol solutions (1.0 mM in absolute ethanol), and SAMs were allowed to assemble for 12 hr. Surfaces were characterized by contact angle and X-ray photoelectron spectroscopy.⁶ Prior to FN coating, SAMs were rinsed in ethanol, dried with N₂, and allowed to equilibrate in Dulbecco's phosphate buffered saline (DPBS: 137 mM NaCl, 2.7 mM KCl, 4.3 mM Na₂HPO₄·7H₂O, 1.5 mM KH₂PO₄, 0.9 mM CaCl₂·2H₂O, 1 mM MgCl₂·6H₂O, pH 7.4) for 15 min. SAMs were coated for 30 min at room temperature with FN diluted in DPBS to produce equivalent FN surface densities among SAMs (40 ng/cm²) and subsequently blocked for 30 min in 1% heat-denatured bovine serum albumin as described previously.^{6,7}

Proliferation

Confluent MC3T3-E1 cells were synchronized by culturing under serum-free conditions (α -MEM + 0.1% albumin) for 3 days. Cells were then seeded at a low density (20 cells/mm²) to insure logarithmic growth, in α MEM supplemented with 10% FBS onto FN-coated (40 ng/cm²) SAMs. After 30 minutes, a 1:10 dilution of alamarBlue™ was added to cells, as well as to cell-free controls. Reduction of the alamarBlue™ dye, monitored by fluorescence (485 nm excitation/ 595 nm emission) at 1, 2 and 3 days after

plating, was utilized as a convenient method to quantify proliferation. Since this method is an indirect measure of cell number (reduction alamarBlue™ of is proportional to metabolic activity), measurement of cell number through DNA incorporation of SYBR Green I (Molecular Probes; Eugene, OR) intercalating dye was quantified as an independent measure of cell number. Cells were lysed in PBS with 0.1 % SDS, lysates were incubated in SYBR Green I (diluted 1:10,000 in 10 mM Tris-EDTA, pH 8.0, per manufacturer's instructions) and incorporation was measured by fluorescence (485 nm excitation, 535 nm emission) and converted to cell number using a standard curve.

Osteoblast-Specific Gene Expression

MC3T3-E1 cells were seeded (100 cells/mm²) on FN-coated (40 ng/cm²) SAMs in α MEM with 10% FBS, 1% penicillin-streptomycin (day 0). Subsequent media changes, starting on day 1, were supplemented with 50 μ g/mL ascorbic acid and 3 mM Na- β -glycerophosphate. Day 7 cultures were lysed and homogenized by QIAshredder column. Total RNA was isolated using the RNEasy RNA isolation kit. cDNA synthesis was performed on DNaseI-treated (25 Kunitz units, for 15 min) total RNA (1 μ g) by oligo(dT) priming using the Superscript II Preamplification System. Real-time PCR using SYBR Green was performed with the ABI Prism 7700 Sequence Detection System (Applied Biosystems; 40 cycles; melting, 15 s at 95 °C; annealing and extension, 60 s at 60 °C).^{35,36} Reaction solutions included SYBR Green PCR Mastermix, 100 μ M forward and reverse primers (**Table 6.1**), and 1 μ L cDNA template in a 30 μ L volume. Gene transcript concentration in template cDNA solution was quantified by generation of a linear standard curve from a decade dilution of an absolute standard for each gene and

plotting the log of concentration versus the C_T value (the cycle number at which a threshold fluorescence value is reached). Standards for each gene were amplified from template cDNA using real-time oligonucleotides and purified using a Qiagen agarose gel extraction kit.^{35,36}

Alkaline Phosphatase Activity

Alkaline phosphatase (ALP) activity was quantified using a modification of the method of Sodek and Berkman.^{35,36} MC3T3-E1 cells were seeded (100 cells/mm²) on FN-coated (40 ng/cm²) SAMs in α MEM with 10% FBS, 1% penicillin-streptomycin. Subsequent media changes, starting on day 1, were supplemented with 50 μ g/mL ascorbic acid and 3 mM Na- β -glycerophosphate. On day 7, cells were rinsed and scraped into ice-cold 50 mM Tris-HCl. Cells were lysed by sonication and normalized for total protein as determined by MicroBCA (Pierce, Rockford, IL). ALP activity was quantified by reaction with 60 μ g/mL 5-methyl umbelliferyl phosphate fluorescent substrate in diethanolamine buffer (pH 9.5). Sample fluorescence was measured on a HTS 7000 Plus BioAssay Reader (Perkin Elmer, Norwalk, CT) at 360 nm excitation, 465 nm emission. ALP activity was calculated using a purified calf intestinal ALP standard.

Matrix Mineralization

MC3T3-E1 cells were seeded (100 cells/mm²) and cultured on FN-coated (40 ng/cm²) SAMs in α MEM supplemented with 10% FBS, 1% penicillin-streptomycin, 50 μ g/mL ascorbic acid, and 3 mM Na- β -glycerophosphate. Following 14 days of culture, cells were fixed in 70% ethanol, rinsed and stained by von Kossa.³⁷ Briefly, 5% AgNO₃

was added to each dish and plates were incubated under uniform light exposure for 30 min. The stain was then fixed in Na₂SO₃ for 2 min, rinsed and dried. Plates were scored for percent mineralization using Image Pro Plus image acquisition and analysis software (Media Cybernetics, Silver Springs, MD). Mineral-phase characteristics of ethanol-fixed cultures were determined by Fourier transform infrared (FT-IR) spectroscopy (Nicolet Magna 550; ThermoNicolet, Madison, WI).³⁶ For FN-blocking antibody experiments, 10 µg/mL HFN7.1 was added to culture media after 24 hours seeding (day 1), and added with media changes for the remainder of the 14 day culture.

Statistical Analyses

Results were analyzed by ANOVA using SYSTAT 8.0 (SPSS Inc., IL). For gene expression, analyses were performed following logarithmic transformation of the data in order to make the variance independent of the mean.³⁶ For treatments that were determined to be significant, pair-wise comparisons were performed using Tukey post-hoc test. A 95% confidence level was considered significant.

RESULTS

Previous work using the same model system indicated that for early adhesion times (under 4 hours), surface chemistry modulates integrin binding and focal adhesion assembly, composition, and signaling.^{6,7} To examine the effects of surface chemistry on long-term cell functions, we evaluated proliferation, osteoblastic gene expression, ALP activity and matrix mineralization for MC3T3-E1 cells cultured on FN-coated SAMs. A fixed FN density (40 ng/cm²) was selected to provide for equivalent ligand densities

among surfaces. This value represents the saturation density for the OH SAM and is the lowest saturation density of all SAMs examined.⁶ Under appropriate culture conditions, the MC3T3-E1 cell line expresses osteoblast-specific genes and produces mineralized nodules, undergoing the developmental stages associated with differentiating osteoblasts.^{38,39} Furthermore, using this cell line, we have previously demonstrated that osteoblastic differentiation and matrix mineralization require binding to FN.³⁵

Cell Proliferation

We investigated the effects of surface chemistry on proliferation of MC3T3-E1 cells seeded on FN-coated (40 ng/cm²) SAMs. Quantification of metabolic activity via alamarBlueTM revealed no differences in proliferation among surfaces, with the exception of a ~30 % increase in cell number on the COOH surface with respect to the OH surface at both day 2 and day 3 (**Figure 6.1**). Since this assay relies on measuring metabolic activity, which may vary as a function of culture confluence, total DNA was quantified by SYBR Green incorporation. DNA quantification measurements revealed no significant differences among SAMs, in general agreement with the alamarBlueTM data, as well as with visual inspection of cultures (data not shown).

Osteoblastic Gene Expression is Surface Chemistry-Dependent

Osteoblastic differentiation on FN-coated SAMs was evaluated via real-time RT-PCR. Markers of osteoblastic differentiation, alkaline phosphatase (ALP), osteocalcin (OCN), bone-sialoprotein (BSP), as well as the house-keeping gene β -actin (BA), were quantified. ALP, BSP and OCN gene expression exhibited surface chemistry-dependent

differences following the pattern $\text{OH} = \text{NH}_2 > \text{COOH} = \text{CH}_3$, with expression levels for OH and NH_2 surfaces approximately twice the levels for the COOH and CH_3 (**Figure 6.2**). β -actin gene expression showed no differences among surfaces, demonstrating no differences in cell number among cultures. This is consistent with the small differences observed in proliferation.

Alkaline Phosphatase Activity

Although considerable differences in ALP gene expression at day 7 were observed, ALP enzymatic activity remained relatively constant among SAMs. However, ~40% higher activity on the OH surface with respect to the NH_2 surface was observed (**Figure 6.3**). This is possibly indicative of regulation at the translational or post-translational levels.

Surface Chemistry-Dependent Differences in Matrix Mineralization

Staining by von Kossa, in which phosphate deposits stain black, revealed that matrix mineralization varied significantly among SAMs. The OH and NH_2 functionalities supported high levels of mineralization, comparable to levels observed on FN-coated tissue culture polystyrene (data not shown), while mineralization on the COOH and CH_3 surfaces was negligible (**Fig. 6.4**). In order to determine if the matrix mineralization observed was biologically equivalent carbonate-containing hydroxyapatite or non-biological precipitation, FT-IR spectroscopy was performed (**Fig. 6.5**). A phosphate peak at $\sim 1100 \text{ cm}^{-1}$, indicative of matrix mineral content, and an amide I peak at $\sim 1650 \text{ cm}^{-1}$, representing matrix protein content, was evident on all surfaces. The

presence of a phosphate doublet peak (seen at $\sim 560\text{ cm}^{-1}$ and as a shoulder at $\sim 605\text{ cm}^{-1}$), indicating the presence of crystallized phosphate, for matrices on the OH and NH_2 surfaces, indicates that mineralization on these surfaces is crystalline hydroxyapatite. FT-IR analysis of mineralized samples revealed the presence of a carbonate peak at $\sim 870\text{ cm}^{-1}$ for matrices on the OH and NH_2 surfaces, indicating biologically equivalent carbonate-containing hydroxyapatite on these surfaces.

To examine the role of the pre-adsorbed human FN on SAMs, cells were cultured in the presence of HFN7.1, a monoclonal antibody that blocks integrin binding to the central cell binding domain of human FN, without cross-reacting with either bovine or murine FN.⁴⁰ Importantly, blocking with HFN7.1 antibody completely inhibited mineralization, indicating that adhesion to FN is critical to expression of the osteoblastic phenotype on these substrates and demonstrating the importance of the FN adsorbed prior to cell seeding (**Fig. 6.6**).

DISCUSSION

A fundamental understanding of cell-protein-surface interactions is critical to the rational design of biomaterials to elicit directed cell and tissue response. Previously, using SAMs of alkanethiols on gold, we demonstrated that surface chemistry modulates the adsorbed conformation of the adhesive protein, FN, giving rise to large differences in adhesion strength and the early cell responses of integrin binding, focal adhesion assembly and signaling.⁶ In the present work, we extend this mechanistic examination of substrate-directed control of cell function, focusing on the later cell responses of osteoblastic differentiation. Osteoblastic gene expression and matrix mineralization

demonstrated significant surface chemistry-dependence. The OH and NH₂ surfaces supported elevated levels of expression of osteoblast-specific genes for ALP (cleaves phosphate groups making them available for incorporation into the inorganic phase), BSP (an enhancer of hydroxyapatite nucleation) and OCN (binds hydroxyapatite). The OH and NH₂ surfaces also supported high levels of matrix mineralization that was shown to be biologically equivalent carbonate-containing hydroxyapatite.

The elevated levels of osteoblastic gene expression and matrix mineralization on the OH and NH₂ surfaces correlated well with enhanced $\alpha_5\beta_1$ integrin binding and FAK activation on these chemistries,⁶ consistent with critical roles for $\alpha_5\beta_1$ binding to FN and FAK in osteoblastic differentiation.^{41,41a} Notably, blocking antibodies against the major integrin binding site in FN completely inhibited mineralization on these substrates. This result demonstrates that interactions between integrins and adsorbed human FN are essential to differentiation on these surfaces. Interestingly, the COOH substrate supported insignificant amounts of mineralization, even though this functionality provided for equivalent levels of $\alpha_5\beta_1$ binding and FAK activation as the chemistries that supported mineralization. An explanation for this result is that the pro-differentiation signals triggered by $\alpha_5\beta_1$ binding are inhibited by another adhesive interaction. The COOH surface, in contrast to the NH₂ and OH substrates, exhibited significant $\alpha_v\beta_3$ integrin binding.⁶ Avioli and colleagues demonstrated that $\alpha_v\beta_3$ integrin binding inhibited osteoblastic differentiation and mineralization without altering FAK activation in this cell line.⁴² These results suggest that the interplay between of multiple integrins plays a crucial role in adhesion-mediated cell function. Future efforts in targeting

specific integrins to direct cell response may evolve to targeting multiple integrins in concert.

Numerous studies have shown substrate-dependent differences in osteoblast cell response,^{14,20,21} however, surface properties were not controlled. To address this, model surfaces have been used to examine the individual effects of surface chemistry⁴³ and roughness.^{44,45} Several groups have used SAMs of alkanethiols on gold to examine the effects of surface chemistry on cell function. For example, McClary et al. demonstrated surface chemistry-dependent differences in fibroblast adhesion, spreading and RhoA signaling on FN-coated SAMs of COOH and CH₃ surface chemistries.^{46,47} Scotchford et al. reported modulation of osteoblast adhesion on FN-coated SAMs of COOH, OH and CH₃ surface chemistries, showing qualitative differences in integrin binding and localization of vinculin to focal adhesions as well as seeding efficiency.²⁹

Other work has focused on the use of alkanethiols on gold to examine the effects of surface chemistry on non-biological mineralization. In contrast to the biological hydroxyapatite reported in the present work, non-biological apatite crystallization was reported on SAMs incubated in protein-free saline solutions with the following trend: COOH >> OH = NH₂ >> CH₃.⁴⁸ It is interesting to note the opposite trends in these two forms of mineralization, indicating the very different mechanisms of mineralization in the two systems.

We propose a model in which surface chemistry-dependent differences in FN adsorption induce differences in integrin binding, differentially regulate focal adhesion assembly and signaling which, in turn, modulates the cellular functions of cell adhesion strength, osteoblast-specific gene expression and matrix mineralization. These results

contribute to the development of design principles for the engineering of surfaces that direct cell adhesion for biomedical and biotechnology applications.

ACKNOWLEDGMENT

This work was funded by the Whitaker Foundation and the Georgia Tech/Emory NSF ERC on the Engineering of Living Tissues (EEC-9731643). B.G.K. was supported by an NSF Graduate Research Fellowship. HFN7.1 monoclonal antibody was obtained from the Developmental Studies Hybridoma Bank developed under the auspices of the NICHD and maintained by the University of Iowa, Dept. of Biological Sciences, Iowa City, IA 52242.

Gene	Forward primer	Reverse primer	Product size (bp)	Genbank accession #
ALP	5'-GGGACTGGTACTCGGATAACGA	5'-CTGATATGCGATGTCCTTGCA	71	6671532
OCN	5'-CGGCCCTGAGTCTGACAAA	5'-GCCGGAGTCTGTTCACCTT	68	X04142
BSP	5'-TCCTCCTCTGAAACGGTTCC	5'-GGAACATATCGCCGTCTCCATT	73	L20232
BA	5'-TTCAACACCCAGCCATGT	5'-TGTGGTACGACCAGAGGCATAC	69	X03672

Table 6.1. Real-time PCR oligonucleotides for murine genes.

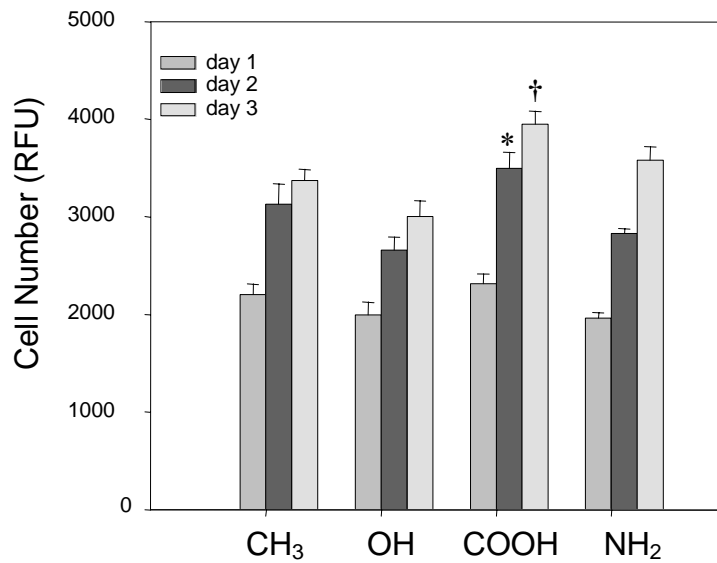


Figure 6.1. Osteoblast proliferation shows little dependence on surface chemistry. MC3T3-E1 cells were cultured on SAMs coated with equivalent FN surface densities (40 ng/cm²). Cell numbers were quantified indirectly through metabolic activity via alamarBlue™ reduction (* - vs. OH (2 days); † - vs. OH (3 days)). Data is plotted as mean ± standard error.

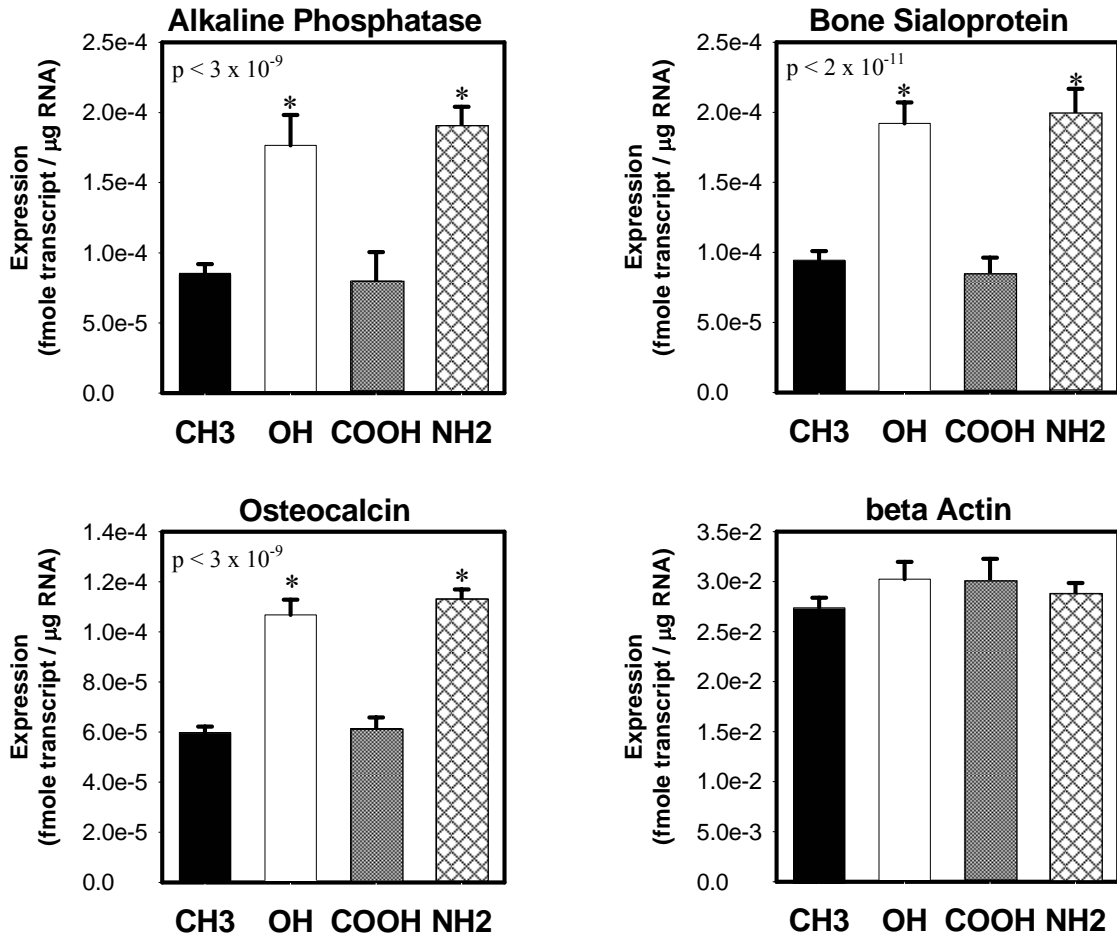


Figure 6.2. Surface chemistry modulates osteoblastic gene expression. MC3T3-E1 cells were cultured on SAMs coated with equivalent FN surface densities (40 ng/cm^2). Osteoblast-specific gene expression was quantified by real-time RT-PCR (* vs. CH₃ and COOH; $p < 8 \times 10^{-6}$). Data is plotted as mean \pm standard error.

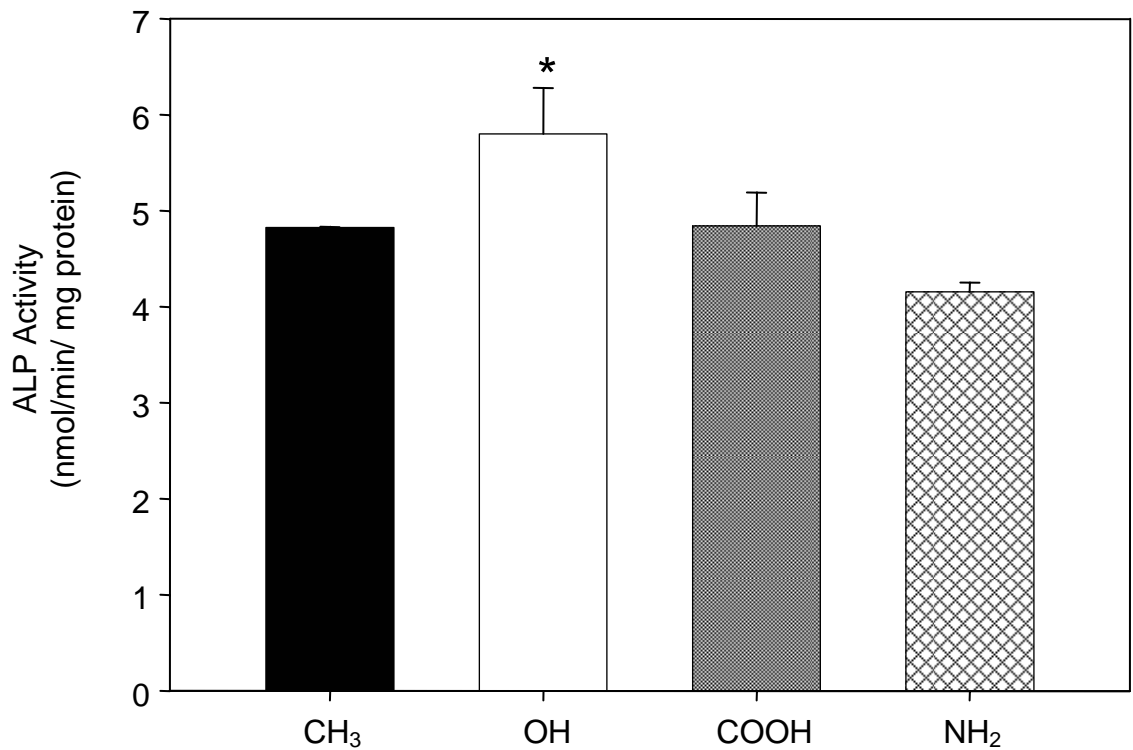


Figure 6.3. Osteoblast alkaline phosphatase activity shows little dependence on surface chemistry. MC3T3-E1 cells were cultured on SAMs coated with equivalent FN surface densities (40 ng/cm²) for 7 days. Pair-wise comparison showed significant differences between two groups (* vs. NH₂). Data is plotted as mean ± standard error.

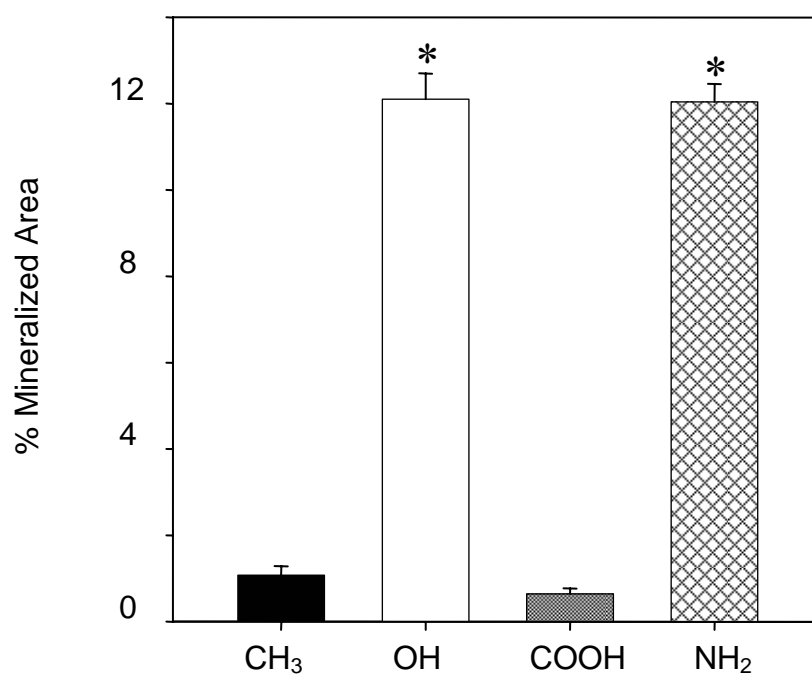
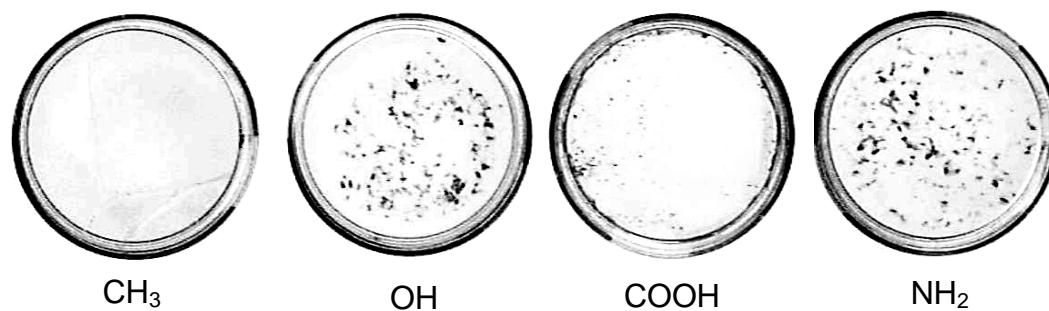


Figure 6.4. Surface chemistry modulates matrix mineralization. MC3T3-E1 cells were cultured on SAMs coated with equivalent FN surface densities (40 ng/cm²). Mineralized deposits (black) at day 14 varied among surface chemistries. Pair-wise comparison showed significant differences between surface chemistries (* vs. CH₃ and COOH; $p < 0.05$). Data is plotted as mean \pm standard error.

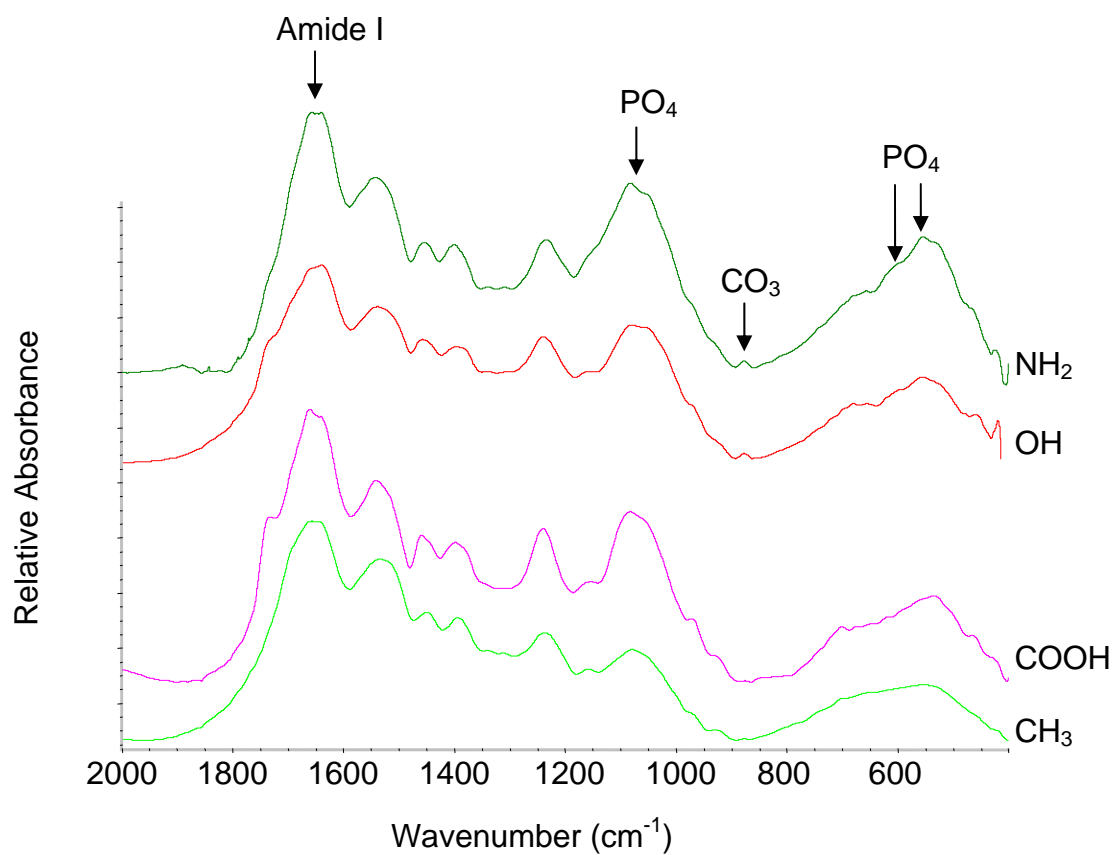


Figure 6.5. Surface chemistry modulates composition and structure of matrix mineralization, as shown by FT-IR. MC3T3-E1 cells were cultured on 14 days on SAMs coated with equivalent FN surface densities (40 ng/cm^2). Spectra show peaks characteristic of biological carbonate-containing hydroxyapatite.

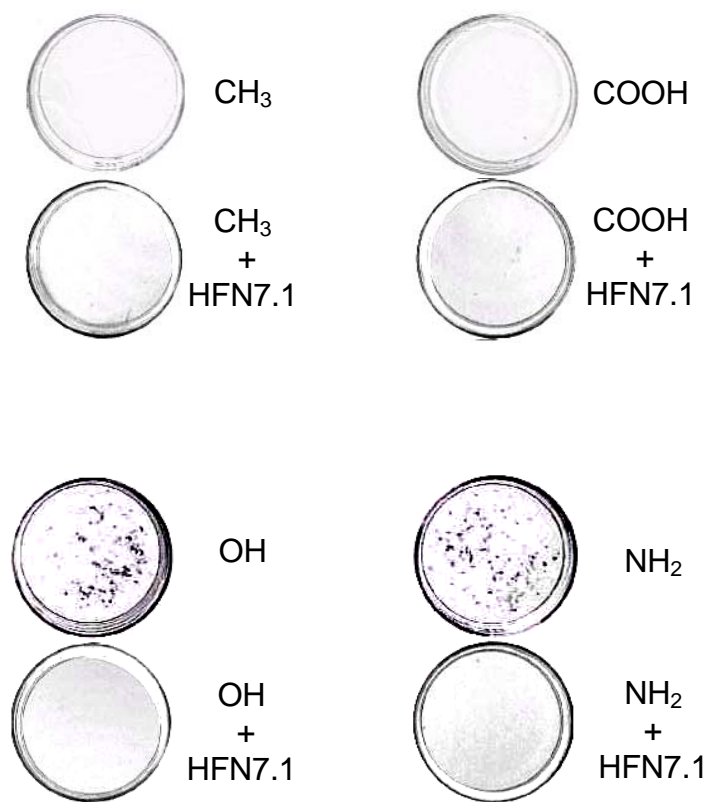


Figure 6.6. Osteoblast differentiation requires integrin binding to FN. MC3T3-E1 cells were cultured on SAMs coated with equivalent FN surface densities (40 ng/cm²). Blocking with HFN7.1 antibody, specific to human FN, demonstrated that integrin binding to pre-adsorbed FN is essential for differentiation.

REFERENCES

1. Sakiyama,S.E., Schense,J.C., and Hubbell,J.A.: Incorporation of heparin-binding peptides into fibrin gels enhances neurite extension: an example of designer matrices in tissue engineering. *FASEB J.* **13**:2214-2224, 1999.
2. Mann,B.K., Gobin,A.S., Tsai,A.T., Schmedlen,R.H., and West,J.L.: Smooth muscle cell growth in photopolymerized hydrogels with cell adhesive and proteolytically degradable domains: synthetic ECM analogs for tissue engineering. *Biomaterials* **22**:3045-3051, 2001.
3. Tsai,W.B., Grunkemeier,J.M., McFarland,C.D., and Horbett,T.A.: Platelet adhesion to polystyrene-based surfaces preadsorbed with plasmas selectively depleted in fibrinogen, fibronectin, vitronectin, or von Willebrand's factor. *J.Biomed.Mater.Res.* **60**:348-359, 2002.
4. Sawada,S., Sakaki,S., Iwasaki,Y., Nakabayashi,N., and Ishihara,K.: Suppression of the inflammatory response from adherent cells on phospholipid polymers. *J.Biomed.Mater.Res.* **64A**:411-416, 2003.
5. Brodbeck,W.G., Patel,J., Voskerician,G., Christenson,E., Shive,M.S., Nakayama,Y., Matsuda,T., Ziats,N.P., and Anderson,J.M.: Biomaterial adherent macrophage apoptosis is increased by hydrophilic and anionic substrates in vivo. *Proc.Natl.Acad.Sci.U.S.A* **99**:10287-10292, 2003.
6. Keselowsky,B.G., Collard,D.M., and Garcia,A.J.: Surface chemistry modulates fibronectin conformation and directs integrin binding and specificity to control cell adhesion. *J.Biomed.Mater.Res.* **66A**:247-259, 2003.
7. Keselowsky,B.G., Collard,D.M., and Garcia,A.J.: Surface chemistry modulates focal adhesion composition and signaling through changes in integrin binding. *Biomaterials* (in press).
8. McFarland,C.D., Thomas,C.H., DeFilippis,C., Steele,J.G., and Healy,K.E.: Protein adsorption and cell attachment to patterned surfaces. *J.Biomed.Mater.Res.* **49**:200-210, 2000.
9. McClary,K.B., Ugarova,T., and Grainger,D.W.: Modulating fibroblast adhesion, spreading, and proliferation using self- assembled monolayer films of alkylthiolates on gold. *J.Biomed.Mater.Res.* **50**:428-439, 2000.
10. Shen,M. and Horbett,T.A.: The effects of surface chemistry and adsorbed proteins on monocyte/macrophage adhesion to chemically modified polystyrene surfaces. *J.Biomed.Mater.Res.* **57**:336-345, 2001.
11. Yamamoto,M., Kato,K., and Ikada,Y.: Ultrastructure of the interface between cultured osteoblasts and surface-modified polymer substrates. *J Biomed Mater Res.* **37**:29-36, 1997.

12. Lim,J.Y., Liu,X., Vogler,E.A., and Donahue,H.J.: Systematic variation in osteoblast adhesion and phenotype with substratum surface characteristics. *J Biomed Mater Res.* **68A**:504-512, 2004.
13. Puleo,D.A. and Bizios,R.: Formation of focal contacts by osteoblasts cultured on orthopedic biomaterials. *J.Biomed.Mater.Res.* **26**:291-301, 1992.
14. Puleo,D.A., Holleran,L.A., Doremus,R.H., and Bizios,R.: Osteoblast responses to orthopedic implant materials in vitro. *J.Biomed.Mater.Res.* **25**:711-723, 1991.
15. Sul,Y.T.: The significance of the surface properties of oxidized titanium to the bone response: special emphasis on potential biochemical bonding of oxidized titanium implant. *Biomaterials* **24**:3893-3907, 2003.
16. Zreiqat,H. and Howlett,C.R.: Titanium substrata composition influences osteoblastic phenotype: In vitro study. *J Biomed Mater Res.* **47**:360-366, 1999.
17. Zreiqat,H., Evans,P., and Howlett,C.R.: Effect of surface chemical modification of bioceramic on phenotype of human bone-derived cells. *J Biomed Mater Res.* **44**:389-396, 1999.
18. Garcia,A.J., Ducheyne,P., and Boettiger,D.: Effect of surface reaction stage on fibronectin-mediated adhesion of osteoblast-like cells to bioactive glass. *J.Biomed.Mater.Res.* **40**:48-56, 1998.
19. Davies,J.E. and Matsuda,T.: Extracellular matrix production by osteoblasts on bioactive substrata in vitro. *Scanning Microsc.* **2**:1445-1452, 1988.
20. El-Ghannam,A., Ducheyne,P., and Shapiro,I.M.: Porous bioactive glass and hydroxyapatite ceramic affect bone cell function in vitro along different time lines. *J.Biomed.Mater.Res.* **36**:167-180, 1997.
21. Vrouwenvelder,W.C., Groot,C.G., and de Groot,K.: Histological and biochemical evaluation of osteoblasts cultured on bioactive glass, hydroxylapatite, titanium alloy, and stainless steel. *J.Biomed.Mater.Res.* **27**:465-475, 1993.
22. Howlett,C.R., Chen,N., Zhang,X., Akin,F.A., Haynes,D., Hanley,L., Revell,P., Evans,P., Zhou,H., and Zreiqat,H.: Effects of Biomaterial Chemistries on the Osteoblastic Molecular Phenotype and Osteogenesis: In Vitro and In Vivo Studies., *In: Bone Engineering.* Ed. J.E.Davies. em squared incorporated, Toronto, Canada, 2000, pp. 240-255.
23. James,K., Levene,H., Kaufmann,E.E., Parsons,J.R., and Kohn,J.: Small Changes in Chemical Structure of a Polymer Can Have a Significant Effect on the Hard-Tissue Response In Vivo., *In: Bone Engineering.* Ed. J.E.Davies. em squared incorporated, Toronto, Canada, 2000, pp. 195-203.

24. Tyler,B.J., Ratner,B.D., Castner,D.G., and Briggs,D.: Variations between Biomer lots. I. Significant differences in the surface chemistry of two lots of a commercial poly(ether urethane). *J.Biomed.Mater.Res.* **26**:273-289, 1992.
25. Silver,J.H., Lewis,K.B., Ratner,B.D., and Cooper,S.L.: Effect of polyol type on the surface structure of sulfonate-containing polyurethanes. *J.Biomed.Mater.Res.* **27**:735-745, 1993.
26. Porter,M.D., Bright,T.B., Allara,D.L., and Chidsey,C.E.D.: Spontaneously organized molecular assemblies. 4. structural characterization of *n*-alkyl thiol monolayers on gold by optical ellipsometry, infrared spectroscopy, and electrochemistry. *J.Am.Chem.Soc.* **109**:3559-3568, 1987.
27. Ulman, A., Eilers, J. E., and Tillman, N. Packing and molecular orientation of alkanethiol monolayers on gold surfaces. *Langmuir* 5, 1147-1152. 1989. Ref Type: Journal (Full)
28. Prime,K.L. and Whitesides,G.M.: Self-assembled organic monolayers: model systems for studying adsorption of proteins at surfaces. *Science* **252**:1164-1167, 1991.
29. Scotchford,C.A., Gilmore,C.P., Cooper,E., Leggett,G.J., and Downes,S.: Protein adsorption and human osteoblast-like cell attachment and growth on alkylthiol on gold self-assembled monolayers. *J.Biomed.Mater.Res.* **59**:84-99, 2002.
30. Webb,K., Hlady,V., and Tresco,P.A.: Relationships among cell attachment, spreading, cytoskeletal organization, and migration rate for anchorage-dependent cells on model surfaces. *J Biomed Mater Res.* **49**:362-368, 2000.
31. Hynes,R.O.: Integrins: bidirectional, allosteric signaling machines. *Cell* **110**:673-687, 2002.
32. Giancotti,F.G. and Ruoslahti,E.: Integrin signaling. *Science* **285**:1028-1032, 1999.
33. Moursi,A.M., Damsky,C.H., Lull,J., Zimmerman,D., Doty,S.B., Aota,S., and Globus,R.K.: Fibronectin regulates calvarial osteoblast differentiation. *J.Cell Sci.* **109**:1369-1380, 1996.
34. Moursi,A.M., Globus,R.K., and Damsky,C.H.: Interactions between integrin receptors and fibronectin are required for calvarial osteoblast differentiation in vitro. *J.Cell Sci.* **110**:2187-2196, 1997.
35. Stephansson,S.N., Byers,B.A., and Garcia,A.J.: Enhanced expression of the osteoblastic phenotype on substrates that modulate fibronectin conformation and integrin receptor binding. *Biomaterials* **23**:2527-2534, 2002.
36. Byers,B.A., Pavlath,G.K., Murphy,T.J., Karsenty,G., and Garcia,A.J.: Cell-type-dependent up-regulation of in vitro mineralization after overexpression of the

- osteoblast-specific transcription factor Runx2/Cbfa1. *J.Bone Miner.Res.* **17**:1931-1944, 2002.
37. Dickson,G.R.: Methods of Calcified Tissue Preparation. Elsevier, New York, NY, 1984.
 38. Sudo,H., Kodama,H.A., Amagai,Y., Yamamoto,S., and Kasai,S.: In vitro differentiation and calcification in a new clonal osteogenic cell line derived from newborn mouse calvaria. *J.Cell Biol.* **96**:191-198, 1983.
 39. Choi,J.Y., Lee,B.H., Song,K.B., Park,R.W., Kim,I.S., Sohn,K.Y., Jo,J.S., and Ryoo,H.M.: Expression patterns of bone-related proteins during osteoblastic differentiation in MC3T3-E1 cells. *J Cell Biochem.* **61**:609-618, 1996.
 40. Schoen,R.C., Bentley,K.L., and Klebe,R.J.: Monoclonal antibody against human fibronectin which inhibits cell attachment. *Hybridoma* **1**:99-108, 1982.
 41. Moursi,A.M., Globus,R.K. and Damsky,C.H.: Interactions between integrin receptors and fibronectin are required for calvarial osteoblast differentiation in vitro. *J.Cell Sci.* **110**:2187-2196, 1997.
 - 41a. Tamura,Y., Takeuchi,Y., Suzawa,M., Fukumoto,S., Kato,M., Miyazono,K., Fujita,T.: Focal adhesion kinase activity is required for bone morphogenetic protein--Smad1 signaling and osteoblastic differentiation in murine MC3T3-E1 cells. *J.Bone Miner.Res.* **16**(10):1772-1779, 2001.
 42. Cheng,S.L., Lai,C.F., Blystone,S.D., and Avioli,L.V.: Bone mineralization and osteoblast differentiation are negatively modulated by integrin alpha(v)beta3. *J.Bone Miner.Res.* **16**:277-288, 2001.
 43. Healy,K.E., Carson H.Thomas, Alireza Rezaia, Jung E.Kim, Patrick J.McKeown, Barbara Lom, and Philip E.Hockberger: Kinetics of bone cell organization and mineralization on materials with patterned surface chemistry. *Biomaterials* **17**:195-208, 1996.
 44. Schwartz,Z., Lohmann,C.H., Vocke,A.K., Sylvia,V.L., Cochran,D.L., Dean,D.D., and Boyan,B.D.: Osteoblast response to titanium surface roughness and 1alpha,25-(OH)(2)D(3) is mediated through the mitogen-activated protein kinase (MAPK) pathway. *J.Biomed.Mater.Res.* **56**:417-426, 2001.
 45. Deligianni,D.D., Katsala,N., Ladas,S., Sotiropoulou,D., Amedee,J., and Missirlis,Y.F.: Effect of surface roughness of the titanium alloy Ti-6Al-4V on human bone marrow cell response and on protein adsorption. *Biomaterials* **22**:1241-1251, 2001.
 46. McClary,K.B., Ugarova,T., and Grainger,D.W.: Modulating fibroblast adhesion, spreading, and proliferation using self-assembled monolayer films of alkylthiolates on gold. *J Biomed Mater Res* **50**:428-439, 2000.

47. McClary, K.B. and Grainger, D.W.: RhoA-induced changes in fibroblasts cultured on organic monolayers. *Biomaterials* **20**:2435-2446, 1999.
48. Tanahashi, M. and Matsuda, T.: Surface functional group dependence on apatite formation on self-assembled monolayers in a simulated body fluid. *J. Biomed. Mater. Res.* **34**:305-315, 1997.

CHAPTER 7

CONCLUSIONS AND RECOMMENDATIONS FOR FUTURE WORK

The goal of this thesis research was to engineer well-defined surfaces to direct integrin binding and signaling to promote osteoblast differentiation. The approach of controlling cell receptor-ligand interactions through underlying substrata represents a versatile method to manipulate cellular responses for biomaterial and tissue engineering applications. By focusing on osteoblasts, the cells responsible for bone matrix production and mineralization, this research is relevant to the engineering of surfaces that may lead to improvements in biomaterials for orthopedic implants, grafting substrates and tissue engineering scaffolds. By implementing a bioengineering analysis of integrin-mediated adhesion to adsorbed FN as a function of the underlying chemistry, we have made important contributions toward establishing a fundamental framework for the engineering of surfaces to direct cell function. A significant advantage of our experimental system over previous studies is the use of model surfaces consisting of SAMs of alkanethiols on gold presenting well-defined chemistries. Using this model system, we conclude that surface chemistry-dependent differences in FN adsorption induce differences in integrin binding, differentially regulate focal adhesion assembly and signaling which, in turn, modulate cell adhesion strength, osteoblast-specific gene expression and matrix mineralization. Specifically, OH and NH₂ chemistries provided enhanced functional presentation of adsorbed FN, targeting integrin $\alpha_5\beta_1$ and promoting osteoblastic differentiation. The CH₃ chemistry most likely performed poorly due to FN inactivation upon adsorption to this hydrophobic surface, while the functional presentation of FN

adsorbed on the COOH surface, able to support high levels of many adhesive functions (integrin binding, focal adhesion assembly and signaling), most likely failed to promote osteoblastic differentiation due to a lack of integrin binding specificity. In addition, new methods to quantify integrin binding and focal adhesion assembly were introduced and validated. Overall, this thesis makes important contributions to the development of design principles for the engineering of surfaces that direct cell adhesion for biomedical and biotechnology applications.

Recommendations for future experiments include many exciting possibilities. Functional antibody blocking experiments could be carried out in order to further elucidate the role specific integrins in surface-mediated cell response. Similarly, important information could be gained by further determination of the signaling pathways giving rise to surface chemistry-dependent differences in cell function. The use of siRNA to block expression molecules involved in cell adhesion, including the ones mentioned above, as well as focal adhesion proteins and adhesive proteins could be employed to gain additional insight into surface-dependent cell function.

The identification of surface chemistries that promote osteoblastic differentiation raises the question of whether osteoblastic cell response to surface chemistry has a “minimum surface chemistry density” to invoke a similar response, and whether surface chemistry effects may be additive or synergistic. This could be addressed through mixed surface chemistry experiments using SAMs. Also, interesting work may be carried out with surface chemistry gradients of mixed chemistries, with one possible goal of potentially overcoming difficulties in non-homogeneous cell population of synthetic grafts. Finally, *in vivo* experiments with model surfaces should be conducted in order to

address whether or not surface chemistry similarly modulates cell response at the tissue level and with the enormous amount of added complexity from being placed in the *in vivo* environment.